Online Electromagnetic Wave Monitoring System for Petroleum Industry Applications

Salem Hasan Hamad Alhajeri

A thesis submitted in partial fulfillment of the requirements of Liverpool John Moores University for the degree of

Doctor of Philosophy

Radio Frequency and Microwaves Group

General Engineering Research Institute

January 2010

Dedicated to my parents Hasan and Saad'a

Acknowledgments

I would like to express my greatest thanks to my principle supervisor Professor. A. Al-Shamma'a for his advice, guidance, and encouragement during the course of this research. I would also like to thank my second supervisor Dr. Steve Wylie who has been close at hand, when I required the benefit of his knowledge and experience in the area of Radio Frequency (RF) and Microwave.

I would like to thanks Dr. Jeff Cullen for his general help in many aspects during this research. Also, I would like to say a huge thanks to my colleagues in the RF and Microwave group, and the General Engineering Research Institute for their help and continued support, particularly, Dr. Eduardo Lopez, Dr. Alex Mason, M. Aljader, Eric Bader, Lio, and Goh. I would like to thank Helen Pottle and Nina Wylie for heir hard work on the admin side of things, allowing the process to run smooth and efficiently.

I also wish to take the opportunity to thank all the technicians for their technical support. Finally, I would like to thank my family for their patience, support and encouragement.

Abstract

The general demand for automating industrial processes in the oil industry has increased rapidly in parallel with sensors and their underlying technology. Since the early 1980s, the particular problem, which has been representing the extremes in complexity in the oil industry, is the measurement of multiphase flow components, the mixing ratio of oil, water, and gas flowing in a pipeline. Electromagnetic (EM) Wave sensors can provide an attractive solution, because microwave signals can penetrate most materials allowing the measurement to be representative for the cross section of the pipeline.

In this thesis, EM wave sensors operating at microwave frequencies are developed for measuring multiphase flow components in a pipeline. These sensors are based on cylindrical cavity, and they use the resonant frequencies related to changes of permittivity to detect and measure (oil, gas, and water) components flowing in a pipeline. Special emphasis has been given to three main design principles. The principle of designing a completely non intrusive sensor, the choice of resonance mode to achieve the best measurement accuracy, and the possibility of designing a new software application to allow online implementation of the sensors. The first principle is shown to allow sensors

with completely non intrusive structures to be designed. The two fundamental modes in cylindrical cavity resonators were therefore analysed.

A sensor for measuring the mixture ratio of oil and water flowing in a pipeline is developed. We called it a EM wave (EMW2) for measuring two phase. Both the experiment results and the HFSS results are compared and analysed.

A sensor for measuring multiphase flow (oil, gas, and water mixtures) in a pipeline in real time is developed. We called it a EW wave (EMW3) sensor for multiphase fractions measurement. The emphasis is on the measurement accuracy with the desired resonant frequency mode, and the possibility of designing a software programme to explore the functionality of the sensor for online measurement. The accuracy of the sensor measurements is achieved by comparing and analyzing the HFSS simulated results and experimental results.

A sensor suitable for measuring online the components of mixtures of (hydrocarbons, gas, and water) flowing in a pipeline is developed based on the EMW3 sensor. We called it a EM Wave monitoring and control system. Consequently, online controlling and monitoring, on the other hand, are achieved and the online results are shown. Finally, the research is concluded and future works is discussed.

Table of Contents

List of Figures

List of Tables

List of Symbols

Symbol	Description	Units
a	width of the broad wall in rectangular waveguide	m
b	width of the narrow wall of rectangular waveguide	m
B	magnetic flux density	weber / m^2
c	speed of propagation of EM wave in free space	m/s
D	electric flux density	coulomb/ m^2
D	diameter of a cylindrical waveguide	m
d	cylindrical Waveguide length	m
E	electric field intensity	volt/m
f	Frequency	Hz
H	magnetic field intensity	ampere/m
J	electric current density	ampere/ m^2
R	radius of a cylindrical waveguide	m
v_g	Group velocity	m/s
v_p	phase velocity	m/s
Z_0	line characteristic impedance	Ω

Z_L	load impedance	Ω
Γ	reflection coefficient	1/m
ε_r	relative permittivity	F/m
ε'	real part of relative permittivity	F/m
ε''	complex part of relative permittivity	F/m
λ	wavelength of EM wave in free space	m
λ_c	cut off wavelength	m
λ_g	guide wavelength	m
μ_r	relative permeability	H/m
μ'	real part of relative permeability	H/m
μ''	complex part of relative permeability	H/m
ρ	volume charge density	coulomb/m^3
Ø	reflection angle	radian

CHAPTER 1

Introduction

1.1 Current Three-Phase Systems Technologies

The need for sensors has grown rapidly with the automatization of the industrial processes. Measuring oil, gas, and water quantities flowing in a pipeline is a significant problem in the petroleum industry. An attractive solution can be provided by microwave sensors, because microwaves penetrate most materials.

Accurately measuring and continually monitoring multiphase flow fractions [1] is a particular problem that has been representing the extremes in complexity in the oil industry since the early 1980s. Since then, several efforts have been made to develop multiphase flow measurement instruments suitable for use in the oil industrial environment. Such instruments need to be $\pm 5\%$ accurate, non intrusive, reliable, flow regime

independent and suitable for use over the full component fraction range [1, 2].

The output of an oil well is a multiphase fluid or a natural combination of oil, gas, and water components (non homogeneous mixture). The component for each phase of this combination needs to be known separately in real time [3]. Water must be removed before oil can be delivered to the oil industry processing facility or sale points.

Gas and water also may be injected at various points into the oil well to maximize the amount of oil that can be retrieved. The injected water and gas are used to maintain the pressure and reduce the viscosity of the oil within that well respectively. The operators need to be able to regularly monitor the output of each well in the field for optimizing the production and life of an oil field. The conventional way of doing this is to use a traditional test separator [4]. Test separators are expensive, occupy valuable space on a production platform and require a long time to monitor each well because of the stabilized flow conditions required. In addition test separators cannot be used for continuous well monitoring.

The output of each well can vary greatly, depending on the location and age of well. Allocation metering is needed when a common pipeline is used to transport the output from a number of wells owned by different companies to a processing facility [4, 2]. This can be achieved by passing the output of each well through a test separator before it enters the common pipeline. In addition to the disadvantages of the test separator, described above, dedicated test pipelines to each well are also required.

Multiphase flow measurement instruments enable the oil and gas industry to continuously measure and monitor the amount of oil, water and gas flowing in a pipeline rather than relying on the occasional test separator measurements [5, 6].

The current developed three phase systems for measuring multiphase flow component fractions are based on various technologies, either two or a combination of several. The two most commonly methods used to measure multiphase flow fractions are based on the electrical impedance measurement and dual-energy Gamma-Ray absorption technologies [7].

Microwave amplitude and phase shift techniques, Pulsed Neutron Activation (PNA), and Nuclear Magnetic Resonance (NMR) are some forms of alternative methods currently applied in the development of multiphase flow Measurement systems.

1.1.1 Dual Energy Gamma-Ray Attenuation Principles

In principle, dual-energy γ-ray attenuation methods are elegant, but in practice a number of difficulties have to be overcome. As with all radiation measurement methods, the greater the required accuracy, the longer the measurement period. More intense sources can be used to reduce the measurement period, but this comes at the expense of increased safety precautions [8]. Despite the ability of the gamma ray technology to measure complete range of component fraction in a multiphase flow, the salinity of the mixture can cause error in the measurement [1, 9]. This is because of the high attenuation coefficient of salt compared to water. Thus, changes in salinity of the water phase will significantly affect the phase fraction measurement.

Whenever the fluid properties changes, there is need for recalibration of the

sensor. This situation is very important for a single energy gamma attenuation system. Changes in the oil density or water density will require a new attenuation coefficient before the system can be used accurately. An example of a commercially three phase system uses this technology is the Framo Engineering product. The accuracy of this system for (oil, gas and water mixture) flow was within ± 5% over the full range fraction [1, 7].

1.1.2 Electrical Impedance Measurement Principle

The basic principle for component fraction measurement using the impedance method is to measure the electrical impedance across two electrodes, between which an oil, water, and gas mixture is flowing. The resistance and capacitance depends on the permittivity and conductivity of the oil, water and gas components, the void fraction and water fraction, the flow regime and the excitation frequency of the detection electronics. As with γ-ray attenuation methods, two independent measurements are required to determine the oil, water and gas fractions [10, 11, 12, 13]. Impedance based methods suffer from two important limitations. They cannot be used over the full component fraction range and are flow regime dependent.

Electric Impedance is an important parameter used to characterize electric and electronic circuits, components, and the materials used to make them. The measurement of capacitance can be accomplished by measuring impedance. A capacitor is an electrical device which can be used to store electrical energy in the form of an electric field between a pair of conductors separated by an insulating dielectric material. A typical capacitor probe uses a cell composed of two plates or an open circuited center rod with a circular pipe. The mixture of oil, gas and water flows through the space separating the inner and outer electrodes. The capacitance of the capacitor is directly proportional to the dielectric constant of the dielectric material and is given by equation 1.1.

$$C = \frac{\varepsilon_0 \varepsilon A}{d} \tag{1.1}$$

where ε_0 is the dielectric constant (dielectric permittivity in vacuum), ε is the dielectric constant of the dielectric material (multiphase fluid), A is the area of the capacitor probe, and d is the distance between the capacitor plates. From the capacitance equation above, either ε, A or d can be variable in order to obtain varying degree of capacitance. The dielectric constant of water is in the range of 68-80, oil is 2.5, and air is 1 [1]. Considering the

wide variation between these dielectric constants, varying capacitance is observed when a mixture of oil, water and gas is used as the dielectric material.

The measurement of the impedance *Ze* of the mixture of multiphase flow across the two electrodes shown in figure 1.2 would give the measured resistance *Re* and capacitance *Ce* as:

$$R_e = \frac{1+\omega^2 R^2{}_m (C_m + C_p)^2}{\omega^2 R_m C_p{}^2} \tag{1.2}$$

$$C_e = \left[\frac{1+\omega^2 R_m{}^2 C_m (C_m + C_p)}{1+\omega^2 R_m{}^2 (C_m + C_p)^2}\right] C_p \tag{1.3}$$

where *Rm* and *Cm* are the resistance and capacitance of multiphase flow (oil, gas and water) in the pipeline, and *Cp* is the capacitance created between the metal pipeline and the capacitor plates.

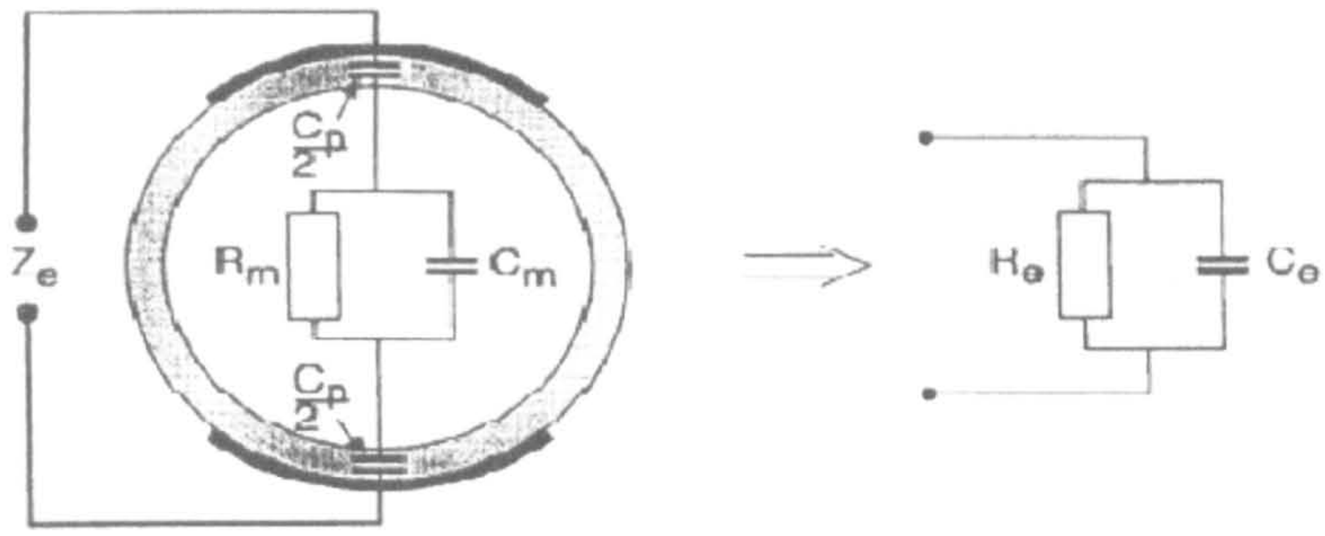

Figure 1.1: Component fraction measurement using impedance method [1]

The measured resistance Re and capacitance C_e are not only a function of R_m, C_m, the circuit excitation frequency, ω, but also the geometry and the material of the sensor. The mixture resistance R_m, and capacitance C_m, depends on certain factors which include: the oil, water and gas permittivity and conductivity, the void fraction and water fraction and the flow regime prevalent in the system [1]. The application of this method is limited for two reasons:

- It cannot be used for full water fraction range
- It is flow regime dependent

For a water fraction above 60%, the two electrodes (plates) becomes short circuited, thus the water fraction remains constant even when the actual water fraction increases [1]. Fluenta 1900V is a commercially example of

available three phase system which is based on a single energy γ-ray attenuation method combined with electrical impedance method to measure three phase (oil, gas and water) fractions. Gas flow rate has been measured with an accuracy of ± 10% of actual flow rate over gas fraction ranges of 30 to 60%, and with accuracy of about ± 15% over the range 60 to 80%. [1, 7].

1.1.3 Microwave Attenuation and Phases Shift Principles

In principle, microwave attenuation and phase shift measurement are based on the measurement of the dielectric properties of the flowing mixture at microwave frequencies. This can be achieved by measuring the amplitude and phase change of a microwave signal after it has passed through the flow [14], or by using a resonant cavity technique [15]. A limitation of resonant cavity methods used here, not including the target sensors of this thesis, is that they cannot be used with water continuous flow, as the cavity will not resonate if the conductivity of the mixture is too high. Although microwave methods require more complex excitation and detection circuitry than impedance methods, they have been used successfully in a number of three-phase flow meters [16]. Microwave sensors are described in sections (2.8-2.9).

1.1.4 Pulsed Neutron Activation (PNA) Principle

The pulsed neutron activation (PNA) technique uses a high-energy source of neutrons to irradiate the flowing mixture. This causes gamma radiation to be emitted. The spectra produced can be used to determine the chemical composition and phase fractions of the mixture. Electrical or chemical generators can be used as a source but both are complex and not yet suited to applications in the field.

The technology associated with PNA is expensive, but this technique is not sensitive to the flow regime and can be used to measure two phase component fractions [1].

1.1.5 Nuclear Magnetic Resonance Principle

Nuclear magnetic resonance (NMR) is a well established technique for analyzing multiphase fluid components in many areas of the process industry. In this technique a magnetic field is applied to the flow to align spin states of the nuclei in the mixture. The realignment in spin states that takes place once the mixture has left the magnetic field is related to the chemical composition, and hence the phase fractions. Like PNA, NMR uses complex and high cost technology [1, 16, 18].

1.2 Thesis Aims and Objectives

The scope of this thesis is microwave sensors for real time measurement of multiphase flow fractions in a pipeline. In particular the sensors are based on a cylindrical cavity resonator fitted to a PVC pipeline and they use the resonant frequencies related to changes in permittivity to measure the three phase quantities.

Depending upon the application, the desired characteristics of a microwave sensor for measuring multiphase flow can be varied. They are related to:

- Flow characteristics
- Measurement characteristics
- Frequency response characteristics affecting the measurement
- Mechanical characteristics and manufacturing cost

The aim and objective of the work described in this thesis were to develop non intrusive, accurate, reliable, compact structure and low manufacture cost electromagnetic wave sensors operating at microwave frequency for online measuring and monitoring the oil, gas and water fractions flowing in a pipeline, expressed in % volume.

The emphasis is on the design of the sensors to achieve the desired characteristics. In order to achieve these goals, combinations of two quantitative methods were adopted; they are the quantitative simulation method and the quantitative experimental method [19, 20]. The strategy used for analyzing the results was the descriptive statistic analysis. The descriptive statistic analysis is used to describe the basic features of the quantitative data in a study, as it provides simple summaries about the predicted results and the measured results, together with simple tables and graphics analysis. Generally descriptive statistic is presented along with more formal analyses to give an overall sense of the data being analysed [21, 22].

1.4 Thesis Construction

The remainder of this thesis is structured as follows:

Chapter 2 considers the basic area which forms the basis of this research, the fundamentals of microwave and microwave sensors. In particular, this chapter provides the background of electromagnetic waves theory, microwave sensors, three phase flow measurement principle and flow

regimes, necessary for this research investigation to be understood and successful.

Chapter 3 gives an account of the accuracy of the simulations performed with the High Frequency Structure Simulation (HFSS) software. Two accurate and non intrusive microwave sensors were designed using HFSS simulation. The EMW2 and EMW3 sensors were constructed, and the experiment works were carried out.

Chapter 4 shows the HFSS simulation, and the design and construction of the cavity resonator and pipeline of the electromagnetic (EMW2) sensor developed in this thesis for measuring and monitoring two phase components in a pipeline. The system prototype was introduced, and the experiments were carried out. Finally, the experiment results are presented and compared to the HFSS simulation results.

Chapter 5 presents the electromagnetic (EMW3) sensor developed for multiphase flow measurements. It shows the state of art in the HFSS simulation, and the design and construction of the sensor cavity resonator

and pipeline. The system set up was constructed and presented. Two phase (oil and gas, and water and gas), and three phase (oil, gas and water mixtures) experiments were carried out. Finally, the experiment results are compared to the HFSS simulation results.

Chapter 6 provides an in depth comparison and discussion of the HFSS simulation results and the experimental results for both sensors developed in chapter 4 and 5 of this thesis. The predicted simulation results and the experimental results were analysed using descriptive statistic analysis. It describes the main features of a collection of data in quantitative terms. The analyzed results show the state of art in the accuracy and reliability for both sensors. In particular, the HFSS simulation and experiment results for each sensor are compared and analyzed separately. This was followed by a comparison of the experimental results for both developed sensors. Finally, the multiphase flow experiments provided by the sensor developed in chapter 5 are analyzed and discussed.

Chapter 7 describes the designs and development of the online electromagnetic sensor (the Online EM Wave Monitoring and Control

System), using Lab View software package. A software application was developed to explore the potential in using the (EMW3) sensor to provide online three phase monitoring and measurements. The real time results are presented in term of screen shots captured during online experiments for both two phases (oil and gas) and three phases (oil, gas, and water).

Chapter 8 looks back to achievements of the research and concludes with a discussion for future work.

CHAPTER 2

Microwave Fundamentals

2.1 Introduction

Electromagnetic waves categories include x-rays, microwaves, visible light, ultraviolet light, infrared light, radio waves, and gamma rays. The difference lies in their frequency and wavelength [23].

Electromagnetic waves are classified according the frequency range and wavelength as show in Figure 2.1.

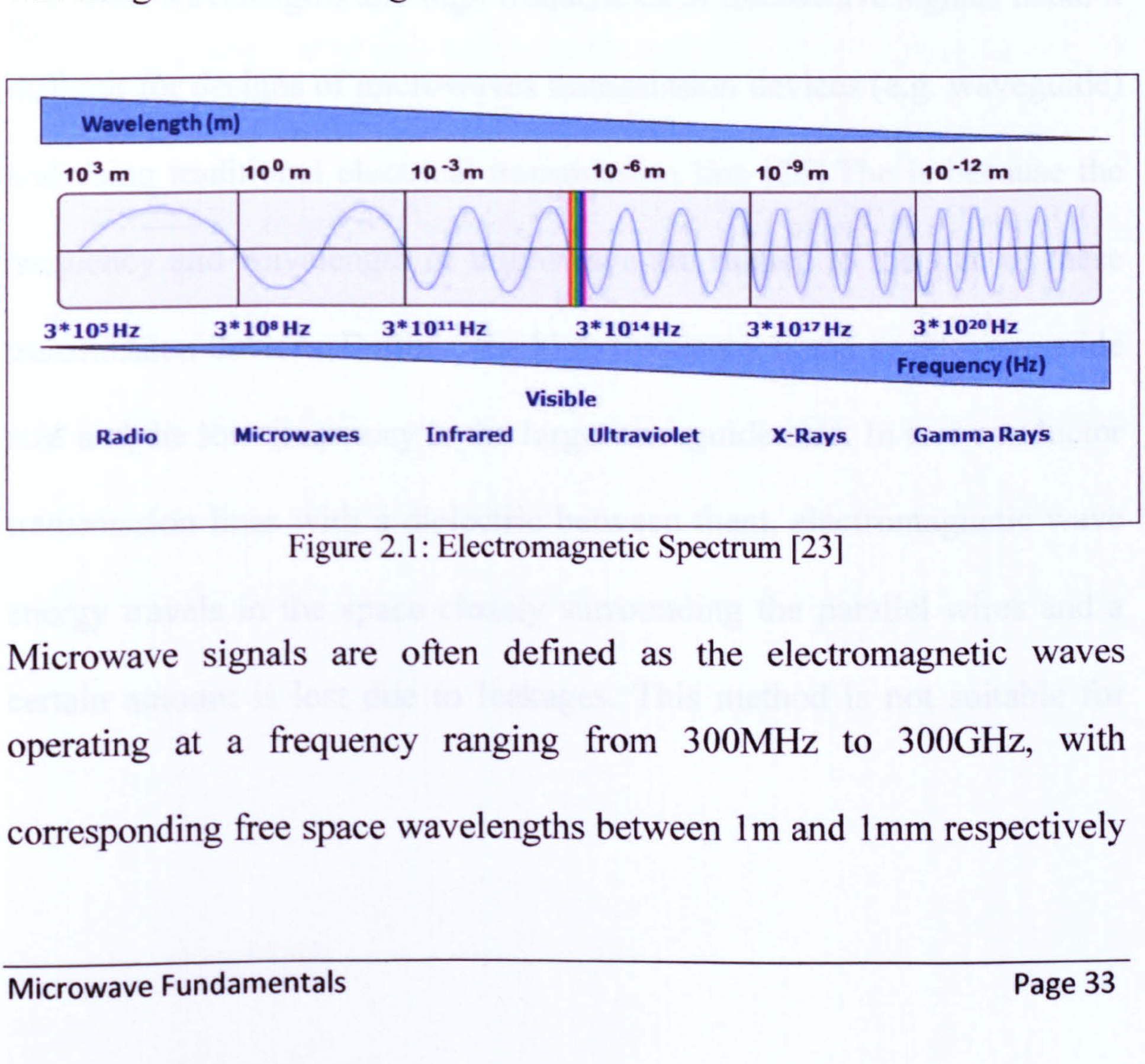

Figure 2.1: Electromagnetic Spectrum [23]

Microwave signals are often defined as the electromagnetic waves operating at a frequency ranging from 300MHz to 300GHz, with corresponding free space wavelengths between 1m and 1mm respectively

[24, 25]. Waves with wavelengths in the order of millimetres are called millimetre waves. The electromagnetic waves frequencies and wavelengths are related to each other through the speed of propagation by Equation (2.1)

$$\lambda f = c \tag{2.1}$$

where λ is the wavelength (m), f is the propagation frequency (Hz), and c is the speed of propagation (m/s). In vacuum all electromagnetic waves propagate with the same speed, the speed of light, $c = 2.998 \times 10^8$ (m/s).

The short wavelengths and high frequencies of microwave signals make it difficult for designs of microwaves transmission devices (e.g. waveguide) and using traditional electrical transmission line [26].The is because the frequency and wavelength of microwave are related to the size of these transmission devices. Further, the high frequency is the small waveguide size and the low frequency is the large waveguide size. In two conductor transmission lines with a dielectric between them, electromagnetic wave energy travels in the space closely surrounding the parallel wires and a certain amount is lost due to leakages. This method is not suitable for

transmitting microwaves, as the loss increases with the frequency (see figure 2.5).

Generally, the physical dimensions of microwave waveguides are in the order of the wavelengths (see section 2.6). However, at higher frequency in which the wavelength is a great deal shorter than the physical dimension of the device, optical design techniques become a sensible strategy for these quasioptical systems. On the other hand, as the short wavelengths and high frequencies of microwaves prevent the use of transmission line, and complicate the design of microwave waveguides, the same issues provide unique opportunities for the application of microwave systems [27]. This is because of the wide bandwidth of frequencies and sight line transmission directivity which are considered as characteristics of microwave signals.

Microwaves are widely used in communication systems such as in mobile phones, wireless networks, military radar, and weather prediction. In addition to the communication systems, microwaves are used in medical diagnostics, global positioning systems, and industry measurement technologies.

2.2 Electromagnetic Wave Equations

In the mid 19th century, the time varying electric field and magnetic field phenomenon was described completely by James Clerk Maxwell [28]. Maxwell noticed the symmetry and other properties of electromagnetic fields, and summarized electromagnetism using four equations, now known as Maxwell's equations. Maxwell found the equation that describes electromagnetism, and noticed that the speed of these waves WAS the same as the speed of light; Maxwell deduced that light was an electromagnetic wave and predicted the existence of other electromagnetic waves. In summary the four equations describe the time varying electromagnetic fields phenomena are given by Equations (2.2-2.5)

$$\nabla \times \mathbf{E} = -(\partial \mathbf{B}/\partial t) \tag{2.2}$$

$$\nabla \times \mathbf{H} = \mathbf{J} + (\partial \mathbf{D}/\partial t) \tag{2.3}$$

$$\nabla \cdot \mathbf{D} = \rho \tag{2.4}$$

$$\nabla \cdot \mathbf{B} = 0 \tag{2.5}$$

where the first equation is Faraday's law of induction; the second is Ampere's law as amended by Maxwell to include the displacement current $\partial \mathbf{D}/\partial t$; the third and fourth are Gauss' laws for the electric and magnetic fields respectively.

The displacement current term $\partial \mathbf{D}/\partial t$ in Ampere's law is essential in predicting the existence of propagating electromagnetic waves.

The quantities **E** and **H** are the electric and magnetic field intensities and are measured in units of [volt/m] and [ampere/m], respectively. The quantities **D** and **B** are the electric and magnetic flux densities and are in units of [coulomb/m^2] and [weber/m^2], or [tesla]. **B** is also called the magnetic induction. The quantities ρ and **J** are the volume charge density and electric current density (charge flux) of any external charges (that is, not including any induced polarization charges and currents.) They are measured in units of [coulomb/m^3] and [ampere/m^2]. The right-hand side of the fourth equation is zero because there are no magnetic monopole charges.

The charge and current densities ρ, **J** may be thought of as the sources of the electromagnetic fields. For wave propagation problems, these

densities are localized in space. For example, they are restricted to flow on an antenna. The generated electric and magnetic fields are radiated away from these sources and can propagate to large distances to receiving antennas. Away from these sources, that is, in source free regions of space, Maxwell's equations take the simpler form

$$\nabla \times \mathbf{E} = - (\partial \mathbf{B}/\partial t) \quad (2.6)$$

$$\nabla \times \mathbf{H} = \partial \mathbf{D}/\partial t) \quad (2.7)$$

$$\nabla . \mathbf{D} = 0 \quad (2.8)$$

$$\nabla . \mathbf{B} = 0 \quad (2.9)$$

2.3 Electromagnetic Waves Propagation

The qualitative mechanism by which Maxwell equations give rise to propagating electromagnetic fields is shown in Figure 2.2.

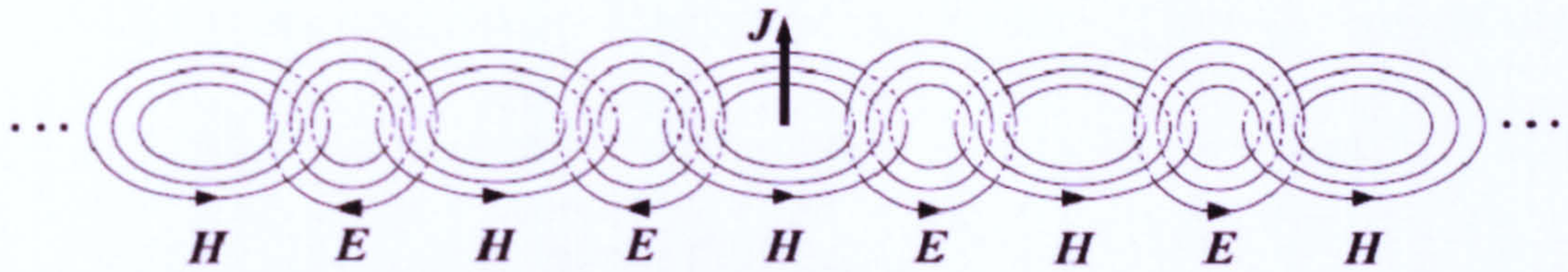

Figure 2.2: The EM Wave propagation in space where the current J generates magnetic field, which in turn generates electric field and son on [28].

The current **J** on a linear antenna generates a circulating and time varying magnetic field **H**, which according to Faraday's law generates a circulating electric field **E**, which through Ampere's law generates a magnetic field, and so on. The cross linked electric and magnetic fields propagate away from the current source.

Figure 2.3 shows the electromagnetic waves in free space. The electric fields and magnetic fields are in phase, mutually perpendicular, and also perpendicular to the direction in which the wave travels. The electric and magnetic fields oscillate together between maximum positive and maximum negative values along the direction of propagation.

In free space, electromagnetic waves travel at the speed of light c, which relates the wavelength to the propagation frequency of the wave, as given by equation 2.1.

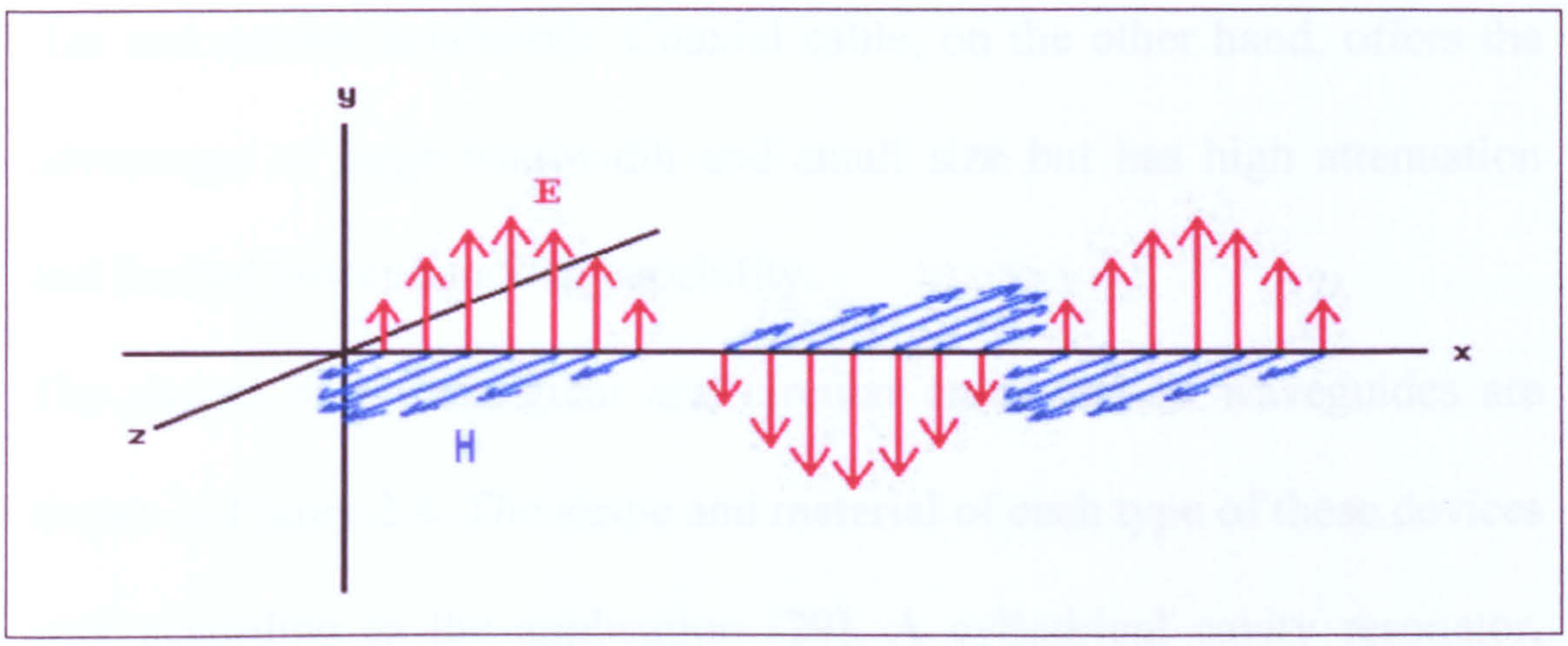

Figure 2.3: Electromagnetic waves propagation in free space. The wave propagates in the x direction, and E and H are transverse [28].

Free space electromagnetic waves are widely used in communication systems and radar. In order to be utilised, electromagnetic waves need to be transmitted and received from one location to another. In microwave sensors designed for industrial applications, microwave signals have to be connected or coupled from the source to the system.

Electromagnetic energy must be transmitted in an efficient manner from the source to the sensors with minimal attenuation. The two commonly used microwave devices are: waveguide (see sections 2.6 and 2.7) and coaxial transmission line. At microwave frequencies, each device offers advantages and disadvantages. On the one hand, waveguides have the advantages of high power handling capability and low loss, but have large

size and narrow bandwidth. Coaxial cable, on the other hand, offers the advantages of large bandwidth and small size but has high attenuation and limited power handling capability.

The shapes of a rectangular and circular cross section waveguides are shown in Figure 2.4. The shape and material of each type of these devices vary according to the application [29]. A cylindrical cavity resonator, which can be made using a cylindrical waveguide with shorted ends, could be fitted to a pipeline, which contains a flow of oil, gas, and water components, as a microwave sensor for measuring the flowing material components.

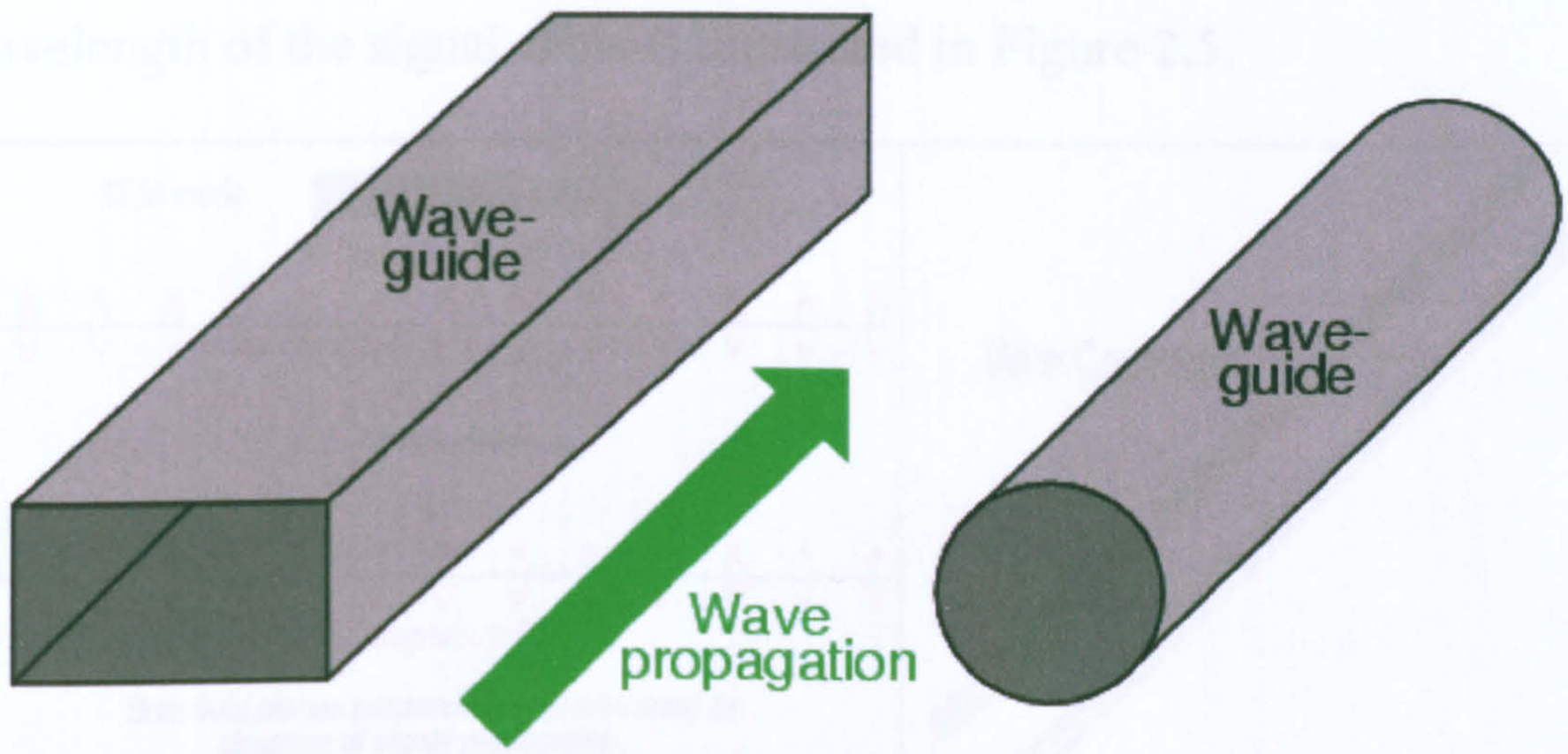

Figure 2.4: Rectangular waveguide (a) , Cylindrical waveguide (b)

2.4. Transmission Lines

All forms of electromagnetic waves consist of electric and magnetic fields propagating in the same direction, but perpendicular to each other, except wave propagations in waveguides or cavity resonators. Along the length of a normal transmission line, both electric and magnetic fields are perpendicular (transverse) to the direction of wave travel. This is known as the principal mode, or (Transverse Electric and Magnetic) TEM mode. This mode of wave propagation can exist where there are two conductors, and it is the dominant mode of wave propagation where the cross sectional dimensions of the transmission lines are small compared to the wavelength of the signal. This is illustrated in Figure 2.5.

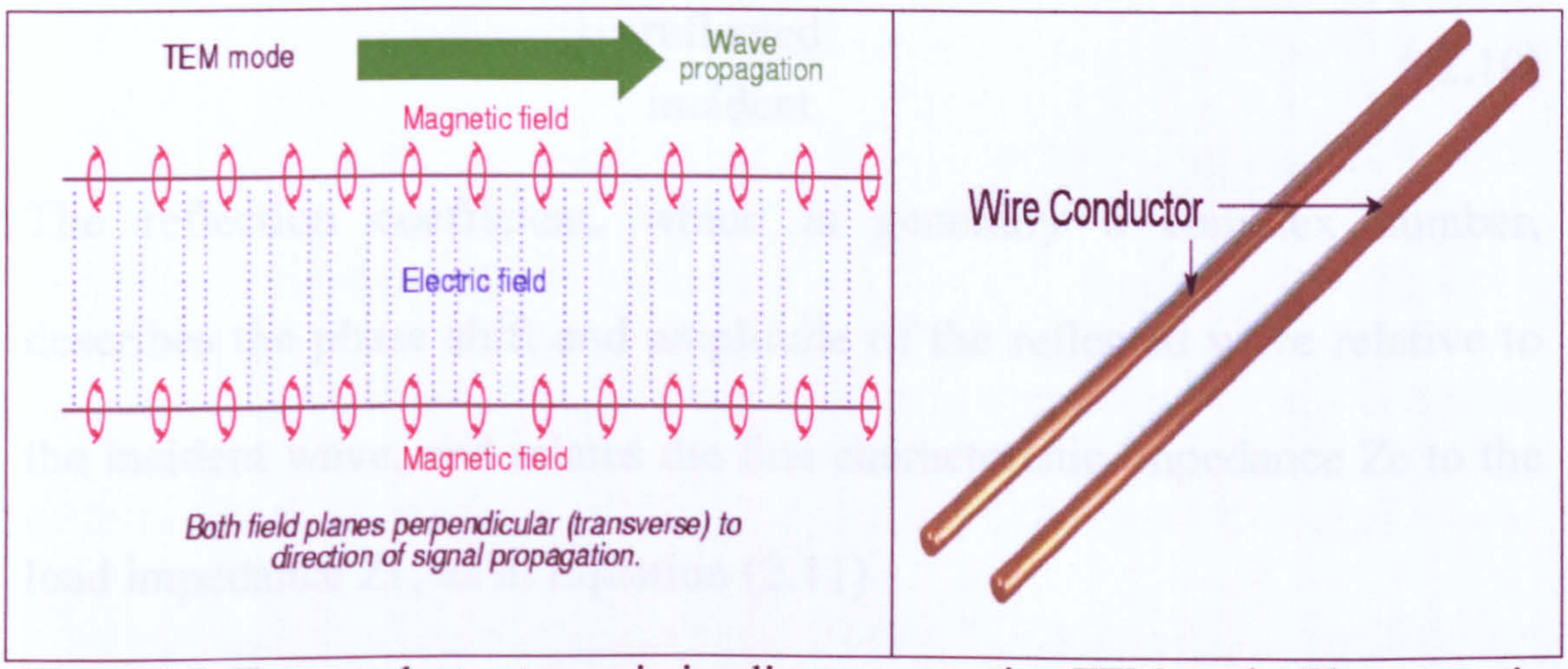

Figure 2.5: Two conductor transmission lines propagation TEM mode. The magnetic field is in red colour and electric field is the blue colour.

At microwave frequency, the two conductor transmission lines of any considerable length operating in standard TEM mode become impractical. In other words, transmitting electromagnetic energy in transmission lines with small cross sectional dimensions with respect to the wavelength, will cause a large power lose due to conductor "skin depth" and dielectric loss between the conductors [30, 26].

The other factor to be taken into account, in addition to the line characteristic impedance (Z_0), is the reflection coefficient, which occurs at the end of a finite line where the load is not matched to the line impedance. The reflection coefficient (Γ) is defined as the ratio of the reflected wave to the incident wave, as shown in equation (2.10)

$$\Gamma = \frac{\text{reflected}}{\text{incident}} \tag{2.10}$$

The reflection coefficient, which is generally a complex number, describes the phase shift and amplitude of the reflected wave relative to the incident wave, and relates the line characteristic impedance Z_0 to the load impedance Z_L, as in Equation (2.11)

$$\Gamma = \frac{Z_L - Z_0}{Z_L + Z_0} \tag{2.11}$$

From equation 2.11 and assuming a zero value for the imaginary part, a reflection coefficient of +1 would be a perfect open circuit, which means the load impedance, Z_L, equals infinity in this case, and the transmitted signal is perfectly reflected and both signals are in phase. A value of −1 of the reflection coefficient would represent a perfect short circuit, and the incident wave is completely reflected but now is 180 degrees out of phase compared to the incident wave. This means that the load impedance equals to zero. A 0 value of reflection coefficient is a perfect match. This means the line characteristic impedance equals to the load impedance, $Z_0 = Z_L$, and the signal is completely transmitted with no reflection, which is the goal in most systems.

Another important factor to be taken into account is the standing wave ratio (SWR), which is in turn a representation of how well matched a line is as the magnitude of the reflection coefficient changes between unity and zero, in term of the line reflected and incident either voltage or power. SWR is defined as the ratio of magnitudes of maximum to minimum of standing wave. As SWR can be a voltage, it is called voltage standing wave ratio VSWR. It is given by

$$VSWR = \frac{|V_{max}|}{|V_{min}|} = \frac{|V_i + V_r|}{|Vi - V_r|} \tag{2.12}$$

$$VSWR = \frac{1+|\Gamma|}{1-|\Gamma|} \tag{2.13}$$

where Γ is the reflection coefficient. Using equation 2.13, the relationship between the voltage standing wave ratio, and the reflection coefficient can be calculated. For example, for a reflection coefficient value of -1 or $+1$, a corresponding value of VSWR is infinity, and if $\Gamma = 0$, the VSWR value will be 1.

Although there are drawbacks to using two conductor transmission lines at microwave frequency, it is more than adequate for low frequency applications. For instance, this type of transmission lines can be found on TV aerial cables. Unlike two conductor transmission lines, coaxial line has advantages over these types of transmission lines, as it has shielding to prevent leakage of radiation, so the entire field is kept within the line as shown in Figure 2.6.

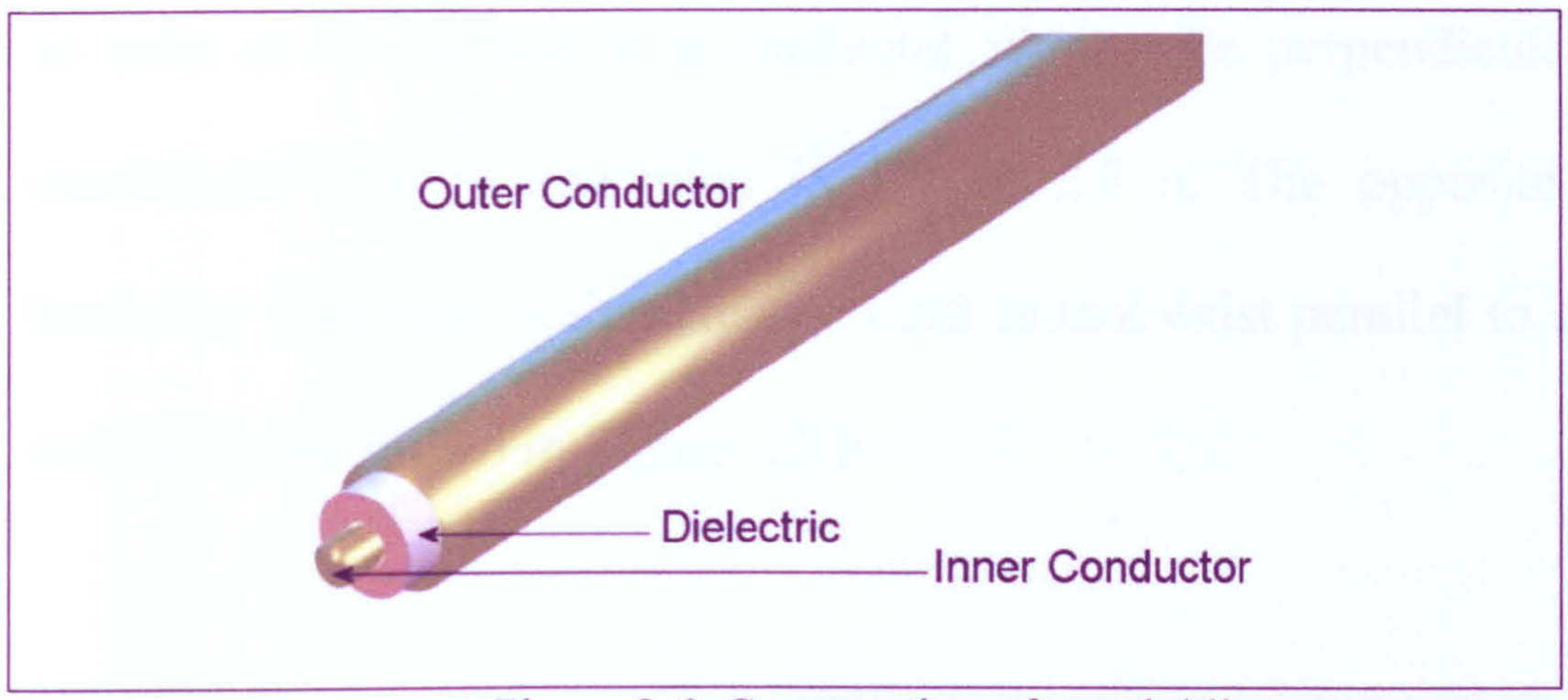

Figure 2.6: Construction of coaxial line.

Fortunately, there are other modes existing at high frequencies of propagation. Waveguide and cavity resonators, on the other hand, are the two most commonly practical methods of propagating TE and TM waves with each having their own advantages and disadvantages.

2.5. Boundary Condition in Waveguides and Cavity Resonators

As discussed earlier, the propagation travel of electromagnetic waves in a waveguide or cavity resonators is not the same as the propagation of electromagnetic waves in free space. The difference is that the electromagnetic wave travelling in a waveguide is confined to the physical limits of the guide. There are two boundary conditions, which must be satisfied for energy to travel through a waveguide or cavity resonator [31, 26]. The first boundary condition is that for an electric field

to exist at the surface of a conductor it must be perpendicular to the conductor. This is illustrated in Figure 2.7 a. The opposite of this boundary condition is that electric field cannot exist parallel to a perfect conductor, as shown in Figure 2.7 b.

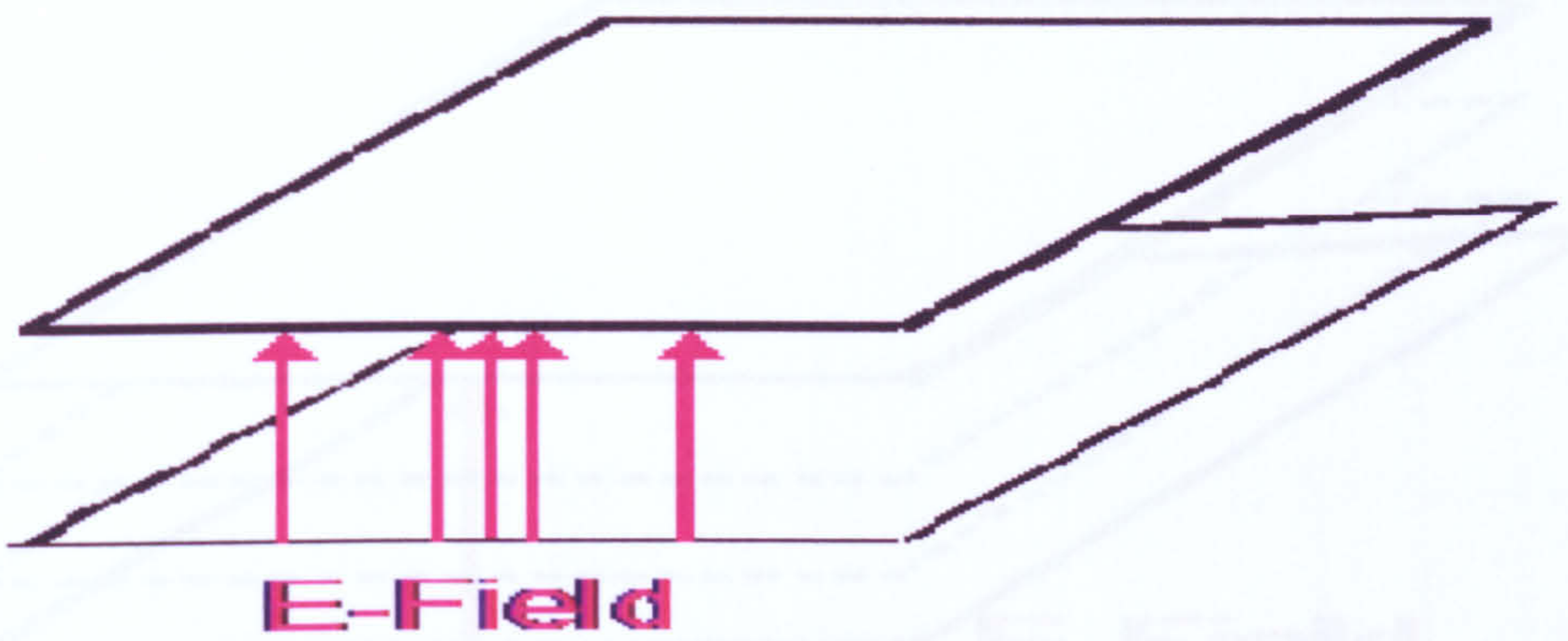

Figure 2.7 a: E- field boundary condition. It meets boundary conditions.

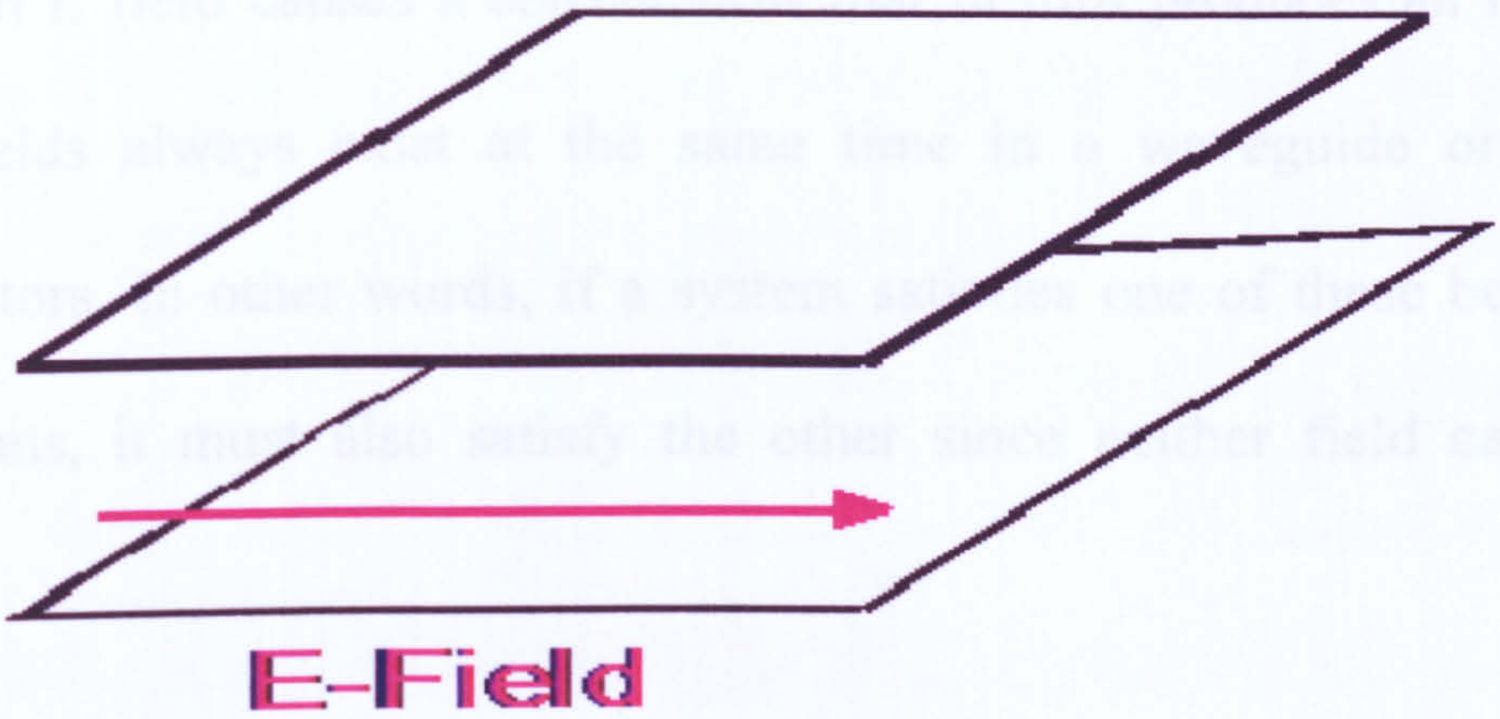

Figure 2.7 b: E field boundary condition. It does not meet boundary conditions.

The second boundary condition is that for a varying magnetic field to exist, it must form closed loops in parallel with the conductors and be perpendicular to the electric field, as shown in Figure 2.8.

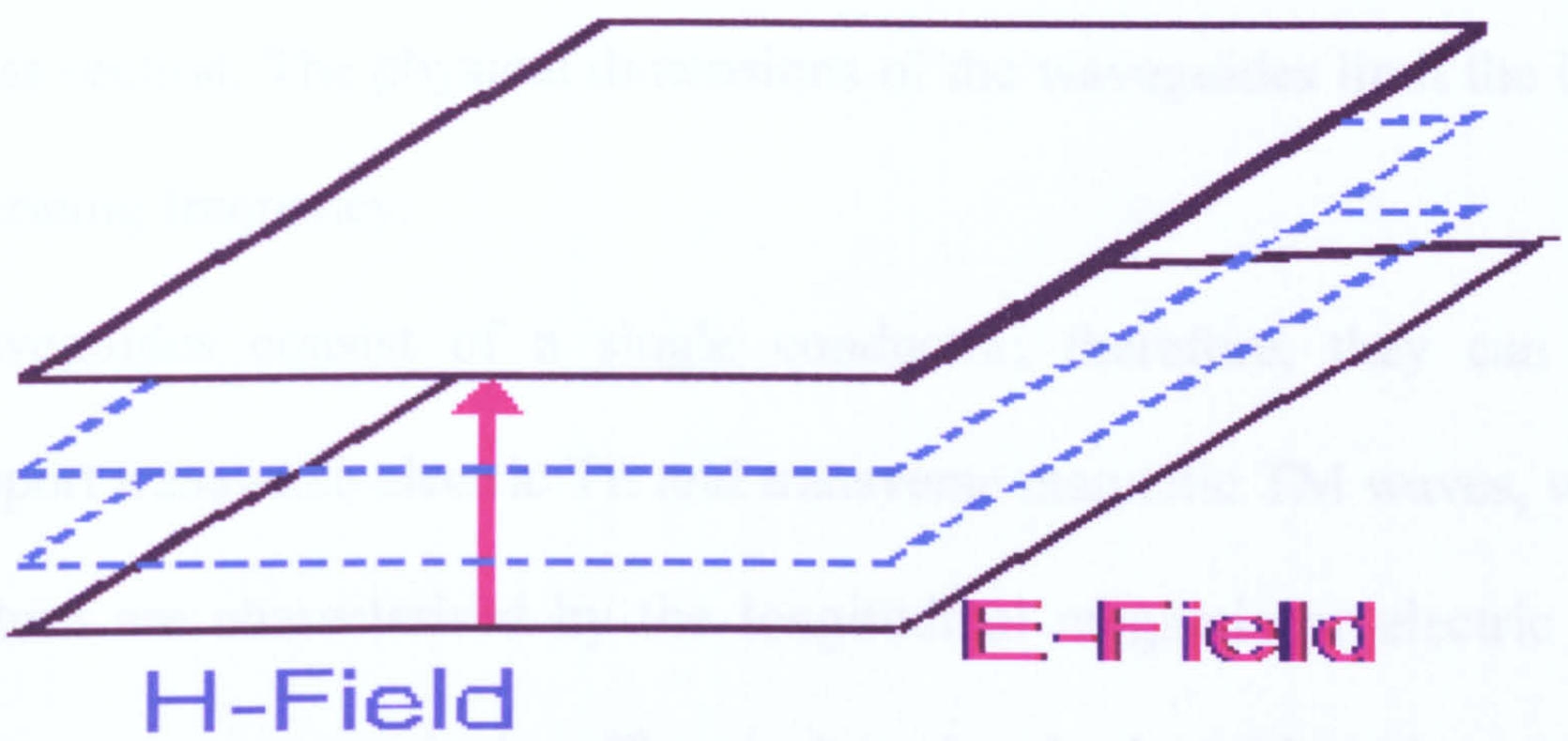

Figure 2.8. H- field meets the boundary conditions.

Since an E field causes a current flow that in turn produces an H field, both fields always exist at the same time in a waveguide or cavity resonantors. In other words, if a system satisfies one of these boundary conditions, it must also satisfy the other since neither field can exist alone.

2.6. Microwave Waveguides

Waveguides or resonance cavities can be described as hollow conducting pipes developed to guide electromagnetic energy at microwave frequencies [32, 29]. Waveguides are made of copper, brass, or aluminium, and can be constructed in either rectangular or cylindrical cross section. The physical dimensions of the waveguides limit the lower operating frequency.

Waveguides consist of a single conductor; therefore, they can only support transverse electric TE and transverse magnetic TM waves, which in turn are characterised by the longitudinal magnetic or electric field components respectively. The major drawback with this type of transmission method is the relation between the physical size of the waveguide and the wavelength of the electromagnetic wave [33]. The width of a waveguide must be approximately a half wavelength at the frequency of the wave to be transported. For example, a waveguide for use at 1 MHz would be about 150 meters wide. This makes the use of waveguides at low frequencies impractical. Cylindrical and rectangular waveguides with internal dimensions are illustrated in Figures 2.9 and 10 respectively.

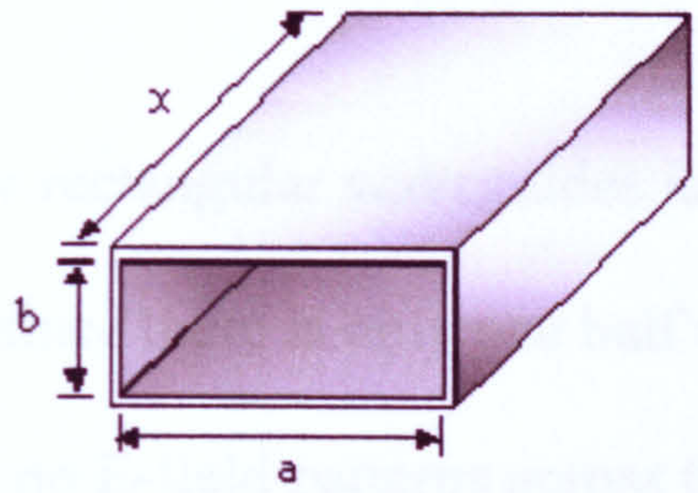

Figure 2.9: Rectangular waveguide with internal dimension a and b.

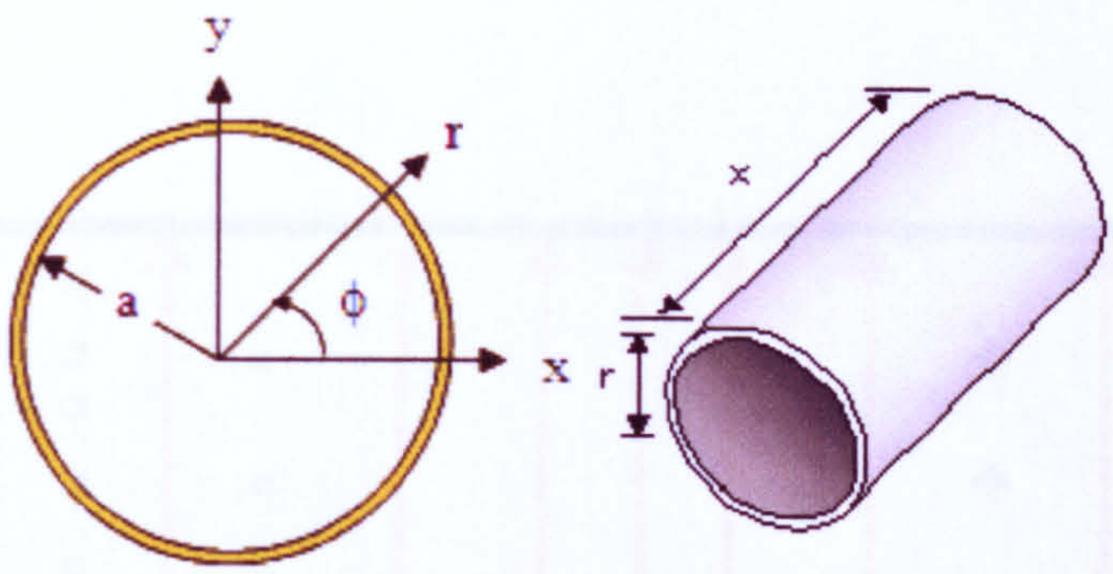

Figure 2.10: Cylindrical waveguide with inner radius, a.

The rectangular and cylindrical waveguides can propagate TE and TM waves but not TEM waves. This is because a unique voltage cannot be defined since there is only one conductor. There are various possible solutions for both TE and TM waves; therefore, subscripts are used to complete the description of the field pattern in the mode to be transmitted. For rectangular waveguide, the first subscript indicates the number of half wave patterns in the *a* dimension, and the second subscript indicates the number of half wave patterns in the *b* dimension.

The dominant mode for rectangular waveguides is shown in Figure 2.11.

The first subscript is 1 since there is only one half wave pattern across the *a* dimension. There are no E-field patterns across the, b dimension, so the second subscript is 0. The complete mode description of the dominant mode in rectangular waveguides is TE_{10}.

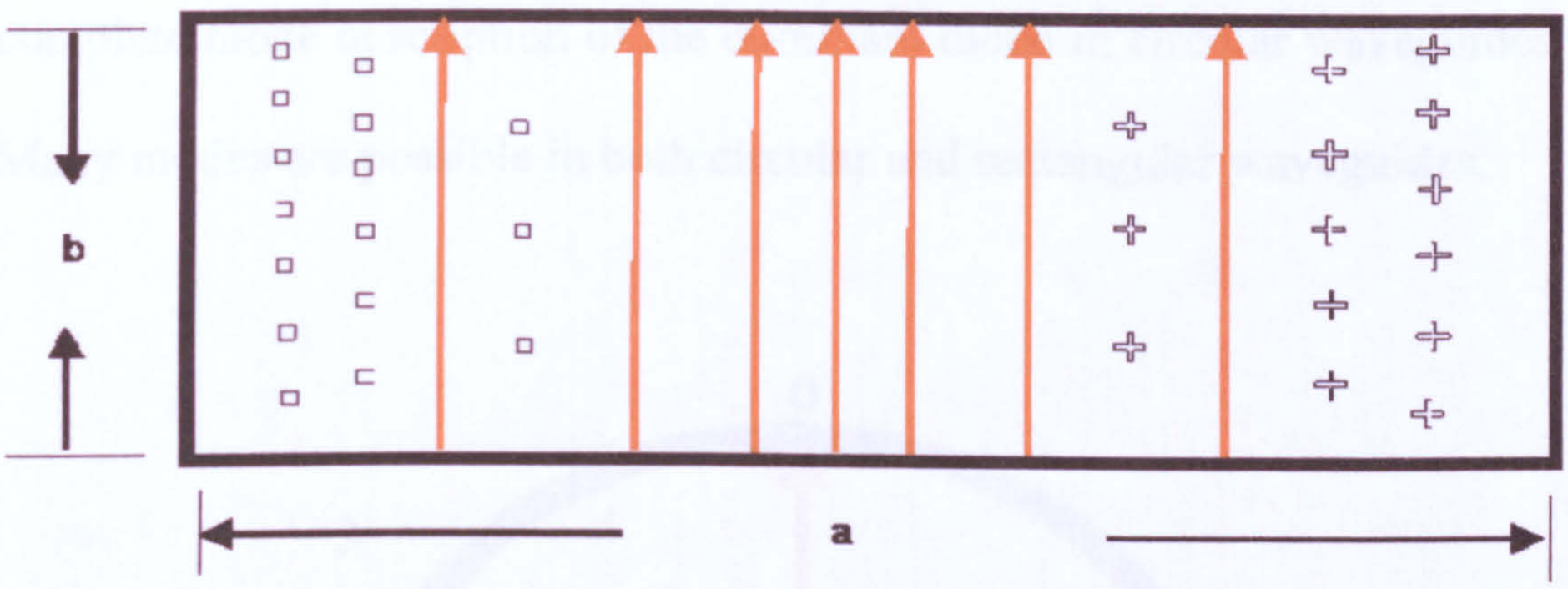

Figure 2.11: Dominate mode (TE_{10}) field configurations in rectangular waveguide.

In circular waveguides the subscripts have a different meaning. The first subscript indicates the number of full-wave patterns around the circumference of the waveguide. The second subscript indicates the number of half-wave patterns across the diameter. In the circular waveguide shown in Figure 2.12, the E field is perpendicular to the length of the waveguide with no E lines parallel to the direction of propagation.

Therefore, it must be classified as operating in the TE mode. If we follow the E line pattern in an anti counter clockwise direction starting at the top, the E lines go from zero, through maximum positive (tail of arrows), back to zero, through maximum negative (head of arrows), and then back to zero again. This is one full wave, so the first subscript is 1. Along the diameter, the E lines go from zero through maximum and back to zero, making a half wave variation. The second subscript is also 1. TE_{11} is the complete mode description of the dominant mode in circular waveguides. Many modes are possible in both circular and rectangular waveguides.

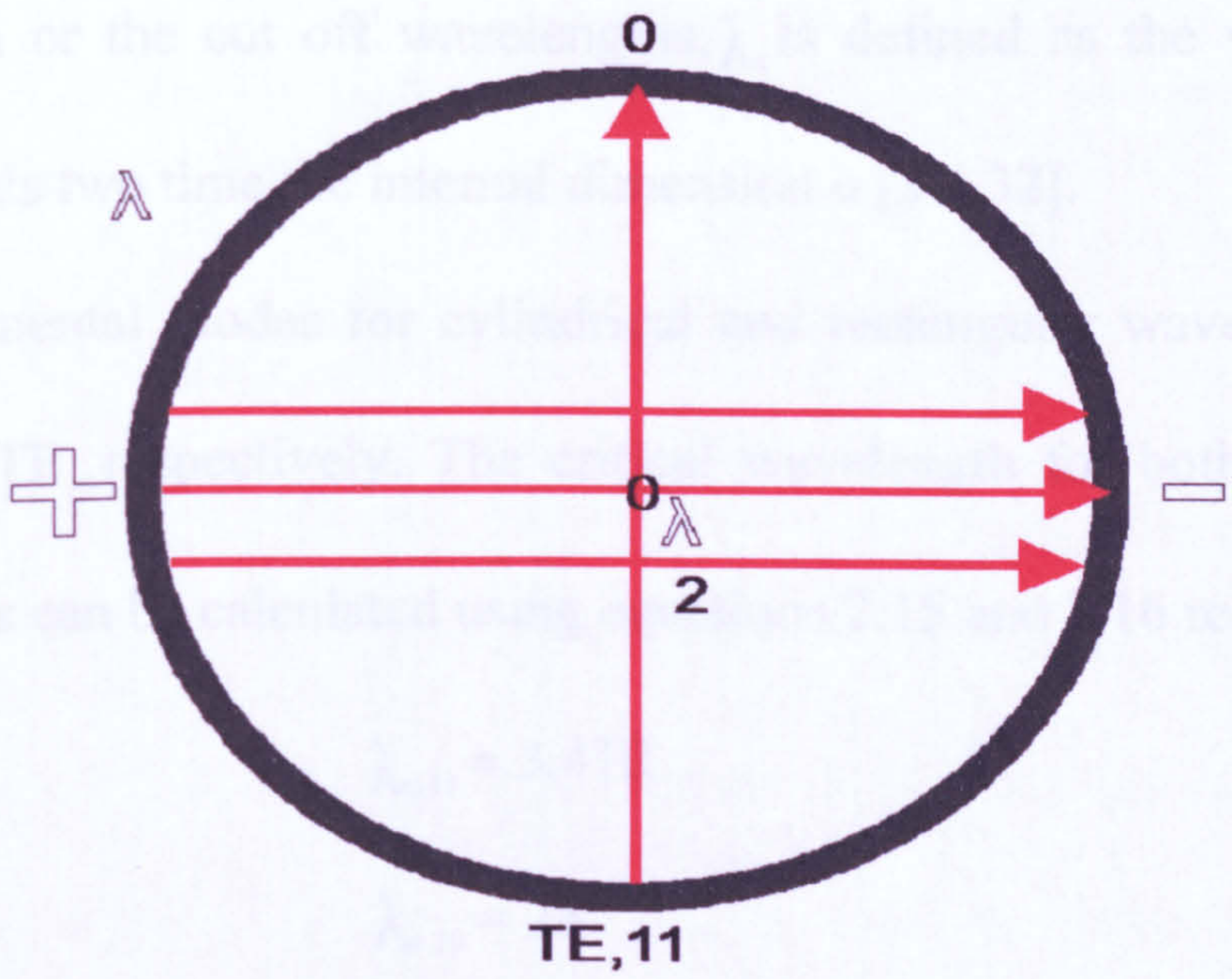

Figure 2.12: Dominate mode (TE_{11}) field configuration in circular waveguide.

The dimension for a waveguide to be operated at a given wavelength is chosen based on the desired mode of operation and the frequencies at which this mode will be operated. In waveguide standard design, set dimensions are based on the cut off frequency of the fundamental mode.

The cut off frequency of a waveguide is defined as the lowest frequency below which energy will not radiate in a waveguide. A lower frequency will attenuate rather than propagate.

Generally, the cut off frequency of a waveguide mode is defined as the lowest frequency below which the mode does not propagate and above which the mode dose [31]. In a rectangular waveguide, the critical wavelength or the cut off wavelengths, λ_c is defined as the wavelength which equals two time the internal dimension *a* [31, 32].

The fundamental modes for cylindrical and rectangular waveguides are TE_{11} and TE_{10} respectively. The critical wavelength for both TE_{11} and TE_{10} modes can be calculated using equations 2.15 and 2.16 respectively

$$\lambda_{c,11} = 3.41R \tag{2.15}$$

$$\lambda_{c,10} = 2a \tag{2.16}$$

where R is the radius of a circular waveguide cross section, and *a* is the longer internal dimension of rectangular waveguide. The cut off

frequency can be related to the cut of wavelength by Equation 2.1. The appropriate radius for TE_{11} in a cylindrical waveguide to be used at a given wavelength λ, can be chosen in terms of cut off frequency and cut off wavelength using Equation 2.17 (a and b) respectively.

$$\frac{c}{3.4R} < \frac{c}{\lambda} < \frac{c}{2.06R} \qquad (2.17a)$$

$$3.4R > \lambda > 2.06R \qquad (2.17b)$$

Where $\frac{c}{3.4R}$ is the cut off frequency of TE11, 2.06R and $\frac{c}{2.06R}$ are the critical wavelength and cut off frequency respectively for the nearest higher mode, which is TE_{21} mode.

The wavelength and velocity of electromagnetic wave in waveguides are not the same as its wavelength and velocity in free space [33]. The propagation of electromagnetic wave in a rectangular waveguide can be represented by two vertically polarized TEM waves propagating in a waveguide, as shown in Figure 2.13a. These waves (wave Ax and waves Bx) are launched between the waveguide walls from the left end and travel to the right by means of multiple reflections between the guide walls. The reflection angles ø, which are created between the guide walls

and each wave directions, are equal to each other and also to the incident angles.

Figure 2.13: Waves zigzag paths (a) and (b) wavefronts for TE Modes, in a waveguide.

The wavefronts for these waves, which are perpendicular to the wave directions and moving with the speed of light c toward each other, are indicated with small arrows in Figure 2.13b.

In free space, the wavelength of electromagnetic wave is defined by the relation $\lambda = \frac{c}{f}$, which was given by Equation (2.1). In waveguide, the wavelength in the guide λ_g or guide wavelength can be defined in a

similar relation (as the free space wavelength), but with a different velocity. This is called the phase velocity (v_p). In order to calculate the guide wavelength, the phase velocity should be understood and calculated. The phase velocity results from the complex zigzag path nature of the wavefronts within the waveguide, as shown in Figure 2.13. The wavefront moves with the speed of light at an angle to the waveguide wall, so a constant phase point of the TE wave must be moving at a velocity that is greater than that of the component waves. This is illustrated in Figure 2.14.

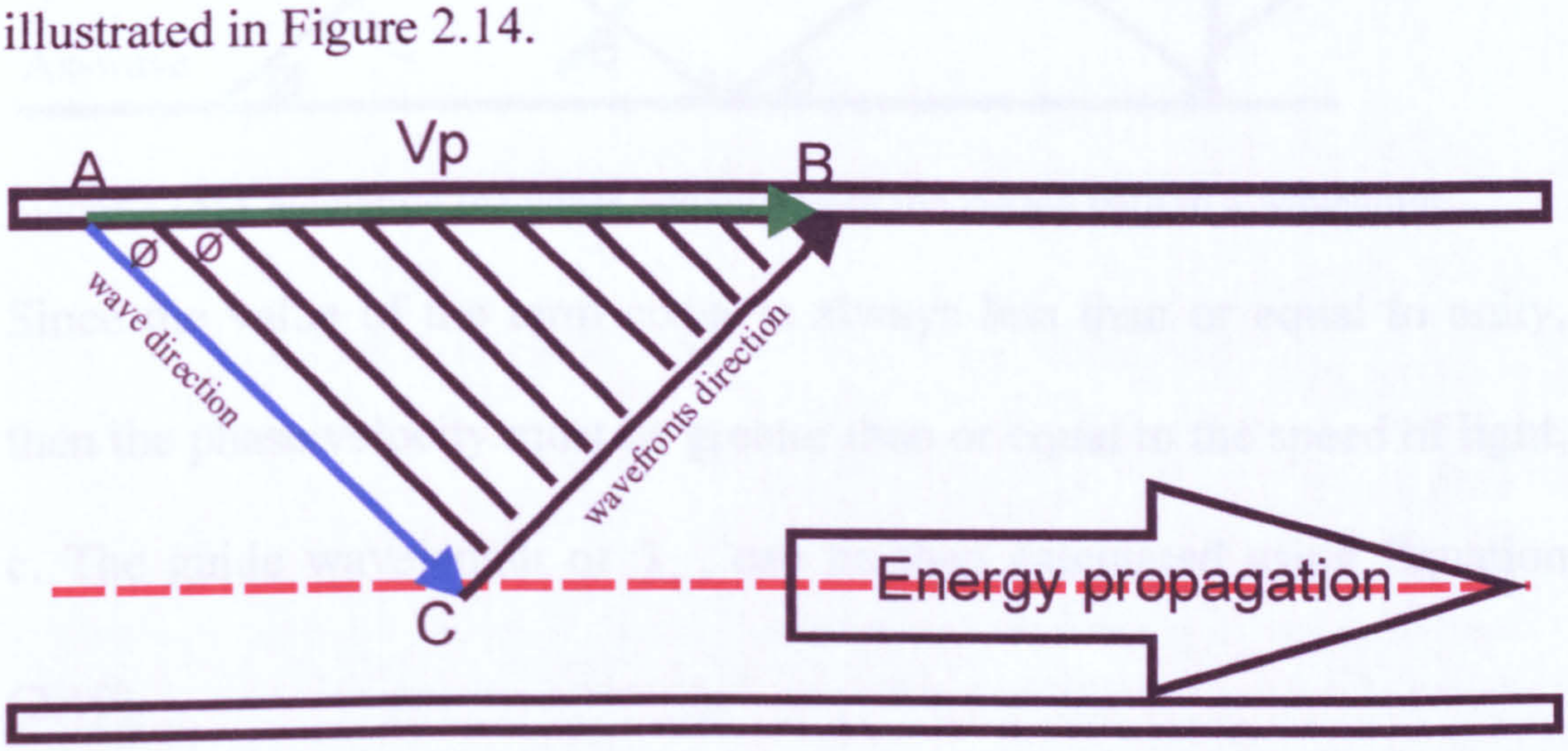

Figure 2.14. Illustration of a constant phase (TE wave) velocity that is greater than the speed of light.

The direction of the wavefronts is indicated by the line CB, and the direction of the component wave is the magnetic line AC. It is apparent from, Figure 2.14, that by the time the component wave moves from

point A to point C at the speed of light, a constant phase point of the TE wave moves along the guide from point A to point B with the speed higher than that of the component wave. From Figure 2.15, and the triangle (ABC), the phase velocity is given by

$$v_p = \frac{C}{\cos\Phi} \tag{2.18}$$

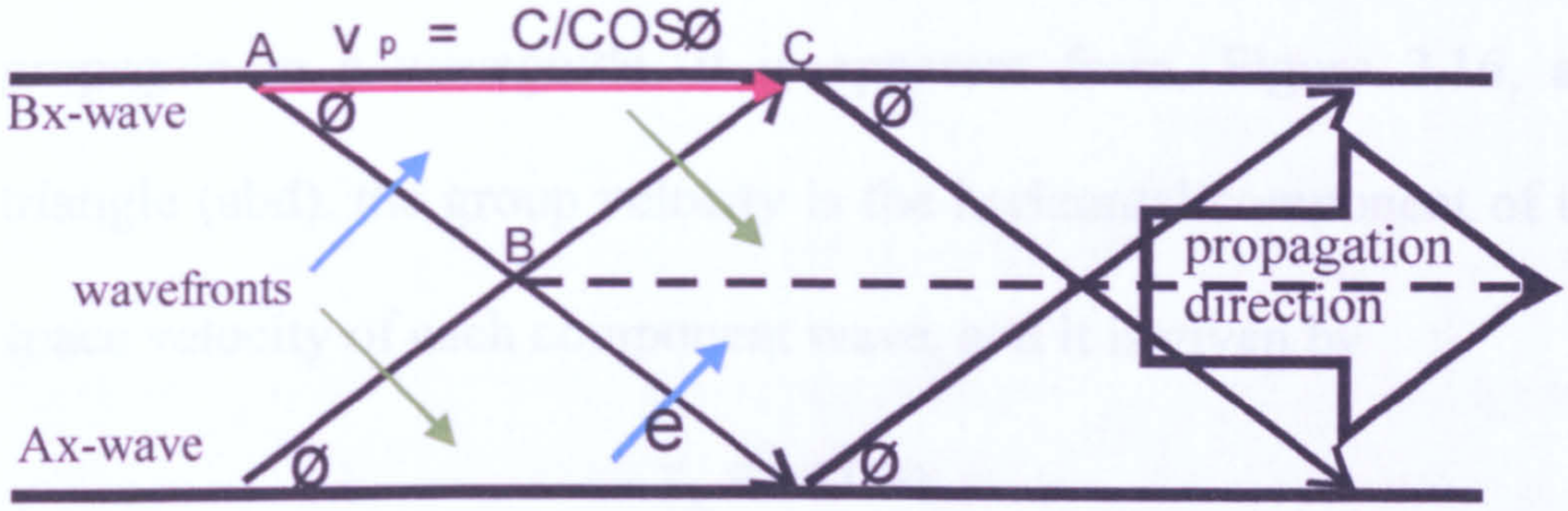

Figure 2.15: Calculation the phase velocity from the zigzag path in a waveguide.

Since the value of the term $\cos\Phi$ is always less than or equal to unity, then the phase velocity must be greater than or equal to the speed of light, c. The guide wavelength or λ_g, can be then calculated using Equation (2.19)

$$\lambda_g = \frac{v_p}{f} \tag{2.19}$$

where f is the propagation frequency. From Equations 2.1 and 2.19, it can be seen that the guide wavelength is longer than the free space wavelength, and they are related by Equation (2.20)

$$\lambda_g = \frac{V_p}{c}\lambda \tag{2.20}$$

Although the phase velocity value is greater than the speed of light c, the energy cannot actually propagate at speeds greater than the speed of light [32, 27, 25]. Accordingly, a new velocity is introduced and called the group velocity which represents the actual velocity the energy can propagate in a waveguide. It is apparent from, Figure 2.16, and the triangle (abd), the group velocity is the horizontal component of the free space velocity of each component wave, and it is given by

$$v_g = c.\cos\emptyset \tag{2.21}$$

Where ø is the reflection angle and c is the speed of light. Furthermore, both, the phase and group velocity are related by Equation 2.22.

$$v_g v_p = c^2 \tag{2.22}$$

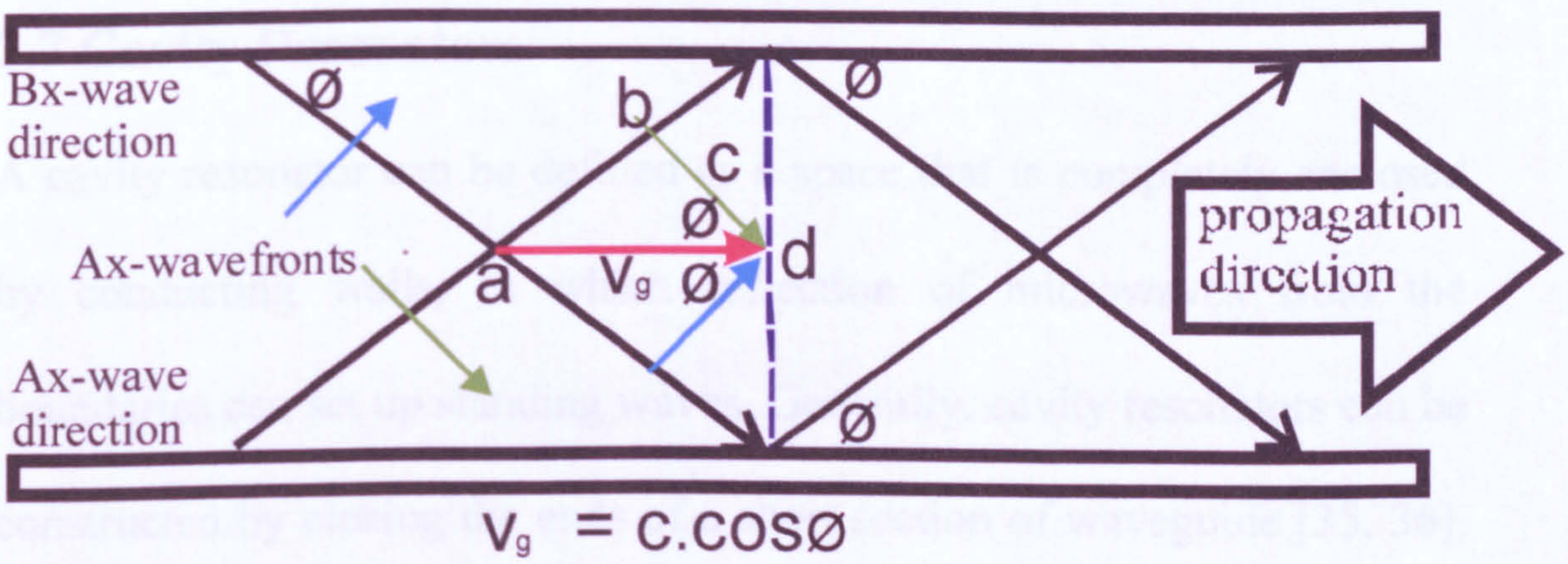

Figure 2.16: Calculation the group velocity from the waves path in a waveguide.

It can be seen from the zigzag path, Figure 2.13, that as the reflection angle varies between zero and 90 degrees, the value of cos ø will vary between 0 and unity. Therefore, the phase velocity can be either equal to or higher than the speed of light. The group velocity, on the one hand, will be either equal to or less than the speed of light. However, at frequencies equal to the fundamental or cut off frequency, the reflection angle will be 90 degrees and the group velocity will be zero. As a result, there will be no EM wave propagation in the waveguide. In other words, the wave will go back and forth in a waveguide, creating a standing wave; however, at frequencies higher than the cut off frequency, the signal will propagate in the waveguide.

2.7 Cavity Resonators

A cavity resonator can be defined as a space that is completely enclosed by conducting walls, in which reflection of microwaves from the boundaries can set up standing waves. Generally, cavity resonators can be constructed by closing the ends of a short section of waveguide [35, 36].

Consequently, cavity resonators are often circular or rectangular in cross section.

The standing wave modes that can exist in the cavity resonator are determined by the cavity resonator size and shape, and the boundary conditions at the walls of cavity resonator. As with the waveguide, the cavity resonator boundary conditions are that, at the conducting wall, the electric field cannot have a component tangential to the surface and the magnetic field cannot have a component normal to the surface of cavity resonators.

Cavity resonators have many advantages and uses at microwave frequencies. The amount of energy that stored at each of the resonant frequencies is defined as the quality factor or Q factor [37]. Cavity resonators, on the other hand, has a very high Q and can be built to handle relatively large amounts of power. The high Q factor gives these devices a narrow pass band and allows very accurate tuning [38].

Although cavity resonators can be designed for different frequency ranges and applications with different shapes, the basic principles of

operation are the same for all. A circular cavity resonator cross section with internal dimensions is shown in Figure 2.17.

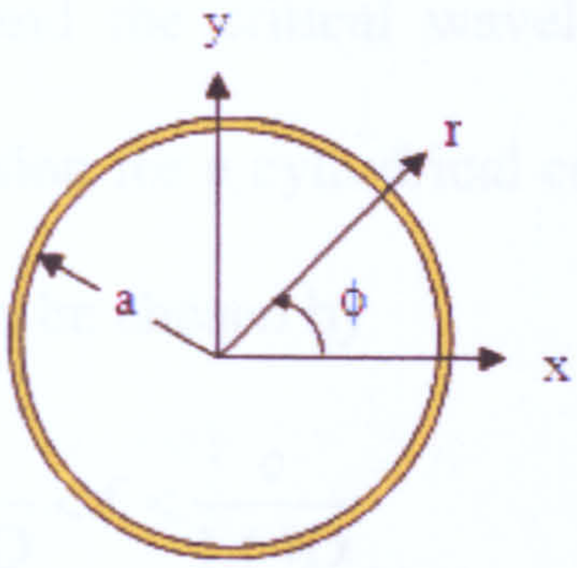

Figure 2.17: Circular cavity resonator.

A cylindrical cavity resonator can be operated in either TEnml or TMnml modes. The subscript n refers to number of full wave patterns around the circumference of the resonantor. The m subscript refers the number of half wave patterns across the diameter. The third subscript refers to the number of half wave variations in the z- direction or length of the cavity resonantor. The two fundamental modes that can exist in the cylindrical cavity resonator for both TE and TM modes are TE111 and TM010 respectively.

The critical wavelength λ_c for the TE111 mode can be calculated using Equation 2.23.

$$\lambda_{c,111} = 1.71D \tag{2.23}$$

where D is the diameter of a cylindrical cavity resonantor cross section. The cut off frequency and the critical wavelength can be related by Equation 2.1. The dimension for a cylindrical cavity resonator to be used at a given frequency f, can be chosen by

$$\frac{c}{1.71D} < f < \frac{c}{1.64D} \tag{2.24}$$

$$\frac{c}{1.71D} < \frac{c}{\lambda} < \frac{c}{1.64D} \tag{2.25}$$

$$\frac{1}{1.71D} < \frac{1}{\lambda} < \frac{1}{1.64D} \tag{2.26}$$

$$1.71D > \lambda > 1.64D \tag{2.27}$$

where $\frac{c}{1.71D}$ and $\frac{c}{1.64D}$ are the cut off frequencies for TE111 mode and the next higher mode, which is the TE011 mode, respectively. For an EM wave to propagate in a cavity resonantor, its wavelength must be shorter than the cut off wavelength of the fundamental mode and longer than the next higher mode cut off frequency. The values of TE111 and TM010 modes can be calculated using Equations 2.28 and 2.29 respectively.

$$f_{TE,111} = \frac{c}{2\pi\sqrt{\mu_r \varepsilon_r}}\left[\left(\frac{1.841}{a}\right)^2 + \left(\frac{\pi}{d}\right)^2\right]^{1/2} \quad (2.28)$$

$$f_{TM010} = \frac{c}{2\pi\sqrt{\mu_r \varepsilon_r}}\left[\left(\frac{2.405}{a}\right)\right] \quad (2.29)$$

Where:

μ_r: is the relative permeability

ε_r: is the relative permittivity

d: is the depth

a : is the radius

2.8 Microwave Sensor Fundamental

2.8.1 Introduction

The general demand for automating industrial processes has come up with an incredible need for sensors. Different types of sensors have solved different problems [1]. The principles of electromagnetic wave sensors operating at microwave frequencies are based on the interaction of signals with the medium material. This type of interaction can be in the form of amplitude attenuation, phase shift for example [39]. Microwave sensors can be divided into groups, depending upon how the measurement is arranged and which interaction the sensor is based on. The most important group related to this research are resonance cavity or waveguide sensors, transmission sensors, reflection sensors, which are used for measuring (oil, gas, and water) flowing in a pipe [39]. The second group are the radar sensor, radiometers sensor, and topographic sensor developed for measuring physical quantities such as distance, movement, shape, and sold material properties. Material measurements with microwave sensors are based on the fact that the relative permittivity and permeability are completely determined the interaction between

microwave signal and the medium material. The relative permittivity and permeability are given by Equations (2.25 - 2.26) respectively.

$$\varepsilon_r = \varepsilon' - j\varepsilon'' \tag{2.25}$$

$$\mu_r = \mu' - j\mu'' \tag{2.26}$$

In this thesis only the real part of the relative permittivity will be considered to affect the interaction (resonant frequency) of microwave signal, unless otherwise stated so that $\varepsilon'' = 0$, and $\mu_r = 1$. As different materials have different permittivity, a mixture permittivity (e.g. oil, gas, and water mixture) depends on the relative large component permittivity as well [40]. In other words, depending upon the permittivity of a mixed materials, the measurement of the applied microwave properties can provide information about the Material Under Measurement (MUM). Further, for a simple case of two components the sum of the permittivity is 100%. In this case, there will be only one unknown if the permittivities of the components are assumed to be known. So that in this case it is possible to deduce the composition from one measurement, e.g. resonant frequency [41, 39]. Increasing the complexity of challenge is such a case where there are more than two components in the mixture. For example

(oil, gas, and water) mixture. In this case multiphase flow sensor or three phase meter is inevitable, where different types of technology based sensors are frequently used to measure mixed components within the three phase system [1, 2].

2.8.2 Microwave Sensors Basic

Microwave sensor can be arranged in several possible ways for the measurement of materials in a pipeline. The different characteristics of microwave sensors make them suitable for different applications. Since the new sensors described in this thesis are all designed for measuring multiphase flow in a pipeline online, a brief overview of the related basic sensors will be discussed in this section. The current microwave sensors are explained in section 2.9.

2.8.2.1 Transmission Sensors

This sensor is constructed such that two dielectric windows are fitted on opposite sides of a metal pipeline with a transmitting antenna on one side and a receiving antenna on the other side as shown in Figure 2.18.

Microwave signal penetrates the material flowing in the pipeline between the antennas [42]. As a result, the phase and the amplitude of the applied signal are affected by the permittivity of the flowing material.

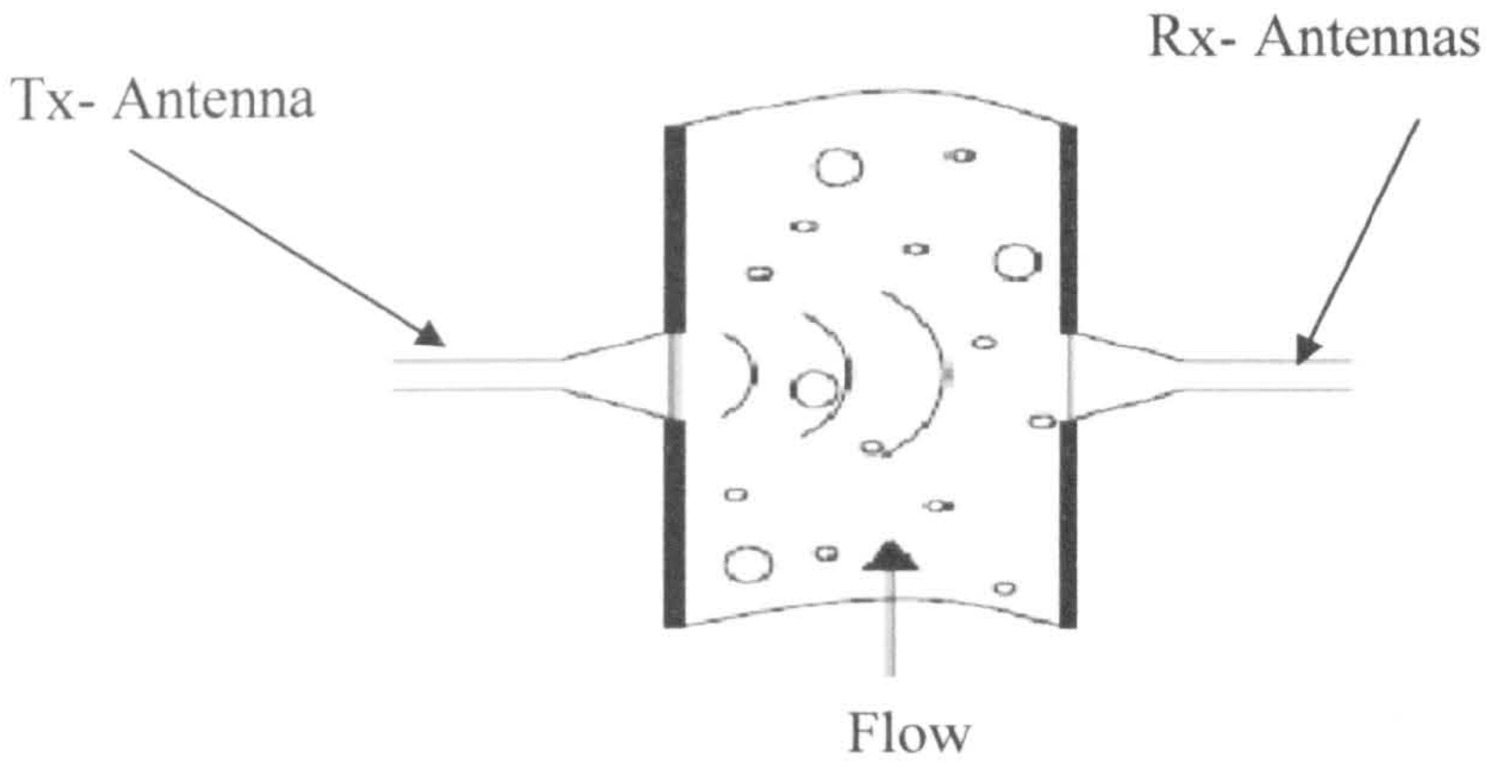

Figure 2.18: The basic geometrical configuration of a transmission sensor [42].

The advantage of this sensor is the simplicity, but the main problem is the sensitivity to reflections in various parts of the system, such as the dielectric windows and interfaces inside the material dependent on the flow regime. The reflections in the system cause ripples on the frequency response, and the amplitude is much more affected than the phase. If the sensor is based on measuring only one microwave parameter, a higher accuracy is therefore achieved by measuring the signal phase shift than by measuring the amplitude attenuation [42].

If the material flowing in the pipe has small losses, the reflections from the pipe walls will also strongly affect the both the phase and amplitude [43]. Especially if the measurement is done on a fixed frequency, the errors will be large, as the moves the cut off frequency of the applied mode frequency.

2.8.2.2 Reflection Sensors

A reflection sensor is based on measuring the reflection coefficient for a wave reflected from the end of a transmission line (see section 2.4). The design is made such that the fringing field (evancent mode) at the end is in contact with the flowing material which affects the phase and magnitude of the reflection coefficient [44, 45].

The open-ended coaxial sensor measures with the fringing field at the front surface of the sensor, it can only measure a small fraction of the mass flowing in the pipe (solid material). This sensor is generally not suited for applications in the petroleum industry, except for emulsions of oil and water with very small drop size because of the small volume affecting the measurement.

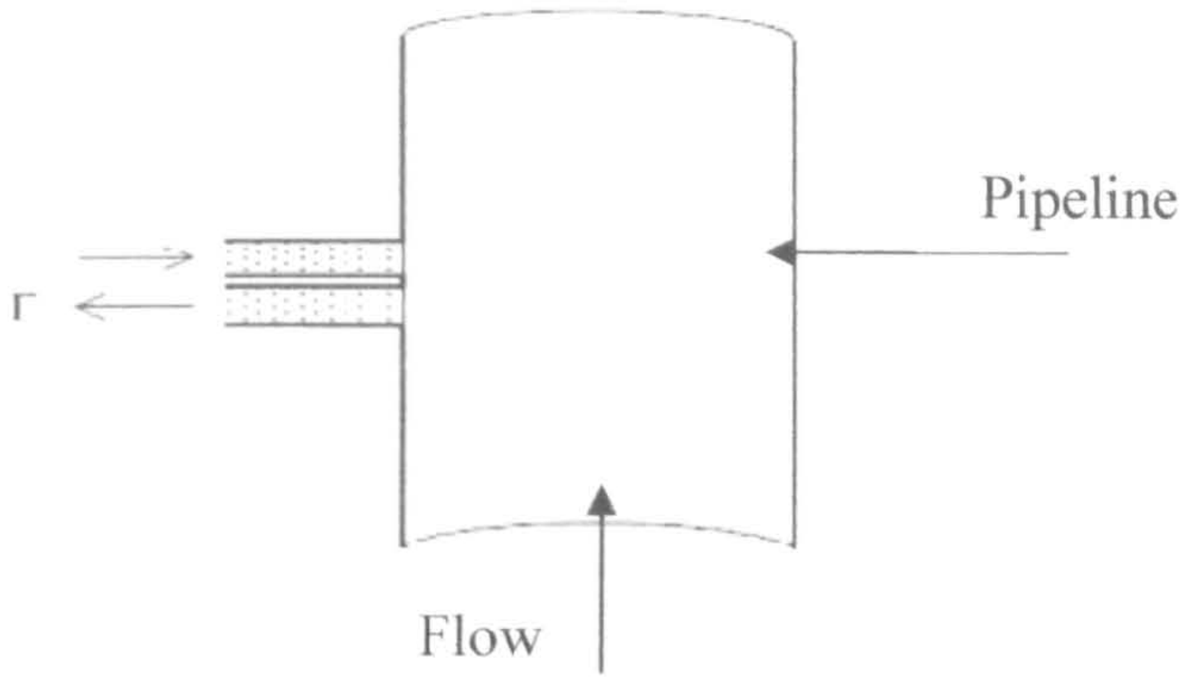

Figure 2.19: The principle of an open-ended coaxial cable as a reflection sensor mounted for measuring on-line in a pipe [44].

2.9 Current Microwave Sensors

The current commercial electromagnetic waves sensors, operating at microwave frequency, used for measuring phase component (e.g. oil and water mixture) are based on microwave resonant cavity or waveguide technologies [46, 13]. When microwave signals are applied to a mixture flowing in a pipeline they will, at a characteristic frequency, resonance and properties of these signals (amplitude or phase shift) are affected by the flow permittivity and then can be measured and used as a measure of phase components in the mixture.

2.9.1 Phase Shift Based Sensor

Agar is a commercial electromagnetic wave sensor based on the measurement of phase shifts and a microwave resonance cavity coaxial (waveguide) [47, 48]. It can measure the phase shift of the applied electromagnetic wave signal as a measure of the component in a mixture. This meter is constructed such that the transmitted signal is received by two antennas, spaced at different distance from the source antenna. The calculated difference, in phase shift between the received signals (with regard to the transmitted signal), is used as a measure of the phase component in the mixture.

The attenuation of electromagnetic waves signals at microwave frequency by oil and water in different measure cause varying degree of attenuation. Attenuation in water medium is relatively very high [47]. This method can be summarized as the detection of energy loss in transmitted microwave signal between a transmitter and a receiver.

The major limitation of this method is that the fluid in close contact with the transmitter dominates the readings [49]. The effect is serious if the fluid is immiscible as it is with oil/water mixture. This lead to false

reading due to uneven distribution of the fluid particles causing the energy loss and phase change.

This technique requires the intrusion of the transmitter and receiver into the flow channel [48, 49]. This is a disadvantage due to pressure drop, and trapping of fluid particle. Since the meter is intrusive, wear and tears of the antennas insulator will often cause replacement of the antennas. In addition, the cleaning of the antenna surface due to fluid clogs will increase operational cost and downtime.

This results in overall increases in the cost and rate of maintenance. Implication is that the meter will not be satisfactory for use in a remote environment due regular maintenance required.

2.9.2 Attenuation Based Sensor

Roxar phase component sensor, on the other hand, is based on an open ends hollow cavity or waveguide [46, 50]. This sensor is constructed such that the electromagnetic waves transmitted into a particular flowing mixture will, at a characteristic frequency, resonate to produce distinct peak amplitude. This peak corresponds directly to the phase fraction or

component, e.g. water content [51]. In other words, the mixture components produce different and distinct peak amplitudes at the resonance state. This is because their dielectric constants are different. These peaks, on the other hand, are translated directly as a measure of the phase component contained in the mixture.

The major limitation of this sensor is that it can only be used with a low loss media. A loss media simple means an oil continuous fluid. This is because water continuous fluid absorbs energy too fast for resonance to occur [50, 51].

2.10 Multiphase Flow Measurement Principles

The measurements of three phases in a pipeline have different methods to express the quantities of each phase. The volumetric flow rate and or mass flow rate of the oil, water and gas components in the flow is the primary information required from the user of a three phase flow instrument [13].

The ideal three phase flow meter would make independent direct measurements of each of these quantities. A direct volumetric flow or

mass flow instrument does not exist at all for use with three phase flows. The alternative to direct volumetric flow rate measurement is to use an inferential technique measurement which requires the superficial or phase velocity, density and cross sectional fraction of each phase to be known in order to calculate the individual component volumetric and mass flow rates (Figure 2.20).

The volumetric flow rate Q of each phase and the total (mixture) flow rate can be determined by Equations 2.27 and 2.28 respectivilly

$$Q_g = A\alpha v_g;\ Q_w = A\beta v_w;\ Q_o = A\gamma v_o \qquad (2.27)$$

$$Q_t = Q_g + Q_w + Q_o \qquad (2.28)$$

where α, β and γ are the gas, water and oil phase fractions. The v_g, v_w and v_o are the superficial velocities of the oil, water, and gas phases in the mixture. A is the cross sectional area of the pipe section. The superficial phase velocity is defined as the flow velocity of one phase, assuming the phase (gas, oil or water) occupies the whole pipeline.

The phase mass flow rate M of each phase and the total mass flow rate can be calculated as:

$$M_g = Q_g\rho_g;\ M_w = Q_w\rho_w;\ M_o = Q_o\rho_o \qquad (2.29)$$

$$Mt = Mg + Mw + Mo \tag{2.29}$$

where ρg, ρw and ρo are the density of the gas, water and oil fractions.

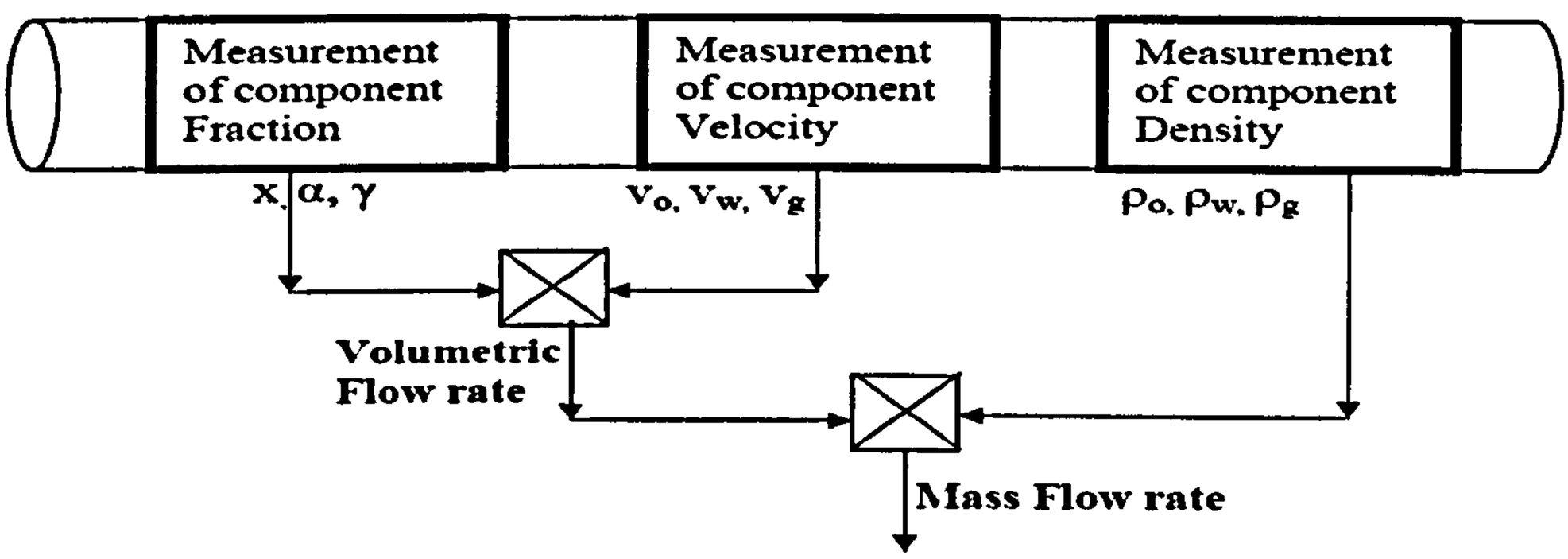

Figure 2.20: Three phase flow measurement using inferential methods [13]

The density information for oil, gas and water phases is readily available from the related database in the oil industry [7]. The measurement of phase density can be achieved using several sensors such as gamma densitometer and coriolis mass flow [1, 13].

2.11 Multiphase Flow Regimes

The physical distribution of the fluid phases in a pipeline section results in the formation of various flow regimes [13]. The magnitude of the force acting on the fluid results to formation of a flow regime. Varying degree of forces such as surface tension, oil, gas and water flow rates and properties, the pipe diameter and pipe inclination can also significantly influence flow regimes.

The general flow regime of (gas, oil and water) streams in horizontal and near horizontal pipe geometry can be classified as: Bubble, plug, stratified, slug, wavy, annular and mist. These flow regimes for vertical and horizontal pipeline geometry are illustrated in Figure 2.21 as a function of superficial liquid (oil and or water) and gas velocities.

The main mechanisms involved in flow regime formation are classified into three effects:

- **Transient effect:** this effect occur due to changes in the system boundaries due to alterations in the flow loop introduced by some system control, such as the closing and opening of control valve.

- **Geometry effect:** this effect is as a result of changes in the pipe line geometry or inclination. The pipelines may be in vertical, horizontal or inclined at an angle.
- **Hydrodynamic effect:** such as fluid flow rate, fluid properties, and a combination of the effects.

In each of these flow effects, the resultant flow can be classified as flows:

- Dispersed flow such as bubble and mist flow in which the phases are uniformly distributed in the radial and axial direction. Water and oil will generally be transported at the same flow rate, but, being immiscible, will produce a dispersed flow regime. If the water fraction or quantity is low, then the fluid will be oil continuous, i.e. drops of water dispersed in a larger volume of oil. If the water fraction is sufficiently large, it will become water continuous.
- Separated flow such as stratified and annular flow, in which the phase distribution is non continuous in the radial and continuous in the axial direction. Stratified flow regime occurs when the superficial phase velocities are low, and annular flow occurs when superficial gas velocity is high.

- Intermittent flow such as churn and slug flow in which the flow is non continuous in the axial direction and as a result, local unsteady behaviour is introduced. Slugs refer to sections 100% liquid.

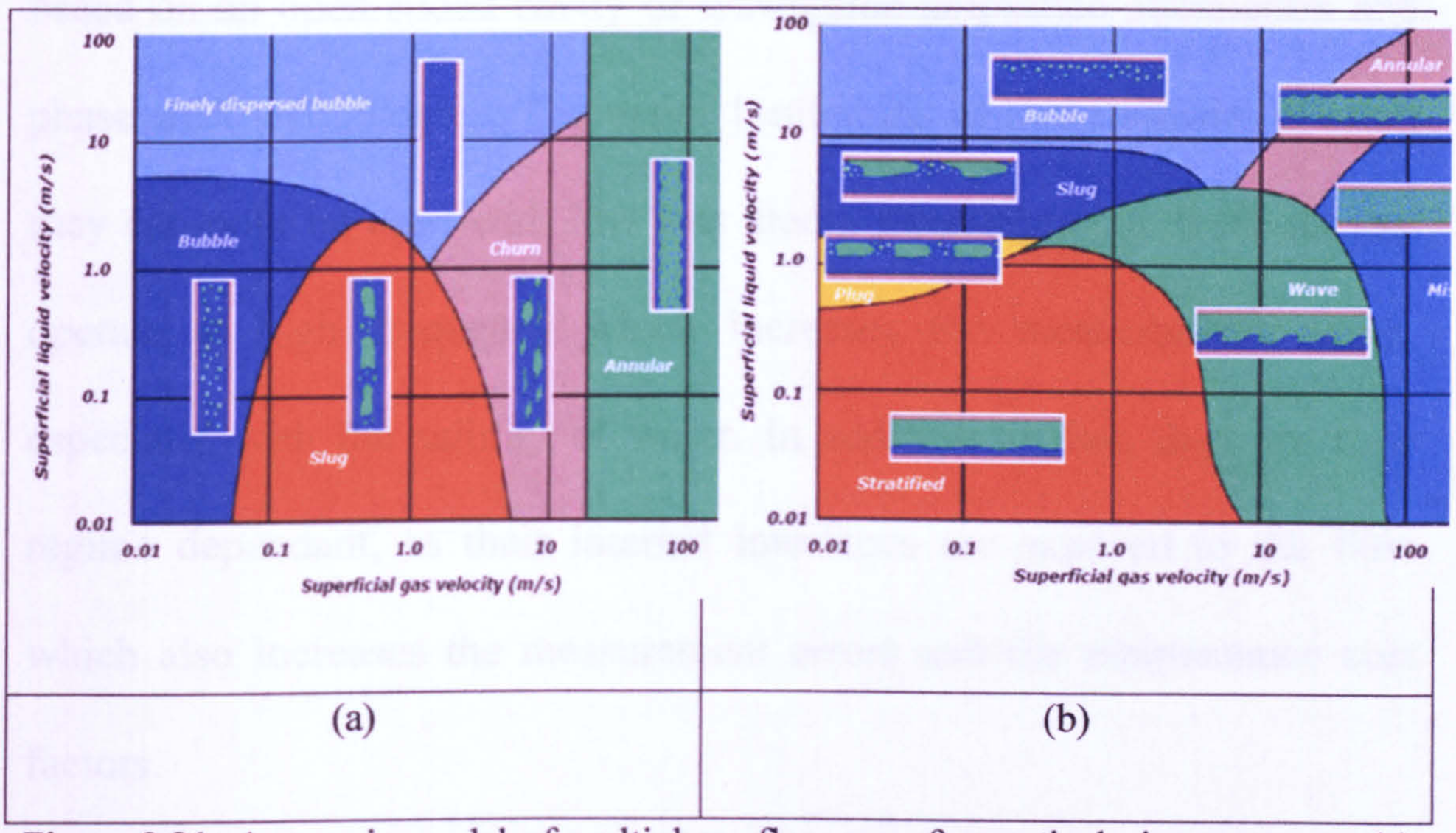

Figure 2.21: A generic model of multiphase flow map for vertical pipe geometry (a) and horizontal pipe geometry in (b)

2.12 Conclusion

A varying time current on a simple antenna can generate a time varying magnetic field which in turn generates a time varying electric field that also generates a magnetic current and so on. EM wave radiates in free space away from the antenna to a large distance with speed of light, to a receiving antenna for example. The energy travels in free space in all

directions, but using appropriate waveguide or cavity resonator the energy can be made to travel in specific directions.

The current microwave sensor used for measuring phase fractions are based on an open-ended cavity or waveguide amplitude attenuation and phase shift technologies. The major limitations of these sensors are that they can only be used with low loss media measurements. Both sensors operate at high frequency which increases the measurement errors, especially with the salinity of water. In addition to that, they are flow regime dependant, as their internal interfaces are exposed to the flow which also increases the measurement errors and the maintenance cost factors.

The new sensors described in this thesis are all cavity resonators based on a partially shorted-ends cylindrical cavity fitted to PVC pipeline, and they used the resonant frequency to measure in real time three phase (oil, gas, and water mixture) quantities in % volume. All these sensors operate at a low frequency, and their interfaces are isolated from the flow. The simulation designs and constructions including the results analysis are described in chapters 4, 5, 6 and 7.

CHAPTER 3

Electromagnetic Wave Simulation

3.1 Introduction

Quality simulation of sensor designs, which based on cylindrical cavity resonator, prior to construction not only saves time, but also money. Even though it is possible to derive a mathematical model for the frequency response of a simple cavity resonator or waveguide, with the introduction of a multiphase flow in a pipeline located at the centre and along the axial direction of a semi open-ended circular cavity resonators, the calculation becomes extremely difficult. The addition of changes in the cavity resonator's properties in the time domain makes a design using simplified mathematical formula impossible. For this reason a powerful simulation software package is required to assess possible designs.

Modelling the sensors has been carried out using the High Frequency Structure Simulator (HFSS) software [52].

3.2 HFSS Basic

HFSS is a full wave electromagnetic wave simulator, designed to model numerous RF and Microwave structures [53]. HFSS is a more modern and more powerful software package than any other existing simulation software. The most important advantage of HFSS is the complexity of geometries that can be created, which were limited in other existing simulation packages [54, 55]. The software design is also superior, for example the undefined division between the design aspect and the simulation of a system, affords a more productive user interaction.

3.2.1 HFSS Computer Aided Design (CAD) Editor

The HFSS CAD, which consists of five main windows and several optional panels, offers a number of features that allow the user to model complex geometry structures [56]. This is useful as it allows the complex structures required during the design of microwave sensor to be created. The HFSS main window is shown in Figure 3.1. The project manager window contains a design tree, which lists the structure of the project. This window allows the user to choose a solution type. In this project, the HFSS solution type used is called Eigenmode or Resonant mode, which is the suitable solution type for calculating the resonant frequencies of

cylindrical cavity resonator structure and the fields at those resonant frequencies. The 3D modeller window, which contains the model and model tree for the active design, allows the user to create 3D models. The property window displays and allows user to change the model parameters. With this window, the user can either assign a material to the model or change the model parameters. The progress window displays the solution progress, and finally, the message manager window allows the user to view any errors or warnings that occur before the user begins a simulation.

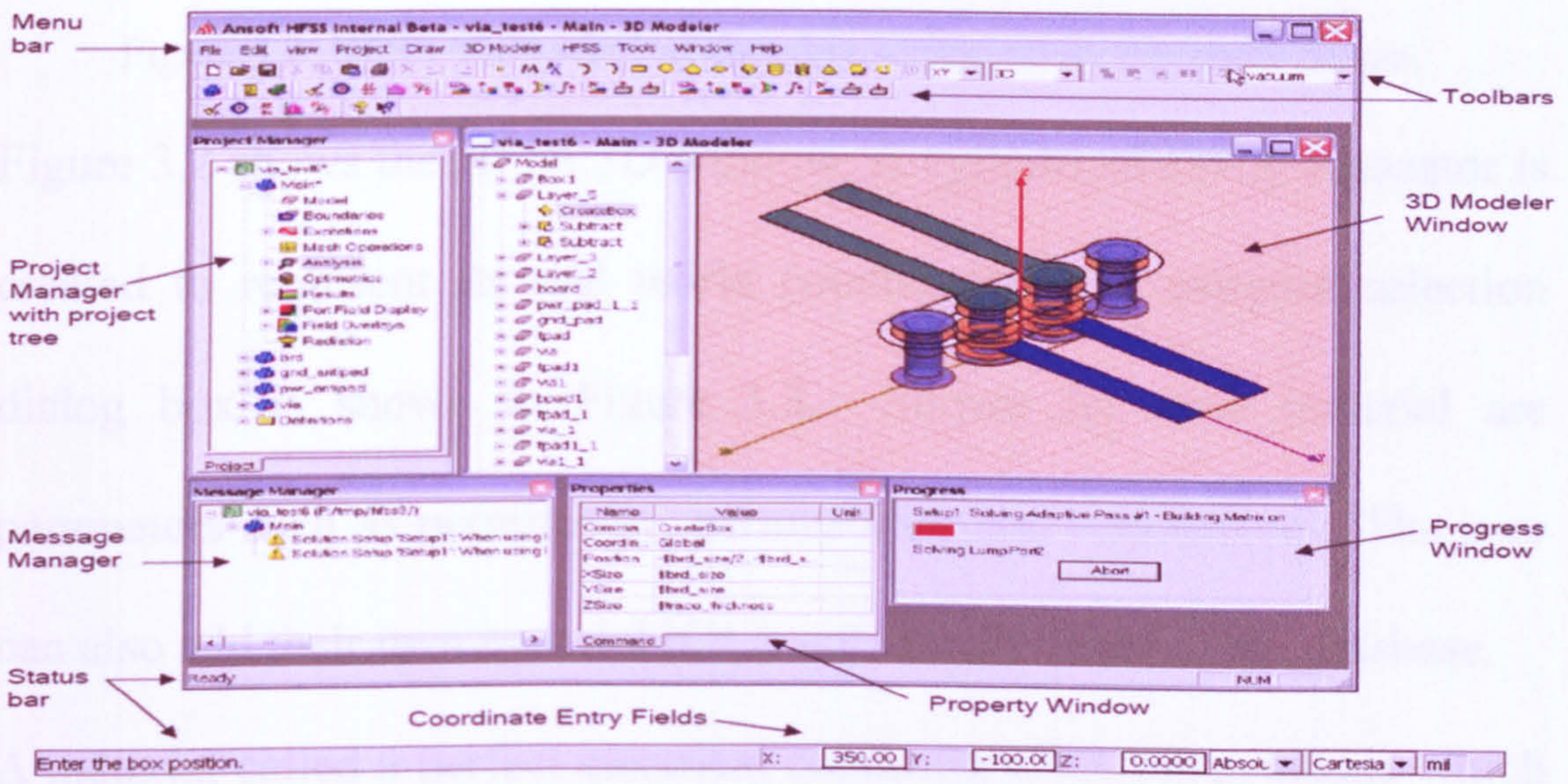

Figure 3.1: HFSS main window showing the graphical user interface (GUI) windows.

Figure 3.2 shows the HFSS 3D window. A cylindrical cavity resonator is created to represent its real world counterpart. When the model is created

and the type of material is chosen, the model can be assigned the solution type and set up.

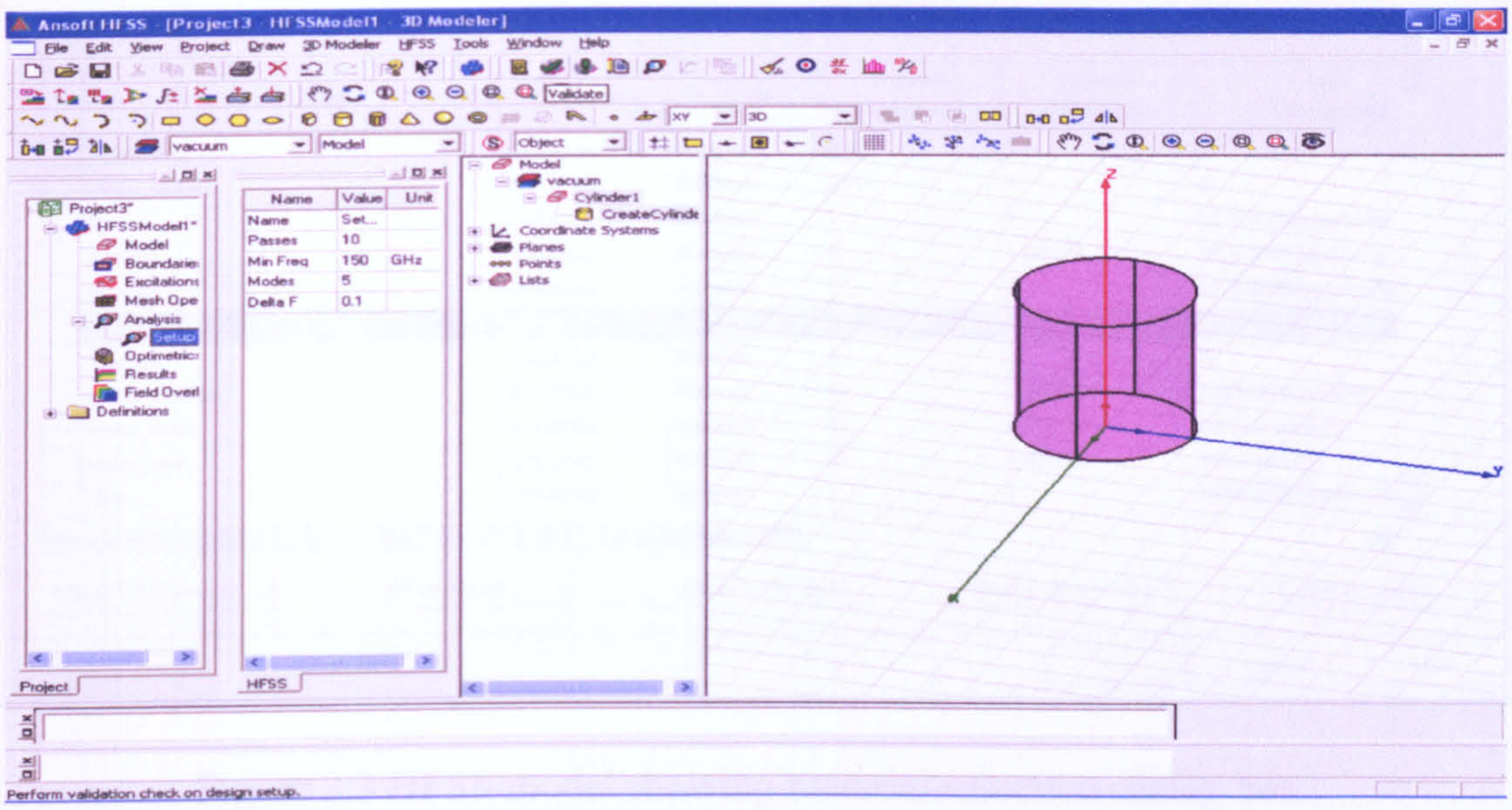

Figure 3.2: HFSS Main window showing sensor cavity resonator design.

Figure 3.2 shows the HFSS 3D window. A cylindrical cavity resonator is created to represent its real world counterpart. The material selection dialog box is shown in Figure 3.3. Shown for each material are parameters such as permittivity, permeability and conductivity. The user can also add their own material if it is not already listed in the database.

A material called a perfect electrical conductor (PEC) is available which can be used to create the walls of an ideal cavity resonator. This has no resistivity, and therefore, no ohmic losses will occur.

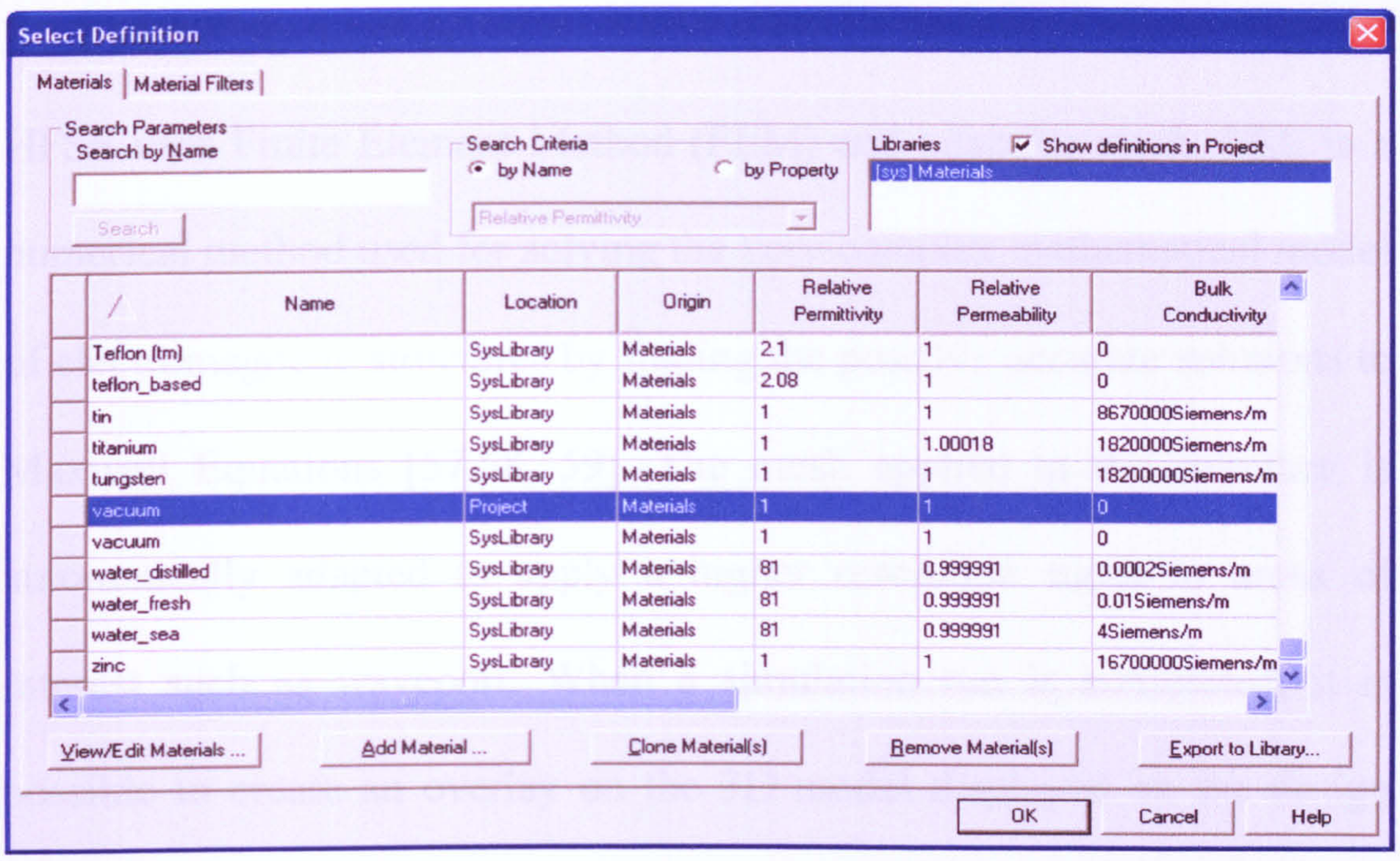

Figure 3.3 HFSS model showing material selection dialog box.

A vacuum can also be used as the air inside a resonator, which again will ignore losses. Both these cases represent ideal, perfect materials, and clearly are not a true representation. However, by doing this, the simulation times are reduced dramatically compared to using non ideal materials such as air and copper. In the example of a cylindrical cavity resonator, the cut off frequency and the number of resonant modes to fined need to be stated before a simulation is started. Only the modes of transmission, having cut off frequencies equal or higher than the 150MHz assigned frequency, are defined.

3.2.2 HFSS Simulation

HFSS uses Finite Element Method (FEM) and adaptive mesh. FEE is a numerical method used for solving the very complex mathematical model of electromagnetic structures by finding the possible accurate solutions to Maxwell Equations [57,58, 59]. The mesh applied to the structure is automatically adapted to apply a higher resolution mesh to areas of interest such as waveport. When a simulation run is completed, it is possible to create an overlay on the 3D model displayed on the design window. Important parameters such as resonant frequency, and E-Field and H-Field can be calculated and viewed on any 2D plane, or as a 3D representation respectively. An example showing the E-field and H-field vectors in the 3D model of the cavity resonator shown in Figures 3.2 is illustrated in Figures 3.4 and 5.

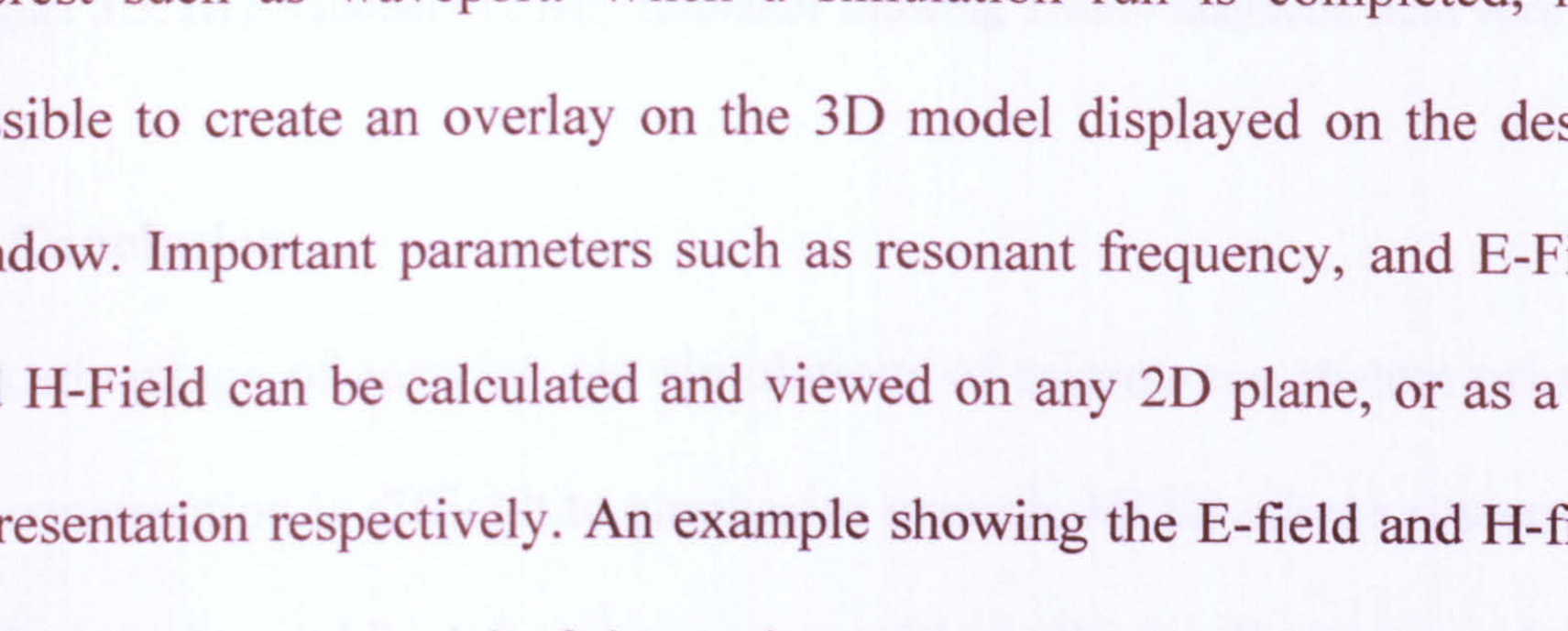

Figure 3.4: HFSS model of cavity resonator showing TM_{010} E-vectors.

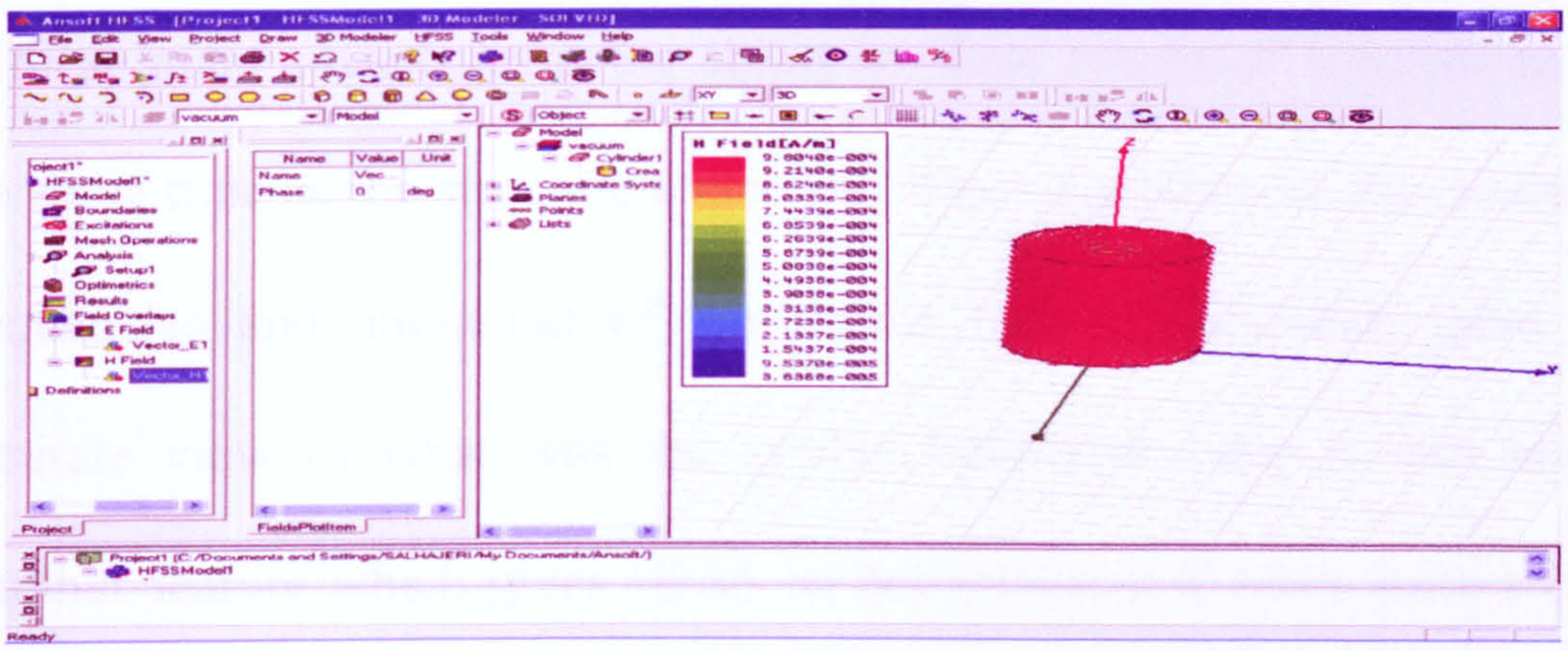

Figure 3.5: HFSS model of cavity resonator showing TM010 magnetic field vectors.

3.3 Conclusion

The advantage of carrying out simulations of microwave system prior to the construction is difficult to emphasise enough. HFSS allows systems to be designed tested in a cheaper manner without the implied cost and time that can be involved in the manufacture. HFSS helped to confirm the best location and dimensions for the structures being fabricated. The creation of the 3D structure in the computer is fairly intuitive. The software can assign different materials to the structures because each material has an associated set of properties (e.g. permittivity).

HFSS has many advantages over their competitor software packages. One of these main advantages is the ability to show results of simulations at the same time as the structure under test. The calculation of the resonant frequencies and animation of the results on the simulation gave an accurate view of what was the system behaviour once it was built. Another feature which gives HFSS an advantage over other software is the possibility of setting up parameters. For example one can set up the position of a structure at a certain variable defined as a parameter. HFSS has the ability to change the parameter position design property automatically and systematically, to make the appropriate calculations for the structure under the conditions of each value for the parameter and then supply the calculated results, giving the user the opportunity to choose the best possible location.

CHAPTER 4

EMW2 Sensor Design and Simulation

4.1 Introduction

A non intrusive electromagnetic wave sensor operating at microwave frequency was designed and constructed to measure and monitor multiphase flow in a pipeline for industrial three phase measurement. This sensor is based on a microwave cylindrical cavity resonator and it uses the resonant frequency shifts and the changes in the related permitivity to monitor and measure two phase (gas and water mixture) component fractions flowing in a pipeline as a volume percentages.

The cavity resonator must be large enough to accommodate the pipeline, and the pipeline material must allow the microwave signals to penetrate inside the pipeline. This was achieved by designing the resonator diameter to be larger than diameter of the pipeline, and by using a dielectric material for this section of a pipeline. This is illustrated in Figure 4.2 as the pipeline is made to be continuous, along the resonator axis [60, 61]. This design not only allowed the

microwave signals to interact with the material in the pipeline, but also protected the transmitting and receiving antennas from the fluid flowing in the pipeline. Marconi Microwave Test Set 6200A or MTS 6200A was used to both sweep through the frequency range and to detect amplitude of the resulting received signals [62]. The main cavity resonator was based on a short circuited cylindrical cavity, and the pipeline was represented by an open-ended PVC pipe. HFSS was used to simulate the cavity resonator and the PVC pipeline to see the effect of changing the various dimensions.

4.2 Related Work

A cavity resonator, which is made using a piece of hollow waveguide, can be circular or rectangular cross section cavity resonator. It is usually short-circuited of both ends with solid metal walls, or with partially open ends to allow the material to flow through online, as with the PVC pipeline used in the new sensor described in this thesis. Consequently, any wave mode that can propagate in a cavity or waveguide, and be reflected at the impedance discontinuities (i.e. the end structures), has resonances in the cavity. In hollow waveguide or cavity the wave modes are called TEnm and TMnm modes,

described early in section 2.3. The resonances for a mode occur at the frequencies, where the length of the cavity is a multiple of the half wavelength of that mode [63]. The resonant modes are called TEnml or TMnml, where the integers n, m, and l refer to the number of electric field maxima in the standing wave pattern along the x, y, and z directions for a rectangular cavity resonator, or ϕ, ρ, and z directions for a cylindrical cavity resonator. Some modes can also be supported with l = 0. This happens for TM modes, when the ends are short-circuited, and for TE modes, when the ends are open circuited. Every cavity resonator has an infinite number of resonances. For a cylindrical cavity resonator the resonant frequency of a TEnml modes and TMnml modes are given by Equations 4.1 and 4.2.

$$f_{TE,nml} = \frac{c}{2\pi\sqrt{\mu_r \varepsilon_r}}\left[\left(\frac{p'_{nm}}{a}\right)^2 + \left(\frac{l\pi}{d}\right)^2\right]^{1/2} \tag{4.1}$$

$$f_{TM,nml} = \frac{c}{2\pi\sqrt{\mu_r \varepsilon_r}}\left[\left(\frac{p_{nm}}{a}\right)^2 + \left(\frac{l\pi}{d}\right)^2\right]^{1/2} \tag{4.2}$$

Where c is the velocity of light, μ_r is the relative permeability, ε_r is the relative permittivity, p_{nm} is the m^{th} root of the Bessel Function of the n^{th} order, p'_{nm}

is the first derivative of the Bessel Function, p_{nm} , a is the radius, and d is the depth or length of the resonator.

In some cases more than one mode will have the same resonant frequency. They are called degenerate modes [64, 65]. For example, TE011 and TM111 modes shown in Figure 4.1 are degenerate modes as they have the same frequency. Because of the large number of resonances in the cavity resonator, it must be designed in such way as to avoid the interference from other modes [65]. This is not a big problem for cavity resonators completely filled with an isotropic (e.g. water) and homogeneous dielectric, because all the resonant frequencies are shifted in the same way as a function of the permittivity. In partly filled waveguide or cavity resonators, the frequency shift of each mode depends on the location of the sample with respect to the electric field of that mode. The order of the resonant modes in the frequency response may therefore change, when the sample is inserted or, when the permittivity of the sample changes.

4.2.1 EM Wave Sensors Design Overview

The dimensions of the cavity resonator should be chosen so that the difference in frequency is as large as possible between the mode, which is used for measurement purposes, and the other modes, especially those identified as potentially interfering modes. A chart showing the order of the resonances in a cylindrical cavity resonator is shown in Fig. 4.1. It has been calculated using Equations 4.1 and 4.2, and the values of p_{nm} and p'_{nm} shown in Table 4.1.

Mode	TM_{nm}			TE_{nm}		
N	p_{n1}	p_{n2}	p_{n3}	p'_{n1}	p'_{n2}	p'_{n3}
0	2.405	5.520	8.654	3.832	7.016	10.174
1	3.832	7.016	10.174	1.841	5.331	8.536
2	5.135	8.417	11.620	3.054	6.706	9.970

Table 4.1: Values of p_{n1} and p'_{n1} for a circular cavity resonator [55]. p_{nm} is the m^{th} root of the Bessel Function of the n^{th} order, p'_{nm} is the m^{th} root of the first derivative of the Bessel Function of the n^{th} order. Bessel function roots are dimensionless [55].

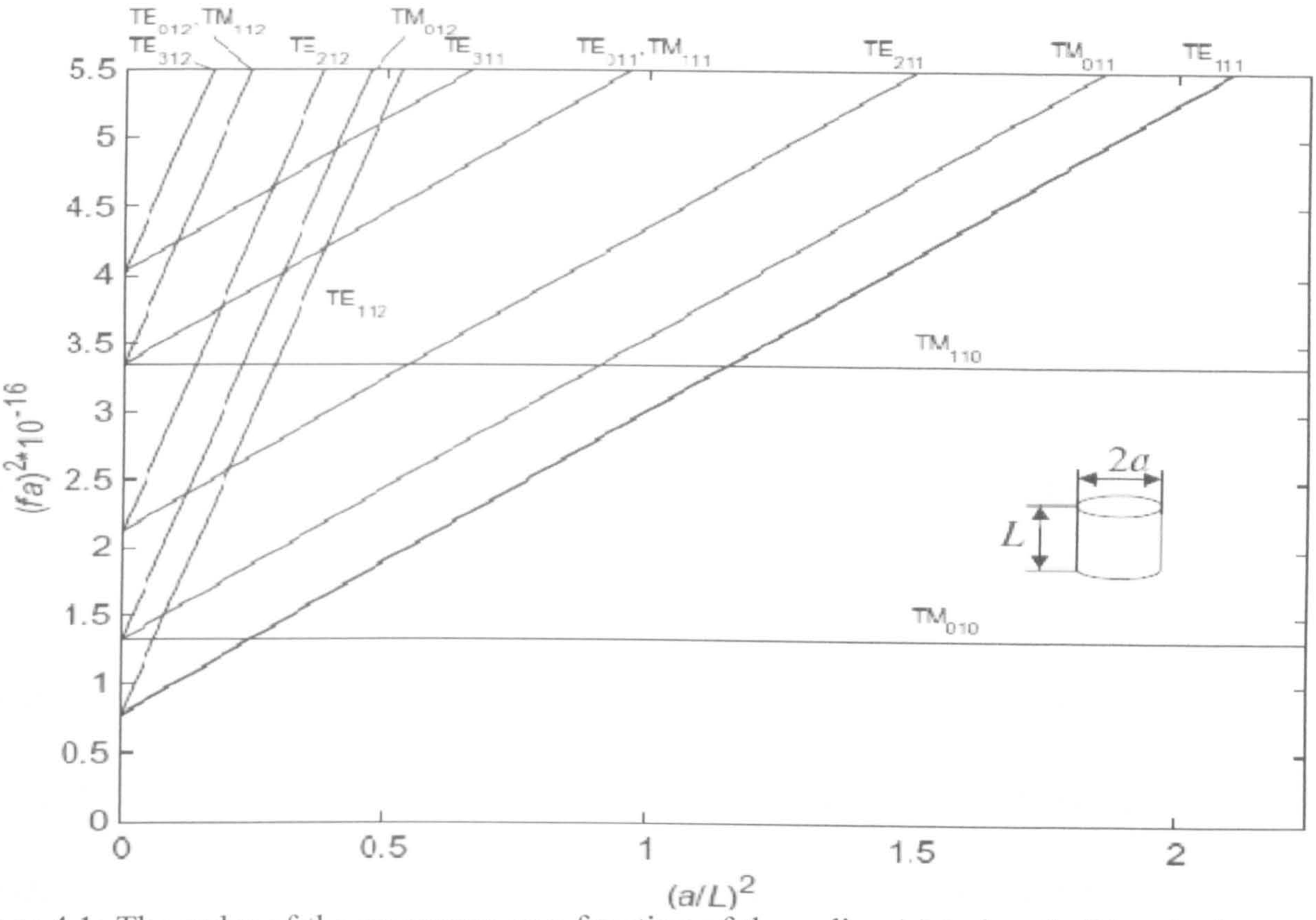

Figure 4.1: The order of the resonance as a function of the radius (a) to length (L) ratio for a circularly cylindrical cavity resonator [55].

Using the chart shown in Figure 4.1, an individual resonator would be represented by a vertical line at the location of the squared ratio $(a/L)^2$ of that resonator. For a cylindrical cavity resonator, dominant mode is TE111, which is the TE mode with the lowest cut off frequency. The TM dominant mode for a cylindrical cavity resonator is TM010.

To design a non intrusive sensor, based on a cylindrical cavity resonator, to accurately measure and monitor the volume percentages of multiphase flow in a

pipeline, the cavity resonator must be large enough to accommodate the pipeline. Figure 4.2 shows the pipeline as it made to be continuous, along the resonator axis centre. This design allows the resonant frequencies to be affected by the contents of the pipeline, and also allows the antennas, which are used to excite the resonant modes, to be separated from the fluid in the pipeline. This both protects the antennas from the moving fluid in the pipeline and enables the pipeline to be cleaned with the sensor in place.

Experimental works show that as the outer part of the cavity resonator is filled with gas (air), no mode of transmission can be propagated. This was regarded to multiple reflections and changes in the speed of the transmitted signal caused by different permittivitty materials (gas / PVC / water / oil) .Therefore, the decision was taken to fully fill the outer part of the cavity resonator with water to reduce the changes of the transmitted signal speed before it can hit the PVC pipeline which can reduce the reflection. This design was applied to all cavity resonators described in this thesis.

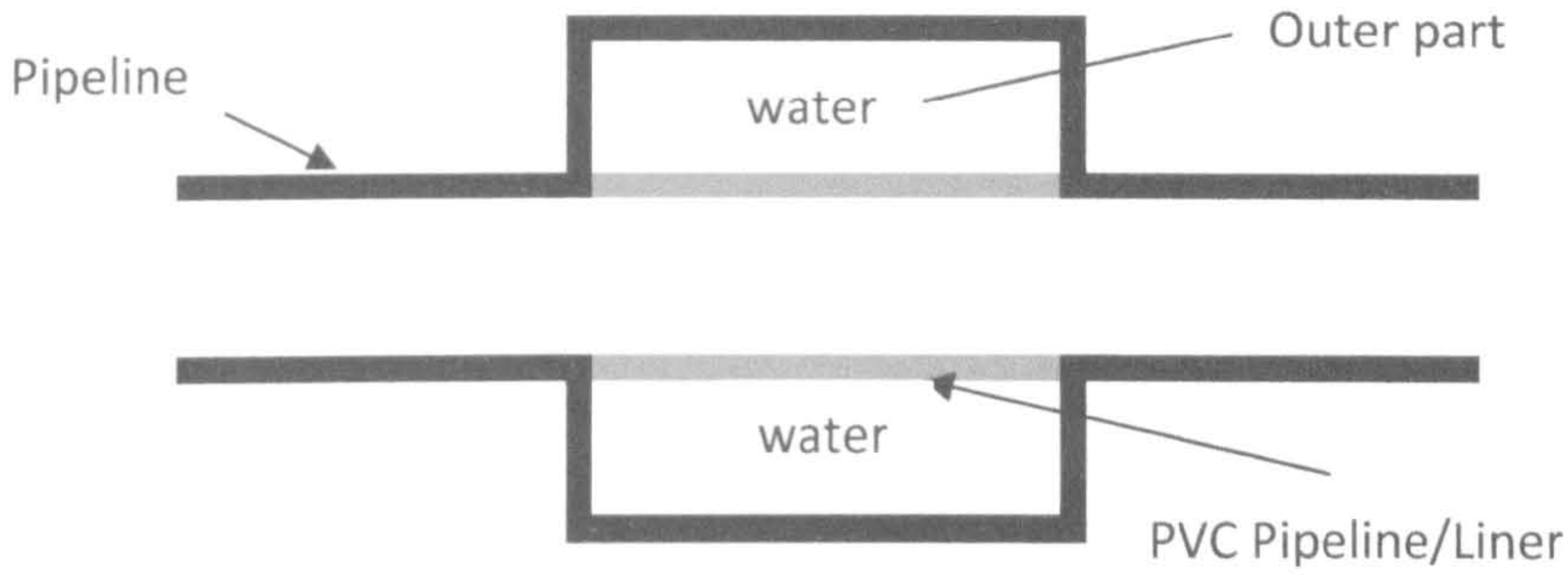

Figure 4.2: the basic designs and construction of the sensor.

The primary dimensions were chosen based on the desired modes of operation cut off frequencies. The cut off frequency of the fundamental mode was chosen so that it operates below the cut off frequency of the PVC pipeline (dielectric liner). The chosen modes of operation were TE111 and TM010. The initial dimensions are listed in Table 4.2.

Table.4.2: The primary chosen dimensions for the sensor and pipeline.

Resonator	Length L	Diameter D	Pipe ID	Pipe OD
Dimension	80 mm	130 mm	42 mm	50 mm

where ID and OD are the inner and outer diameters of the PVC pipeline respectively.

4.3 EMW2 Sensor Simulation

HFSS was used to design a microwave sensor to operate in a frequency ranging from 200 to 400MHz using a cylindrical cavity resonator and a PVC pipeline. The cavity resonator was given the initial dimensions of 130mm × 80mm. The pipeline was assigned an initial radius of 21mm and length of 130mm. The HFSS model is illustrated in Figure 4.3.

It is well-known that the mode of propagation within the main cylindrical cavity resonator is TE111. The cut off frequency of TE111 is given by Equation 4.3.

$$f_{TE111,c} = \left(\frac{p'_{11}}{2\pi a} \frac{c}{\sqrt{\varepsilon_r \mu_r}} \right) \tag{4.3}$$

The cut off frequency for TM010 mode, can be calculated using equation 4.4.

$$f_{TM010,c} = \left(\frac{p_{01}}{2\pi a} \frac{c}{\sqrt{\varepsilon_r \mu_r}} \right) \tag{4.4}$$

The cut off frequencies of both modes, TE111 and TM010 were calculated using Equations 4.3 and 4.4, and Table 4.1, so that $f_{TE111,c} = 150.2\text{MHz}$, and $f_{TM010,c} = 196.14\text{MHz}$ where $\mu_r = 1$ and $\varepsilon_r = 81$. These values were used in the HFSS set up solution before the simulation is started, as explained earlier in section 3.2.

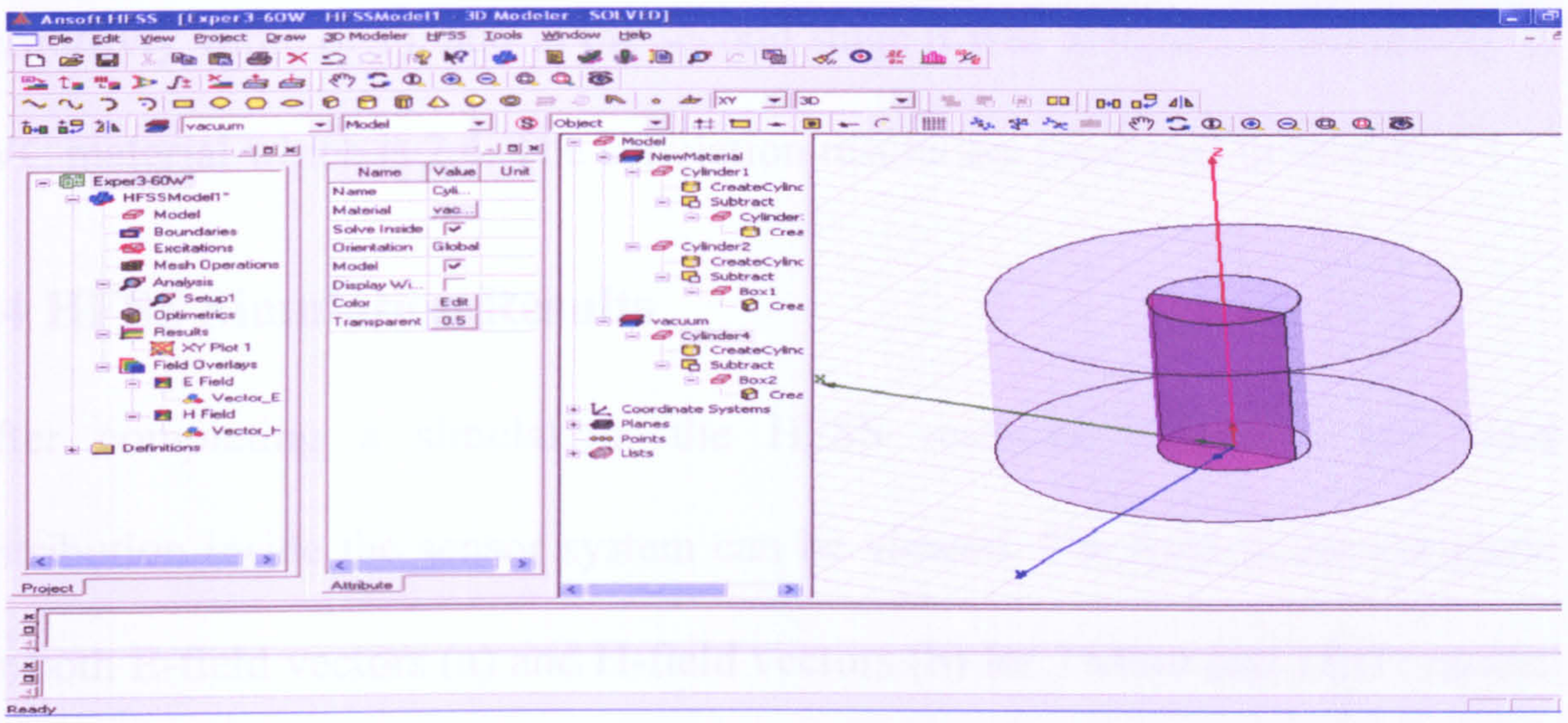

Figure 4.3: HFSS model of the EMW2 sensor using cylindrical cavity resonator and PVC pipe.

In order to design this microwave sensor for multiphase flow in a pipeline, the material used for the pipeline must allow microwave signals to penetrate. This is the reason for choosing a PVC pipeline instead of a metal pipeline, which cannot be penetrated by a microwave signal. However, because of the fully filed water outer cavity resonator and the inner open-ended PVC cavity resonator, the effect of pipeline material type needs to be investigated over full range of the pipeline contents (figure 4.2).

The sensor was modelled, and simulated in two stages over the full range of the pipeline content (water and gas mixture) varying from 0 to 100%. In the first

stage, the PVC pipeline or dielectric liner was simulated as a air (with permittivty value of 1), and in the second stage it was assigned a permittivty of PVC material which is 2.4. The simulation results are presented in section 4.4.

4.4 HFSS Simulation Results

After completing a simulation, the HFSS resonant frequency and field distribution inside the sensor system can be viewed. The field in the y-z plane for both E-field vectors (a) and H-field vectors (b) for TM010 and TE111 modes are shown in Figures 4.4 and 4.5 respectively.

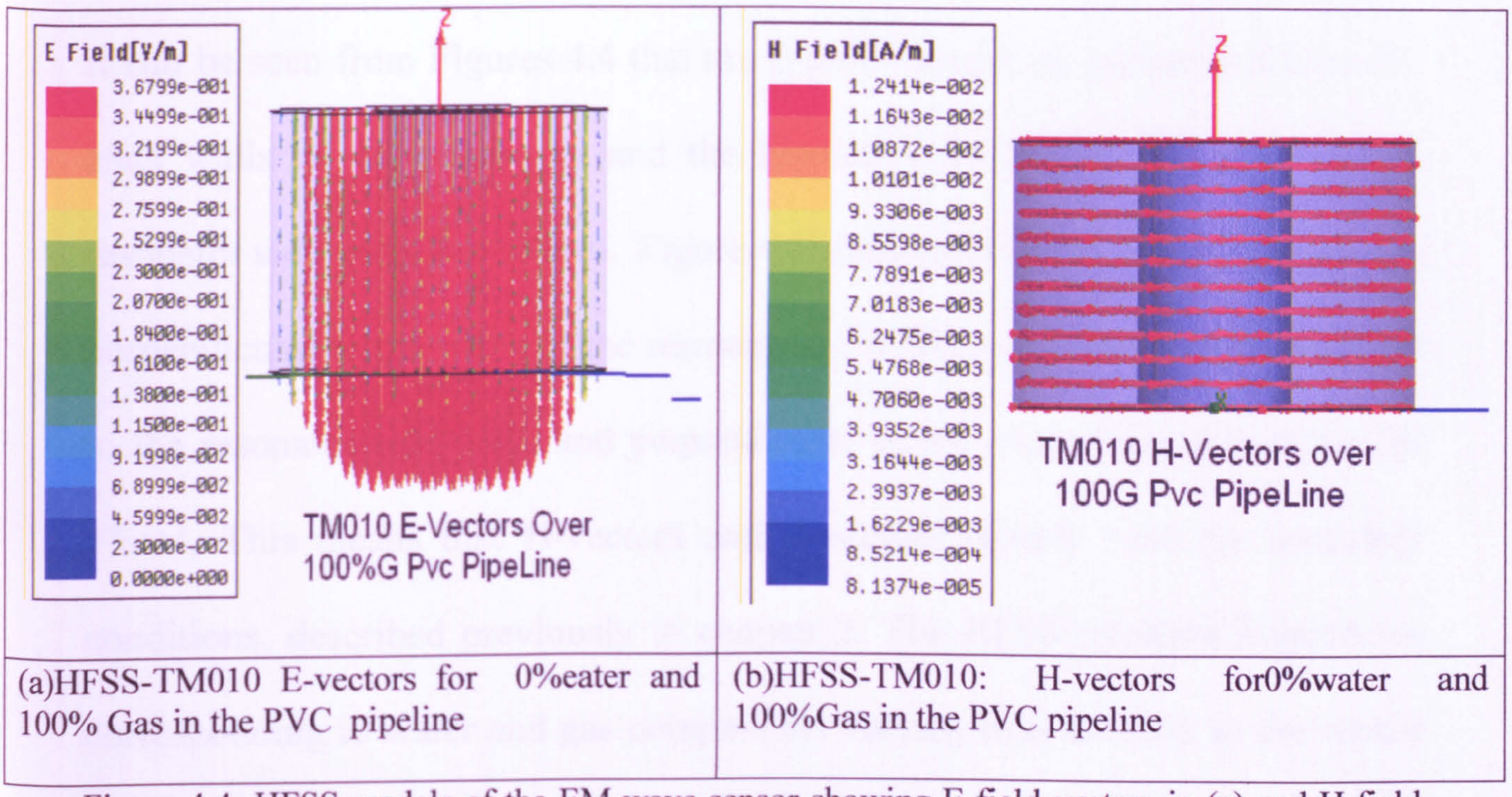

(a)HFSS-TM010 E-vectors for 0%eater and 100% Gas in the PVC pipeline	(b)HFSS-TM010: H-vectors for0%water and 100%Gas in the PVC pipeline

Figure 4.4: HFSS models of the EM wave sensor showing E-field vectors in (a) and H-field vectors in (b) for the TM010 mode.

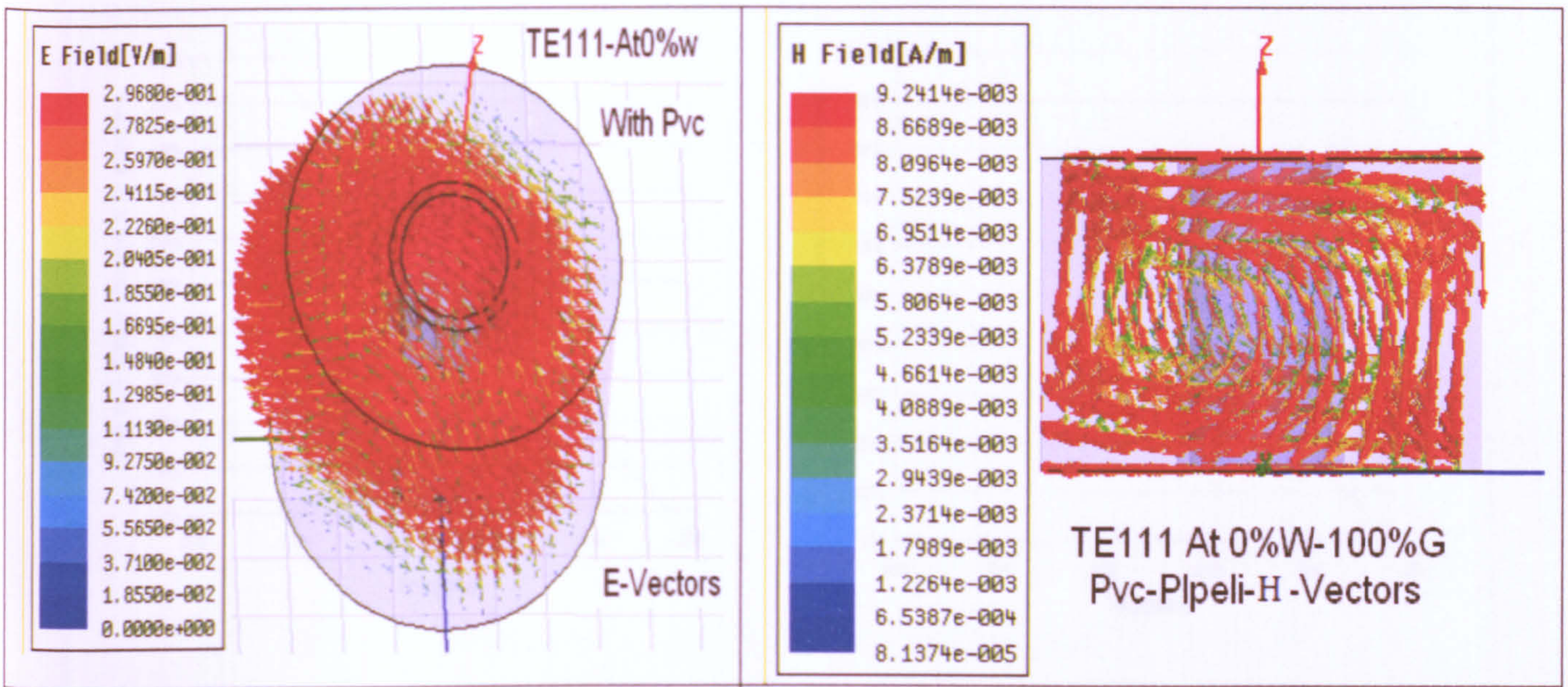

(a)HFSS-TE111:E-vectors for 0%water and 100% Gas in the PVC pipeline

(b)HFSS-TE111:H-vectors for 0% water and 100%Gas in the PVC pipeline

Figure 4.5: HFSS simulation results showing E-field vectors in (a) and H-field vectors in (b) for the TM010 mode at 100%Water, in the pipeline

It can be seen from Figures 4.4 that the E-field vectors are perpendicular to the ends walls of the resonators and the H-vectors are circles tangential to the resonator side walls for TM010. Figure 4.5 shows that as the E-field vectors are perpendicular to the walls of the resonators, the H-vectors are circles tangential to the resonator side walls and perpendicular to the ends of the resonators for TE111. This means that H-vectors and E-vectors comply with the boundary conditions, described previously in chapter 2. The HFSS resonant frequencies corresponding to water and gas components varying over 0-100% in the sensor pipeline can be represented graphically. This is illustrated in Figures (4.6 - 4.7) for TM010 and TE111 modes respectively.

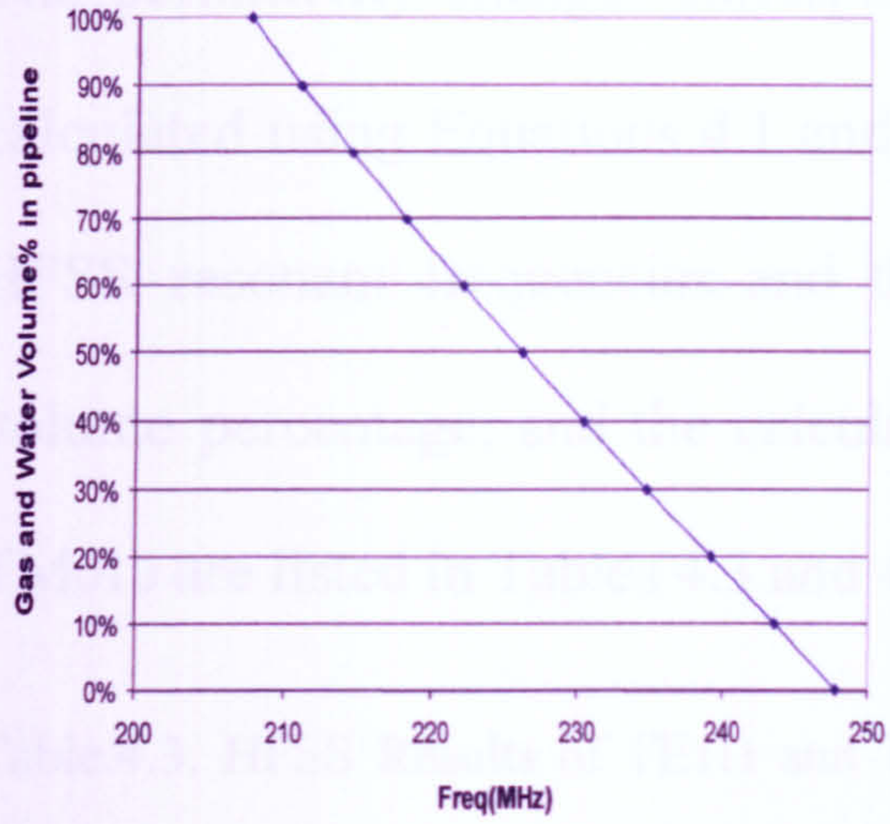

(a) The PVC material of the pipeline is replaced with air in the simulated model

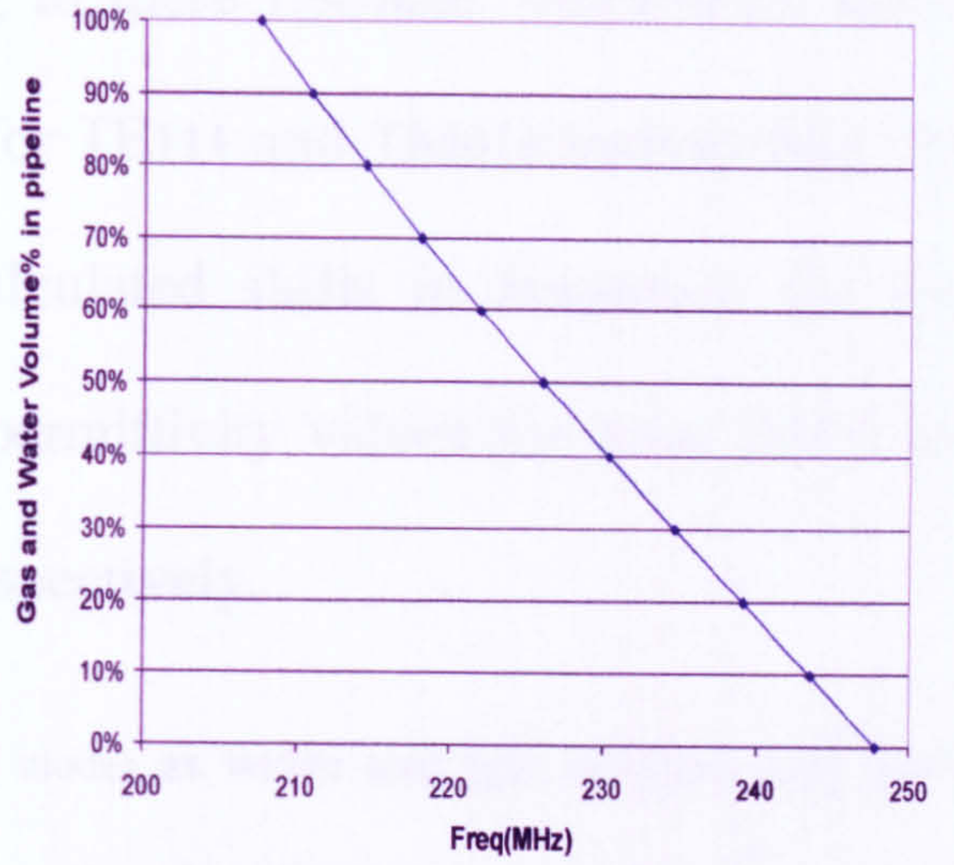

(b)The pipeline is simulated as a PVC pipeline

Figure 4.6: HFSS Resonant frequency results for TM010 mode as the water and gas mixture vary from 0 to 100% in the pipeline.

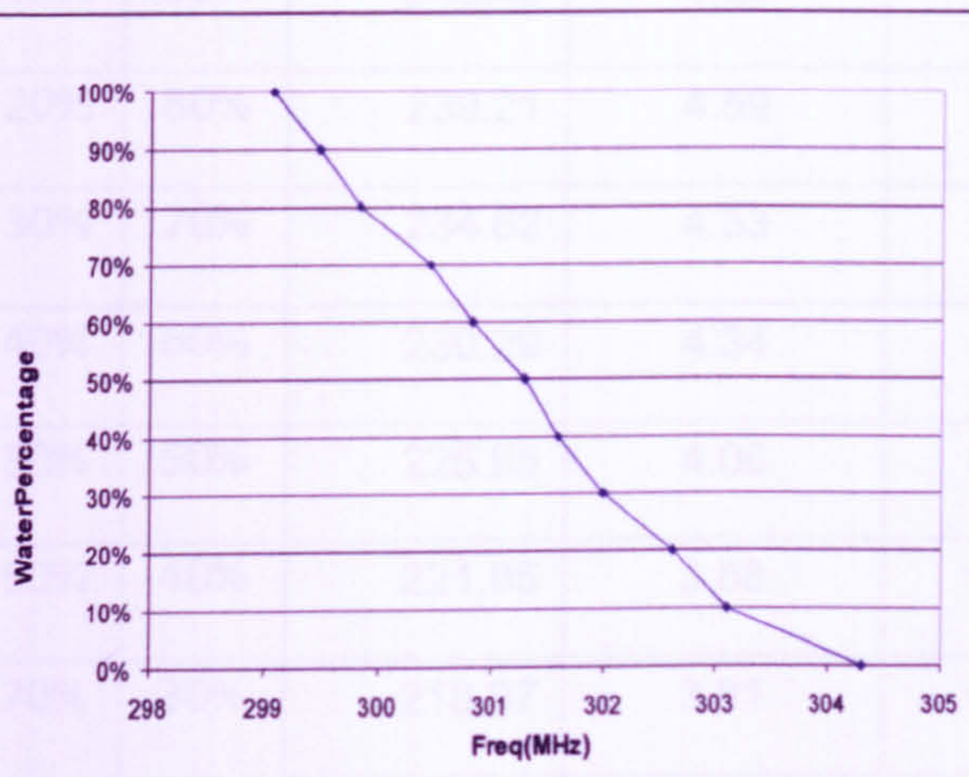

(a) The PVC material of the pipeline is replaced with air in the simulation

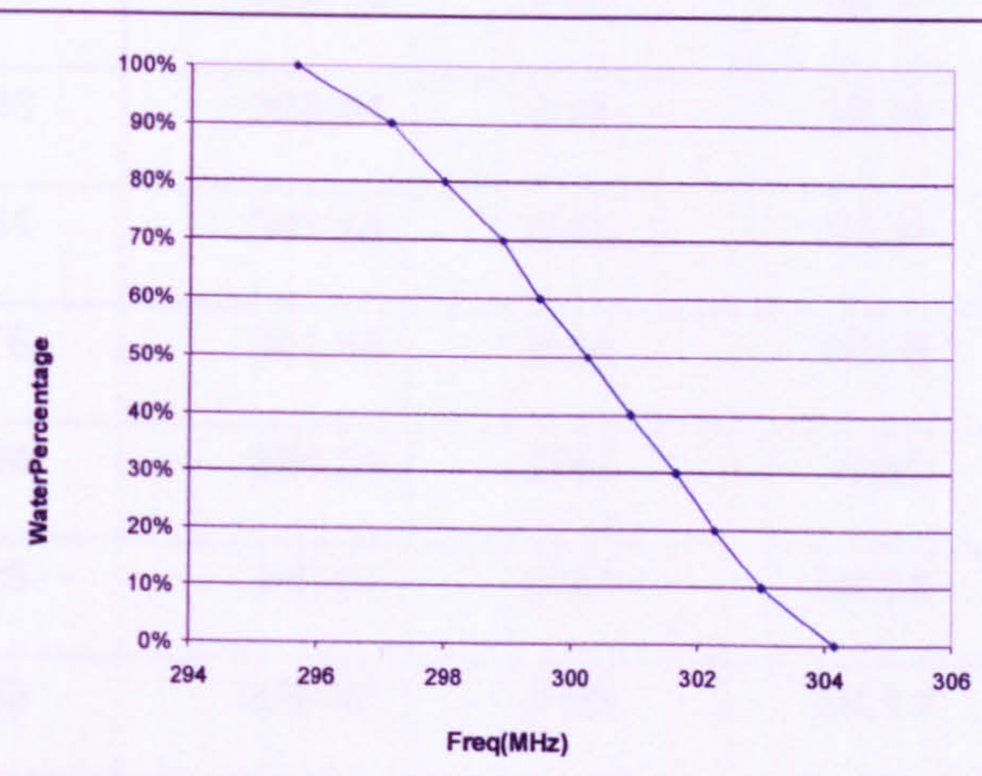

(b) The pipeline is simulated as a PVC pipeline

Figure 4.7: Resonant frequency results for stage1 (a) and stage2 (b) with TE111 mode as the water and gas mixture vary from 0 to 100% in the pipeline.

The permittivity changes corresponding to these resonant frequencies can be calculated using Equations 4.1 and 4.2 for TE111 and TM010 respectively. The HFSS resonant frequencies and the calculated shifts in frequency for each volume percentage, and the calculated permittivity values for both TE111 and TM010 are listed in Tables 4.3 and 4.4 respectively.

Table.4.3. HFSS Results of TE111 and TM010 modes as water and gas mixture vary for 0-100%water. The PVC material of the pipeline is replaced with air in the simulation.

Percentage		TM010 Mode			TE111 Mode		
Water%	Gas%	Freq.(MHz)	Fr. hift(MHz)	Permittivity	Freq.(MHz)	Fr.Shift(MHz)	Permittivity
0%	100%	247.97	4.48	50.68	304.30	1.20	57.64
10%	90%	243.49	4.28	52.56	303.10	0.49	58.10
20%	80%	239.21	4.59	54.46	302.61	0.62	58.29
30%	70%	234.62	4.33	56.61	301.99	0.40	58.53
40%	60%	230.29	4.34	58.76	301.59	0.30	58.68
50%	50%	225.95	4.00	61.04	301.29	0.47	58.80
60%	40%	221.95	3.88	63.26	300.82	0.37	58.98
70%	30%	218.07	3.81	65.53	300.45	0.63	59.13
80%	20%	214.26	3.46	67.88	299.82	0.35	59.34
90%	10%	210.80	3.40	70.13	299.47	0.41	59.52
100%	0%	207.40		72.45	299.06		59.69

These results show that as the permittivity of the mixture changes, the resonant frequency changes as well. Varying the volume percentages for 0-100% in the pipeline (the PVC pipeline was simulated as air in the simulated model) corresponds to a total shift in frequency of 40.57 MHz and 5.24 MHz for TM010 and TE111 modes respectively, as shown in Figures (4.6 - 4.8).

Table 4.4: Stage2: HFSS Results of TE111 and TM010 modes as mixture water and gas vary for 0-100% in a PVC pipeline. The pipeline is simulated as a PVC pipeline.

Percentages		TM010			TE111		
Water%	Gas%	Freq.(MHz)	Freq. Shift	Permittivity(Ɛr)	Freq.(MHz)	Freq. Shift	Permittivity(Ɛr)
0%	100%	247.76	4.23	50.77	304.14	1.145	57.70
10%	90%	243.53	4.42	52.55	302.995	0.74	58.14
20%	80%	239.11	4.44	54.51	302.255	0.61	58.42
30%	70%	234.67	4.38	56.59	301.645	0.74	58.66
40%	60%	230.29	4.27	58.76	300.91	0.67	58.95
50%	50%	226.02	4.1	61.00	300.24	0.76	59.21
60%	40%	221.92	3.84	63.28	299.485	0.58	59.51
70%	30%	218.08	3.71	65.52	298.905	0.94	59.74
80%	20%	214.37	3.49	67.81	297.965	0.83	60.12
90%	10%	210.88	3.39	70.08	297.135	1.50	60.45
100%	0%	207.49		72.38	295.64		61.07

Comparing the total shifts in frequency, on the other hand, for both TE111 and TM010 (as the material type of the pipeline used in the simulated model is PVC and air) shows that the frequency shifts in TE111 is increased from 5.24 to 8.5 MHz. The total frequency shifts in TM010 is decreased from 40.57 to 40.27 MHz (see Tables 4.3 and 4.4).

This effect might be referred immediately to presence of PVC pipeline as if TE111 is negatively affected as its frequency shift is decreased and positively affected TM010 as its frequency shifts is increased. This argument is discussed in details in chapter 6.

4.5 EMW2 Sensor Resonators Design

The sensor system set up, which was illustrated in Figure 4.8, shows the components used to create a complete system. In this system, the microwave source was a Marconi Microwave Test Set (MTS) 6200A, which is capable for generating and detecting electromagnetic waves in a frequency range of 10MHz to 20GHz.

As discussed earlier, this sensor system was carried out using the main cavity resonator, which is constructed out of a brass cylindrical cavity with shorted ends, and a PVC pipeline. The sensor is coupled to the Marconi MTS with

coaxial cables, and two antennas are used for transmitting and receiving the microwave signals to and from the sensor. The sensor system output is connected to a PC data logger, using a National Instrument GPIB interface [66]. Figures 4.8 and 4.9 show the final cavity resonator fitted to the pipeline.

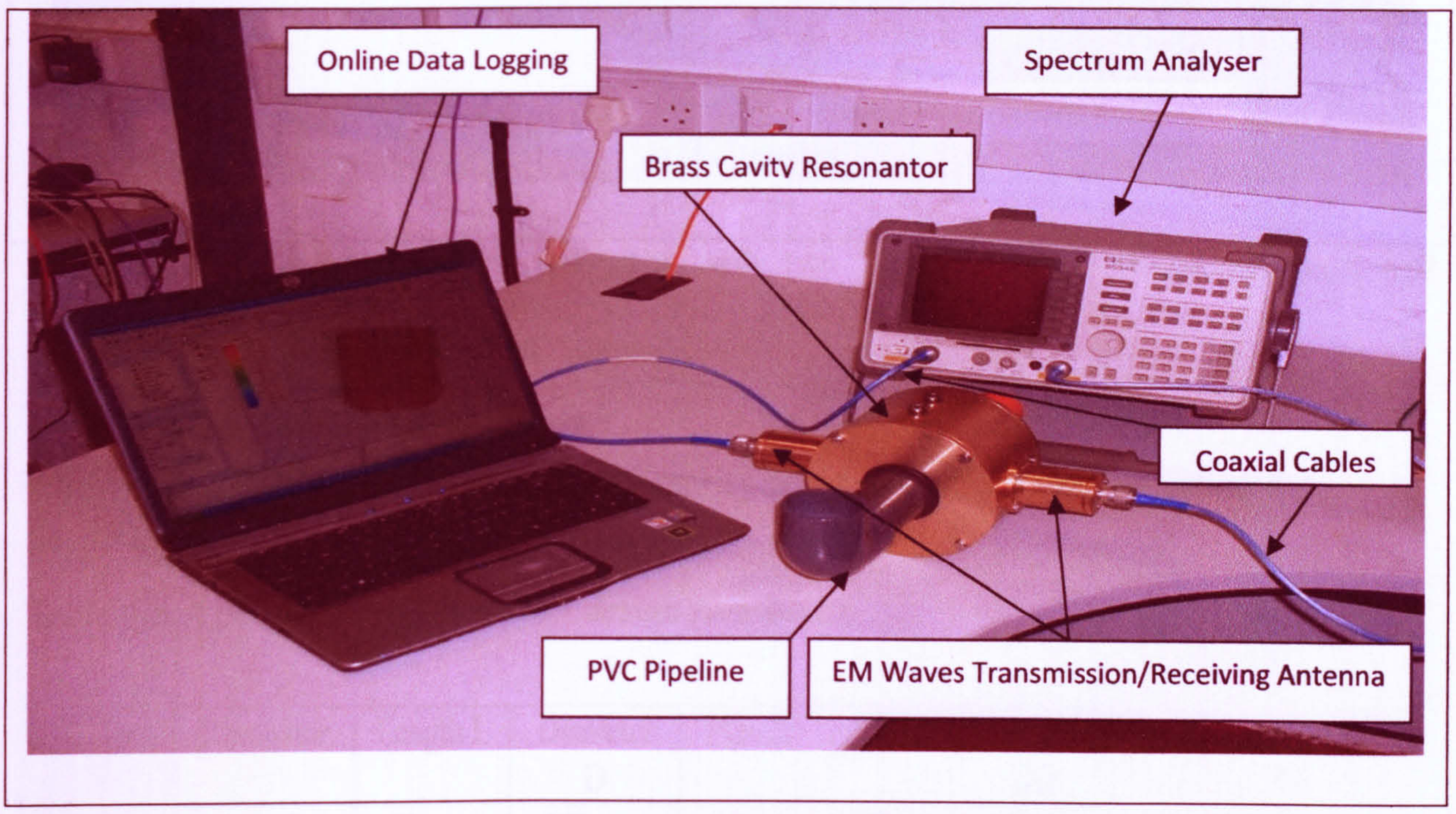

Figure 4.8: EMW2 Sensor System Prototype

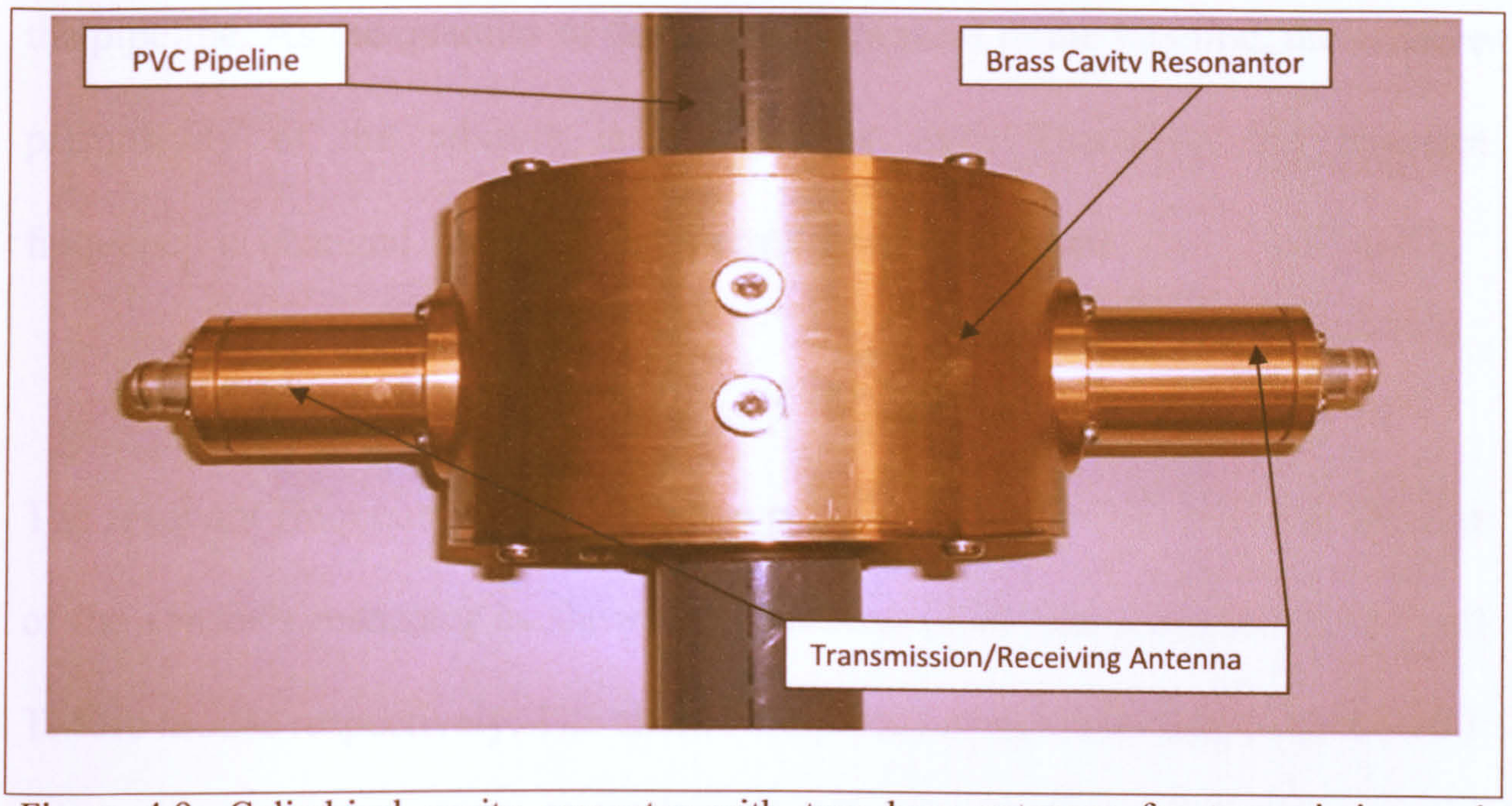

Figure 4.9: Cylindrical cavity resonator with two loop antennas for transmission and receiving EM Waves, and the PVC pipeline.

The final design parameters for the cavity resonator are listed in Table 4.5.

Table 4.5: The final cavity resonator design parameters

Resonator	Length L	Diameter D	Pipe ID	Pipe L	Plastic OD
Dimensions	80 mm	130 mm	42 mm	333mm	50 mm

4.6 Experiments Results

Experiments were carried out using the set up shown in Figure 4.10.The quantities of two phase (water and gas) mixture were varied from 0 to 100% in

the pipeline. As the quantity of the mixture is varied in the pipeline, the relative permittivity of the mixture is changed as well. Therefore, the resonant frequency is changed as the mixture permittivity is changed.

The resonant frequency and the relative permittivity are both related to the size of the sensor's resonator as shown in equations (2.28 and 2.29) for TE111 and TM010 modes respectively. The chosen frequency range described in section 4.1 was not only chosen prevent water salinity effect on the sensor, but also to make it possible to design a large dimension sensor's resonator suitable for a practical oil transmission line.

Consequently, for each experiment carried out, the corresponding resonant frequencies were captured via the data logger with the National Instrument GPIB and capturing software [67]. The spectrums captured during these experiments for both TE111 and TM010 are shown in Figure 4.10.

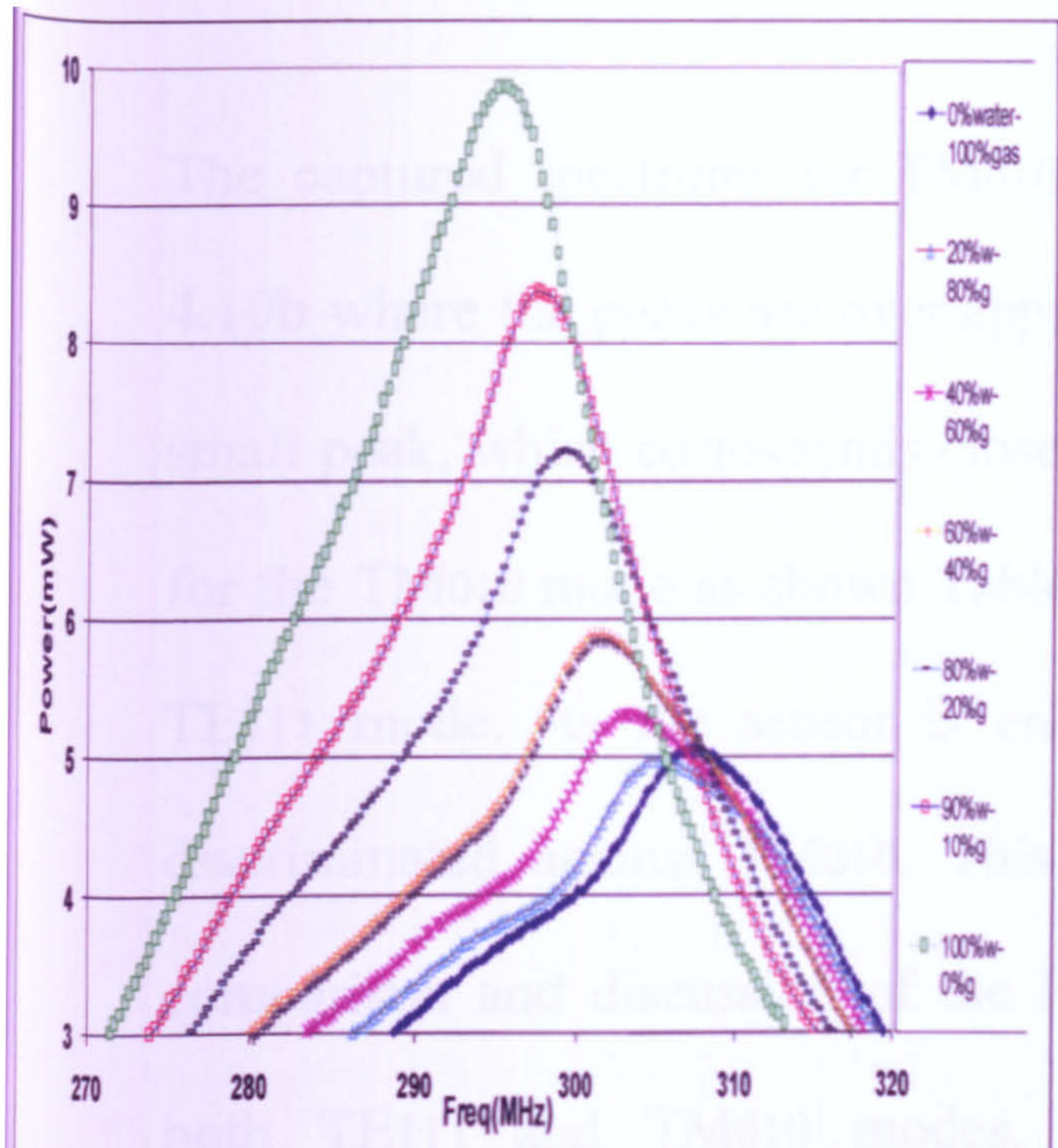

(a)EMW2 Sensor: TE111 Mode peak

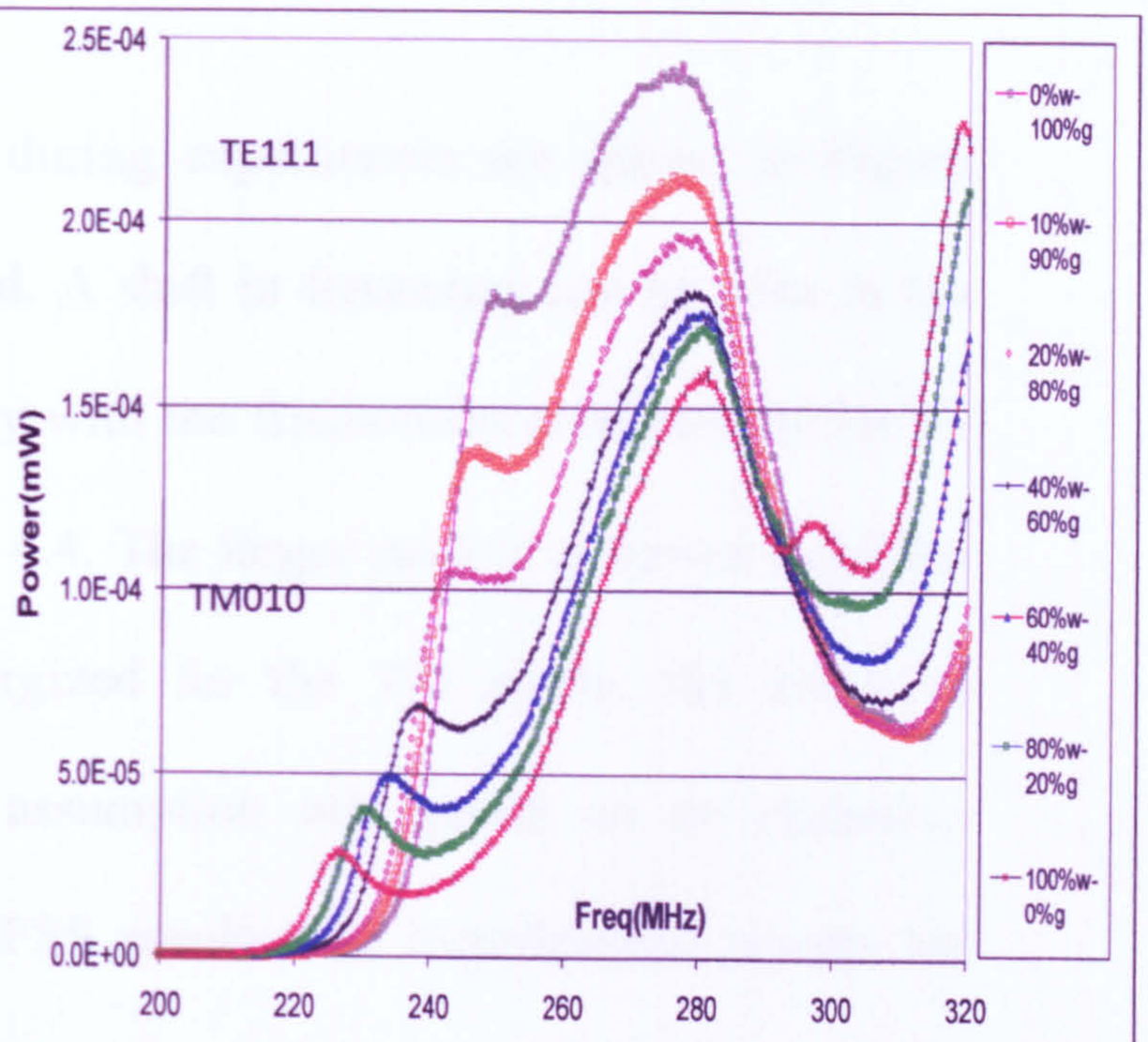

(b) EMW2 Sensor: TM010 Mode peak

Figure 4.10: Experimental results showing the frequency shift in TE111 peak (a) and TM010 (b) peak as the water and gas mixture varies from 0 to 100% in the PVC pipeline.

The shifts in frequency in the TE111 peak are shown in Figure 4.10a. It can be seen clearly from this Figure that as the permittivity is changed the frequency is shifted as well. In other words, as the permittivity is increased, the amplitude is in increased well, but the frequency is decreased. These changes of amplitude can be regarded to the loop antennas used for transmitting and receiving the microwave signals. Analysing these results shows that the resonant frequencies closely correspond to the predicted HFSS simulation results shown in Table 4.4 with a total frequency shift of 12.5 MHz.

The captured spectrums for TM010 during experiments are shown in Figure 4.10b where the peaks are overlapped. A shift in frequency can be seen in the small peak, which corresponds closely with the frequencies predicted by HFSS for the TM010 mode as shown Table 4.4. The larger peak is assumed to be the TE111 mode. As the sensor is energized for the TM mode, the TE111 is discriminated against TM010. This assumption was based on an extensive comparison and discussion of the HFSS results and experimental results for both TE111 and TM010 modes. For the reasons of consistency, these comparisons and discussions have been left until chapter 6. Since then, a decision was taken to develop one more accurate sensor for three-phase (oil, gas, water) measurements. This is described in chapter 5.

4.7 Conclusion

Electromagnetic wave (EMW2) sensor operating at microwave frequencies ranging from 200MHz to 400MHz was simulated, designed and constructed based on a cylindrical cavity resonator fitted in-line to accurately detect and measure two phase (water and gas mixtures) component fractions in real time, expressed in volume percentages.

The HFSS simulation results and the experimental results for the two fundamental modes, TE111, TM010 were presented, compared and analysed. Based on these results, the conclusion can be outlined as follows:

- The sensor was found to be accurate, compact in size, and capable for detecting and measuring the two phase (water and gas) component fractions in a pipeline with the TE111 mode. The total experimental frequency shift was found to be 12.5MHz. The HFSS total frequency shift was found to be 8.5MHz.
- The measuring of two phase component fractions using the TM010 mode was found very difficult. It was found that even when the sensor was energized for TM mode, the TE111 still dominated. This problem was referred to the presence of the (PVC) material of the pipeline.

CHAPTER 5

Electromagnetic Wave EMW3 Sensor Design

5.1 Introduction

A non intrusive electromagnetic wave (EMW3) sensor operating at microwave frequency was designed and constructed for online monitoring and measuring multiphase flow (oil, gas, and water) fractions, expressed in Volume % in pipeline. The sensor is based on a cylindrical cavity resonator, and it uses the shift in resonant frequency to detect and measure the components of multiphase flow in a pipeline [68, 69].

HFSS was used to design both the cavity resonator and PVC pipeline. The cavity resonator was designed based on a short circuited cylindrical cavity, and the PVC pipeline was designed based on an open-ended PVC cylindrical cavity.

Based on the results of the EMW2 sensor, the chosen modes of operation was TE111 mode, which was found the accreted and dominated mode in both the TE and TM modes.

The Marconi Microwave Test Set 6200A was chosen as a microwave source [62]. Then the system was designed and constructed, and coupled to a PC with the National Instruments GPIB interface [66]. An overview of the system prototype set up is shown schematically and graphically in Figures 5.1a and 5.1b respectively.

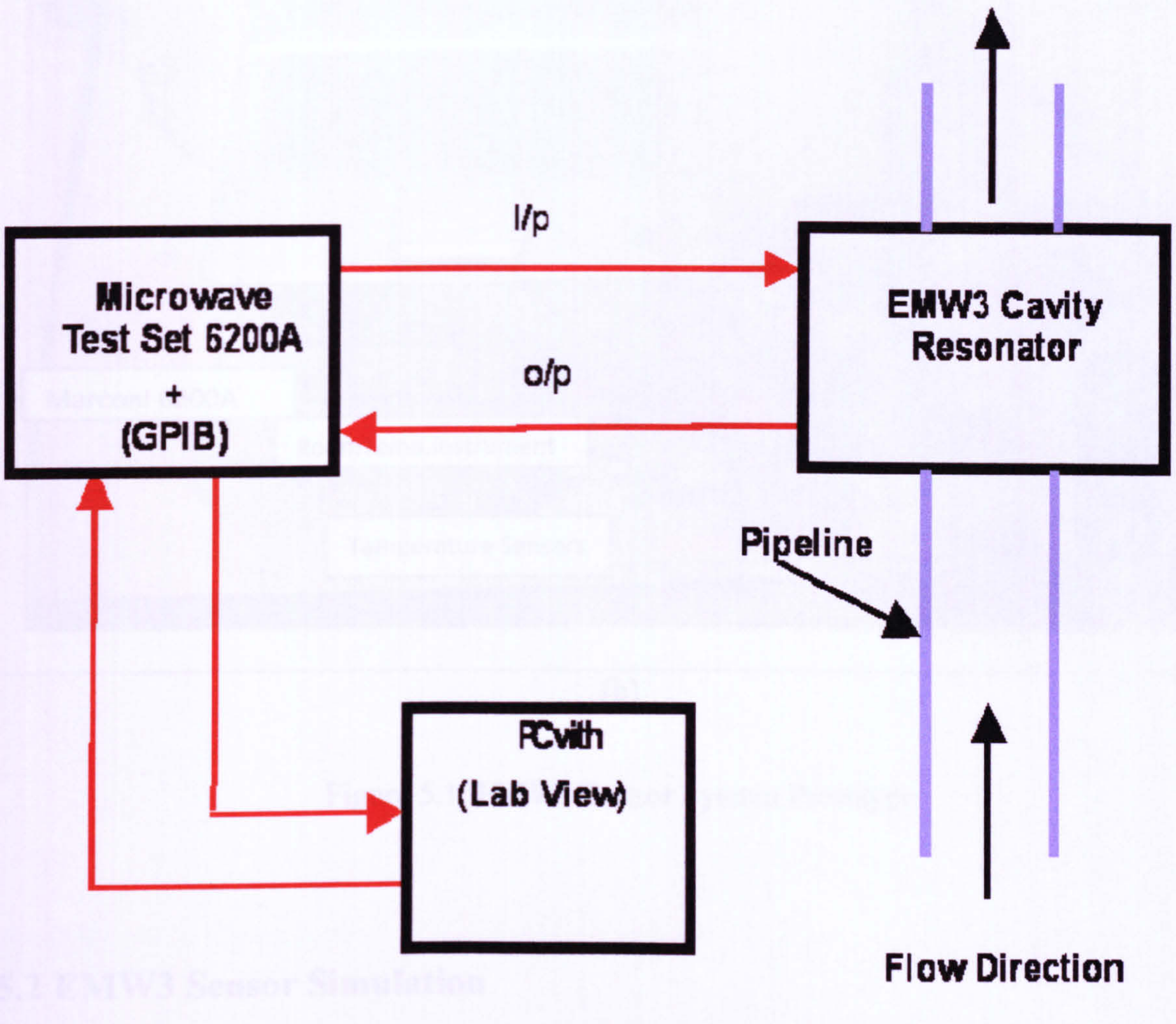

(a)

Figure 5.1: EMW3 Sensor System Prototype

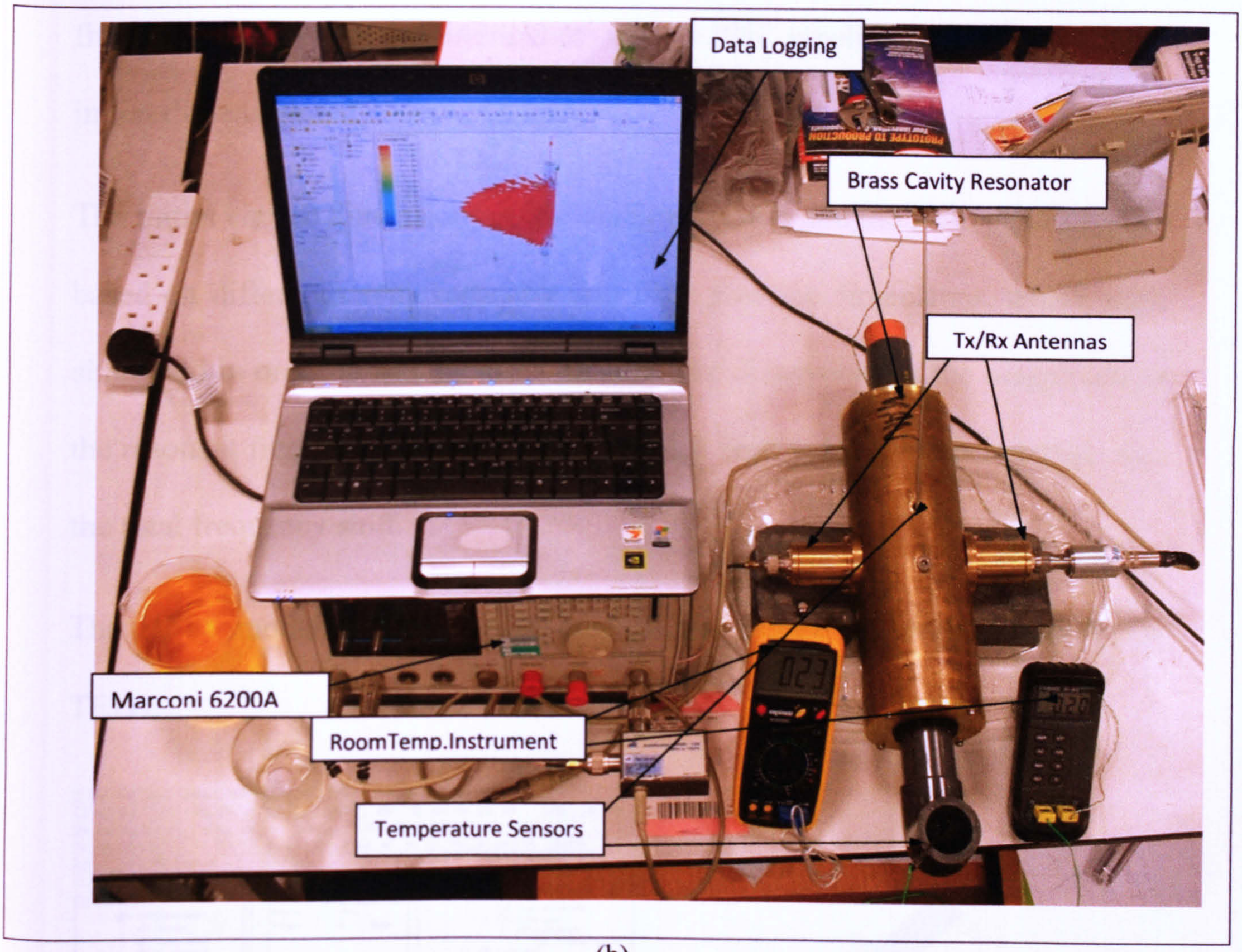

(b)

Figure 5.1: EMW3 Sensor System Prototype

5.2 EMW3 Sensor Simulation

The HFSS software package was used to design a microwave sensor system to operate in frequency ranging from 200 to 400 MHz using a brass cylindrical

cavity resonator with initial internal dimensions of 300mm × 100mm, which is fitted to an open-ended cylindrical cavity as a PVC pipeline which is also given initial dimensions of 300mm × 42mm.

The initial chosen dimensions of the cavity resonator and the PVC pipeline were based on different cavity resonator and PVC pipeline dimensions, which were simulated in order to see the effect of different dimensions in the magnitude of the resonant frequency, the resonant frequency shift per volume percentage, and the total frequency shift.

The HFSS model for this sensor is shown in Figure 5.2 with E-vectors for TE111.

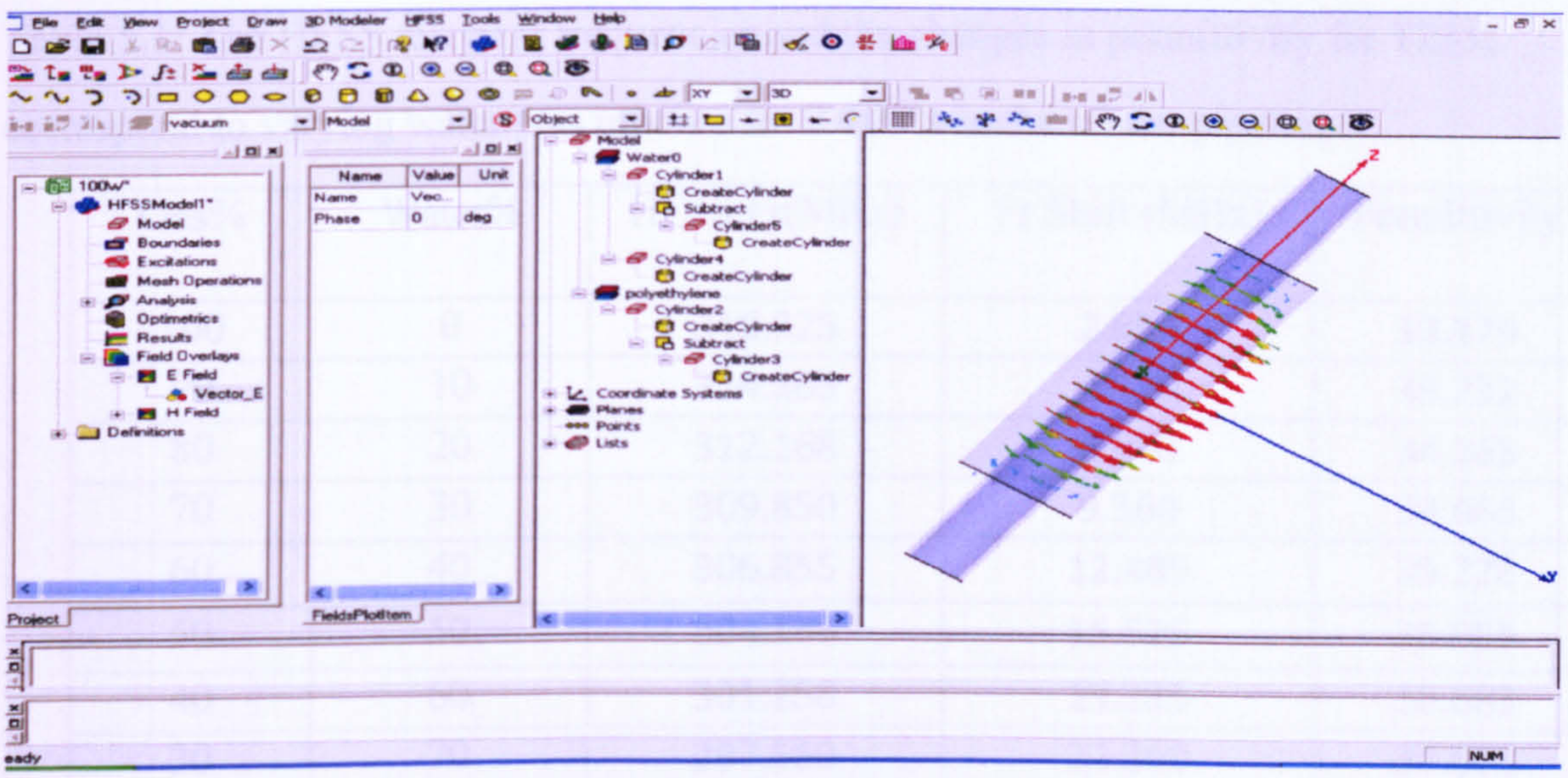

Figure 5.2: HFSS modelling of the EM W3sensor based on a cylindrical cavity resonator and PVC pipeline.

It can be seen from Figure 5.2 that the E-field vectors are perpendicular to the walls of the cylindrical resonators, both the brass resonator and the PVC pipeline. Thus, the boundary conditions described early in chapter two are satisfied.

5.3 HFSS Simulation Results

The sensor model was simulated over full ranges of multiphase flow varying from 0 to 100% in the sensor pipeline. As the permittivity changes for each percentage, the frequency shifts as well. The HFSS resonant frequencies and the corresponding calculated changes in permittivity are tabulated as shown in Table 5.1.

Table 5.1: The HFSS resonant frequencies and the changes in permittivity for TE111 correspond to varying water/Gas mixture for 0-100% in the sensor pipeline.

Gas%	Water%	HFSS.Fr(MHz)	Fr.Shift (MHz)	Permittivity
100	0	316.225	2.610	33.179
90	10	314.105	4.610	33.732
80	20	312.168	6.860	34.165
70	30	309.850	9.360	34.663
60	40	306.855	12.485	35.228
50	50	304.185	15.525	35.955
40	60	301.258	19.235	36.683
30	70	297.550	22.360	37.603
20	80	294.438	26.360	38.404
10	90	290.450	34.235	39.468
0	100	282.590	2.610	41.696

Varying water and gas mixture from 0 to100% in the pipeline corresponds to a total shift in frequency of 35.1MHz. A graphical representation relating the volume percentages to the HFSS resonant frequencies is shown in Figure 5.3.

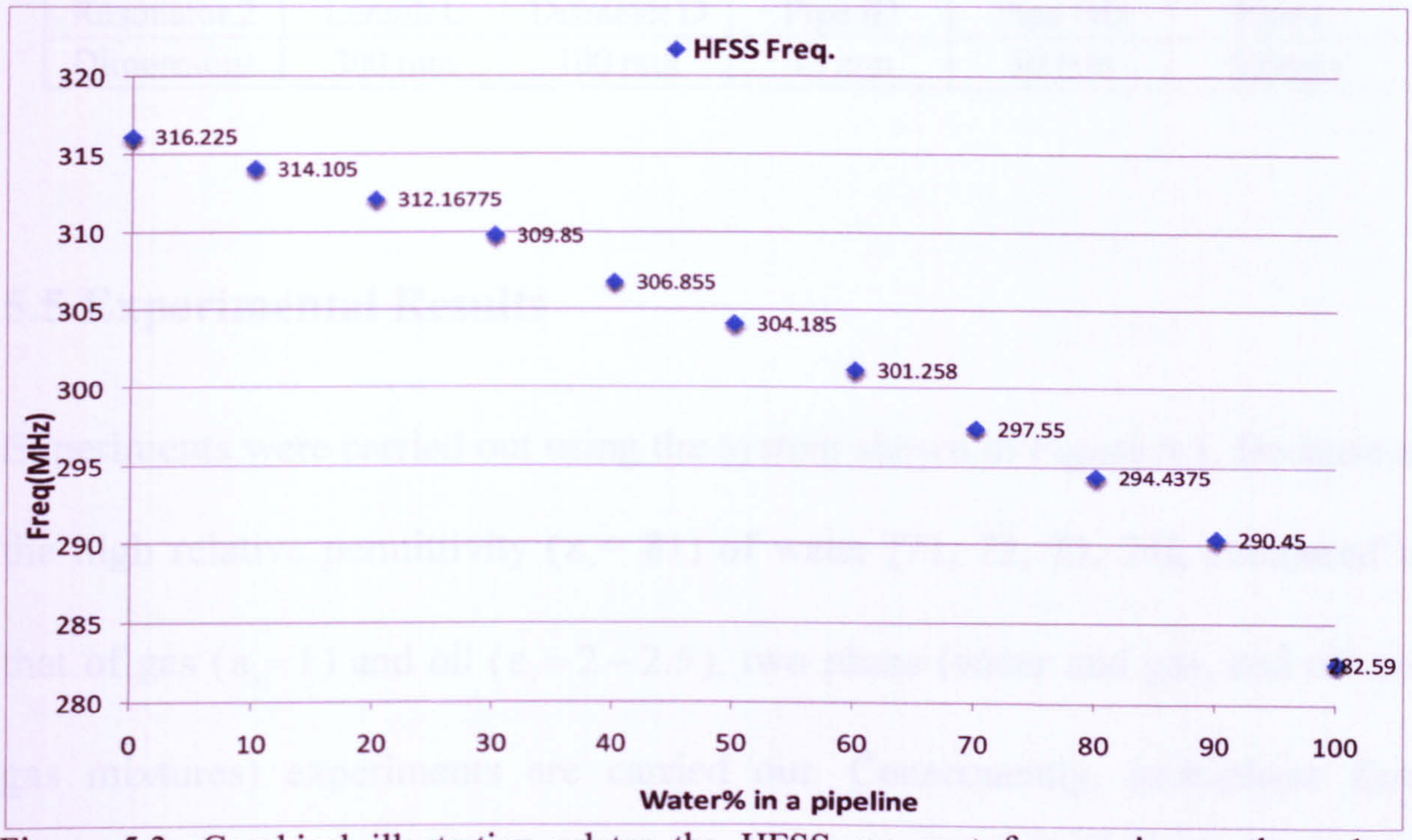

Figure 5.3: Graphical illustration relates the HFSS resonant frequencies to the volume percentages as the water volume changes from 0 to 100% in the pipeline.

5.4 EMW3 Sensor Resonator Design

The system set up described earlier and shown in Figure 5.1b shows the final designed version of the resonator fitted to the pipeline. In addition to the optimal length found for the pipeline, the final design parameters for the sensor are listed in Table 5.2. This design allows a homogeneous mixture (oil, gas and

water mixed components) to pass though a non intrusive pipeline, and protects the antennas from the flowing materials [70].

Table 5.2: The final cavity resonator design parameters

Resonator.2	Length L	Diameter D	Pipe ID	Pipe OD	Pipe L
Dimensions	300 mm	100 mm	42 mm	50 mm	500mm

5.5 Experimental Results

Experiments were carried out using the system shown in Figure 5.1. Because of the high relative permittivity ($\varepsilon_r = 81$) of water [71, 72, 73, 74], compared to that of gas ($\varepsilon_r = 1$) and oil ($\varepsilon_r = 2 - 2.5$), two phase (water and gas, and oil and gas mixtures) experiments are carried out. Consequently, multiphase flow experiments are carried out over the full range of oil, water, and gas mixture flowing in the pipeline, and the measured phase components are measured and expressed in volume%.

A spectrums captured during the experiments of two phases are shown in figure 5.4.

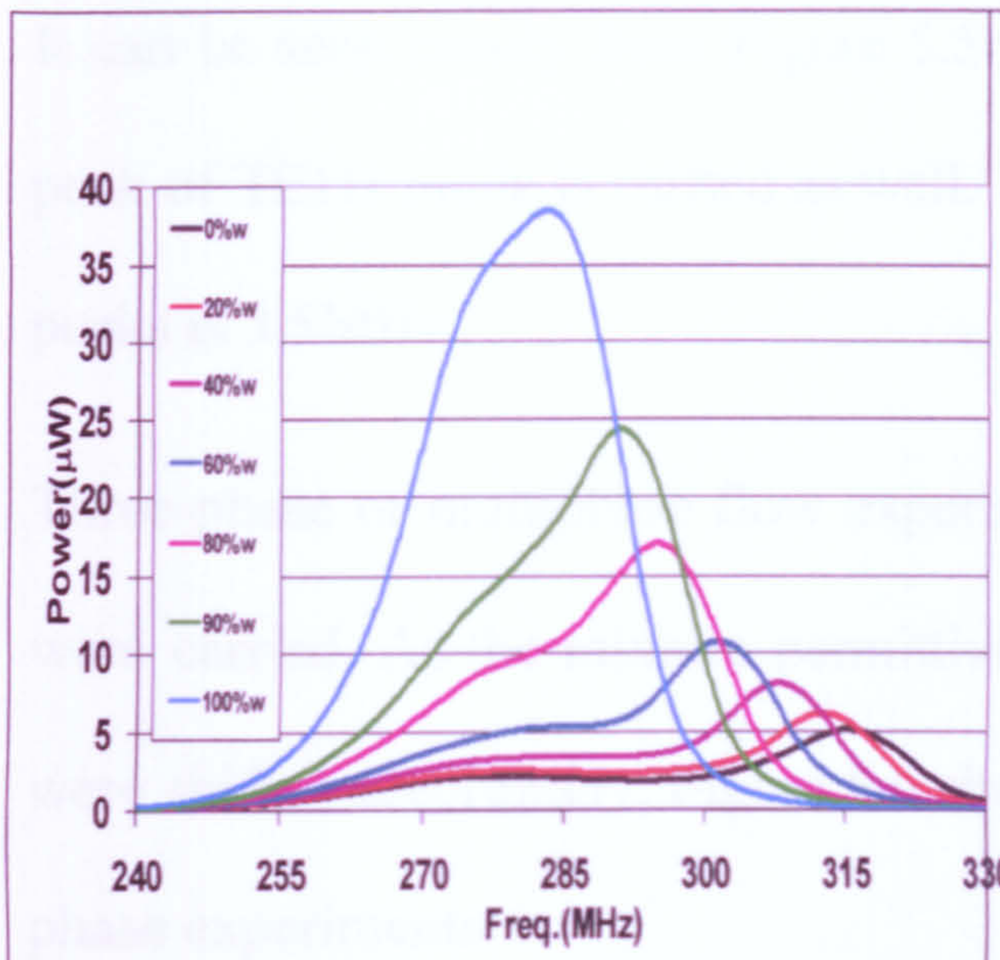

(a) Experiment results two phase (gas and water)

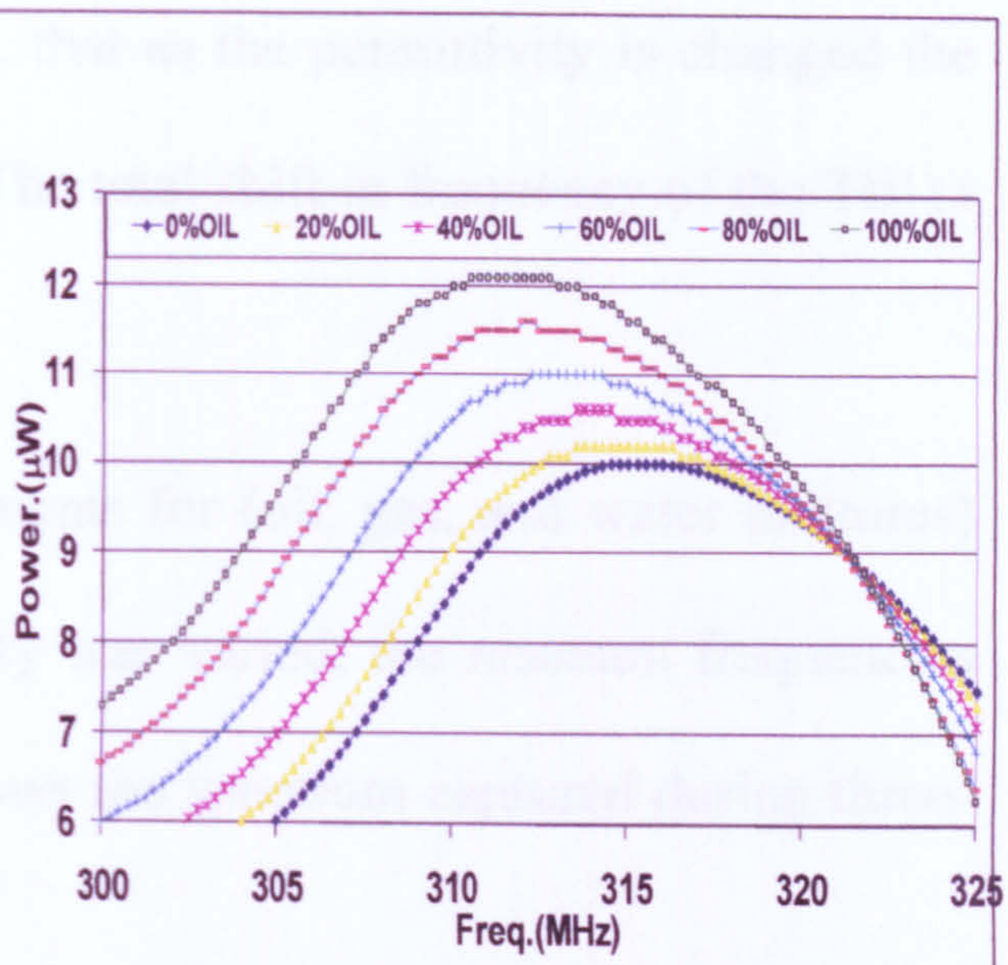

(b) Experiment results two phase (oil and gas)

Figure 5.4: Experimental results showing the captured spectrums for the two phase (gas and water) in (a) and for the two phases (oil and gas) in (b).

It can be seen clearly from Figure 5.4a, that the peak of the TE111 mode is shifted as the permittivity is changed. The total shifts in frequency for varying volume percentages from 0 to 100%, is 32MHz.

As with the two phase (water and gas mixture) fractions experiments, two phase (oil and gas mixture) experiments were carried out as well. Figure 5.4b shows the spectrum captured during these experiments.

It can be seen clearly from Figure 5.5b, that as the permittivity is changed the peak of TE111 mode is shifted as well. The total shift in frequency of the TE111 peaks is 3.5MHz.

Three-phase or multiphase flow experiments for (oil, gas, and water mixtures) were carried. As the mixture permittivity was varied, the resonant frequencies were shifted accordingly. Figure 5.6 shows the spectrum captured during three-phase experiments.

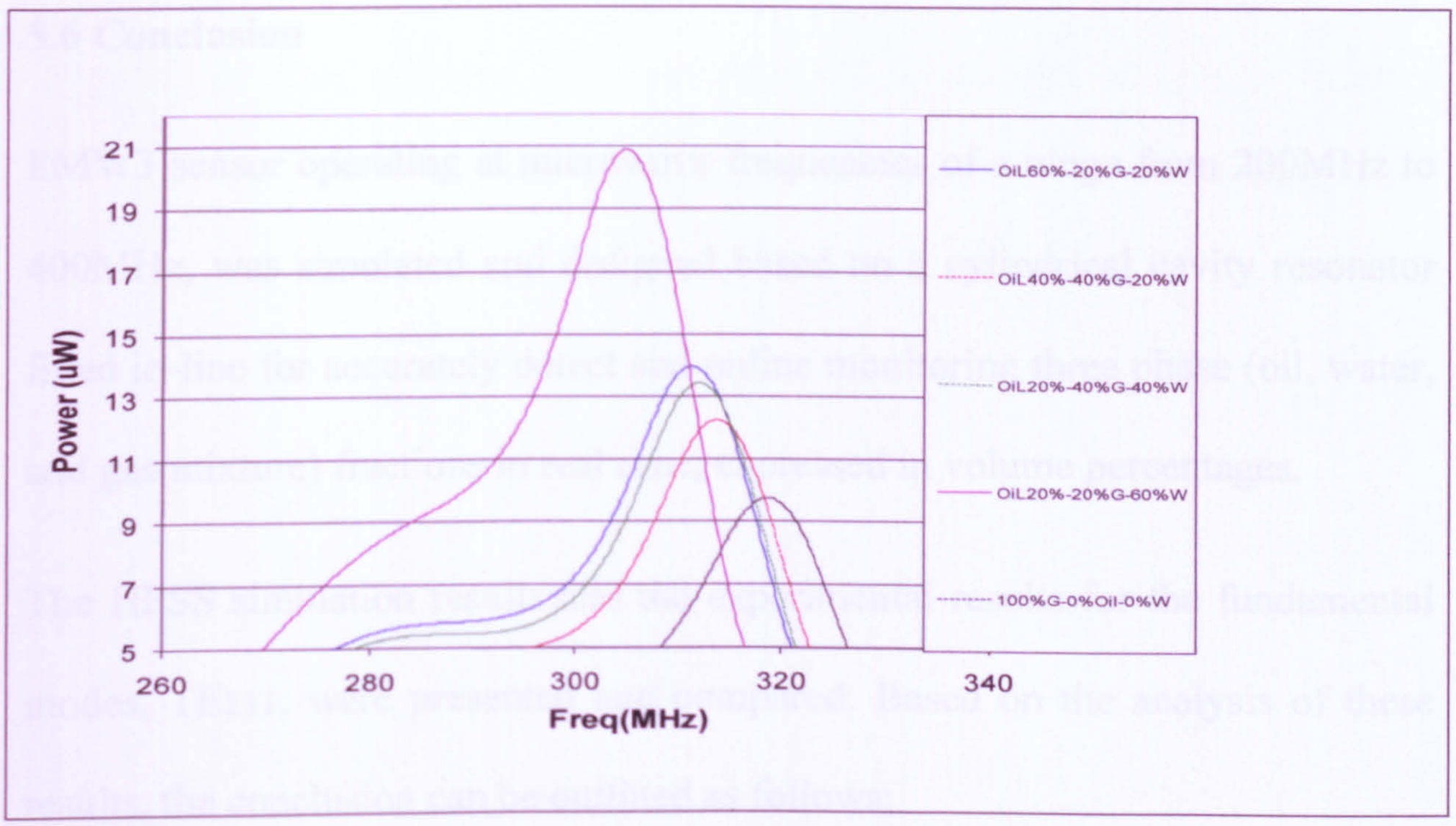

Figure 5.5: The TE111 peak frequency shifts for three-phase (oil and gas and water) mixtures.

Based on these results and their analysis in chapter 6, a new software application programme was developed to explore the power of this sensor to monitor, measure, and control multiphase flow fractions online. This is explained in chapter 7. The two phase experiments results, including the results of the heat effect on frequency shifts, for both sensors will be compared and analysed in chapter 6.

5.6 Conclusion

EMW3 sensor operating at microwave frequencies of a range from 200MHz to 400MHz, was simulated and designed based on a cylindrical cavity resonator fitted in-line for accurately detect and online monitoring three phase (oil, water, and gas mixture) fractions in real time, expressed in volume percentages.

The HFSS simulation results and the experimental results for the fundamental modes, TE111, were presented and compared. Based on the analysis of these results, the conclusion can be outlined as follows:

- The sensor was found to be accurate, compact in size, and capable for detecting and measuring two phase (oil / gas, water gas) and three phase

(oil, gas, and water) component fractions in a pipeline with the TE111 mode.

- The total experimental frequency shift was found to be 34.235MHz, while the HFSS total frequency shift was found to be 33.635MHz.
- The maximum, minimum, and average divergence between the HFSS simulation and experimental resonant frequencies were found to be 0.29%, 0.101%, and 0.145% respectively.
- The main drawback found within this sensor was its sensitivity to the temperature changes. This problem was overcome in chapter 7, as a thermo controlled unit was added to the system to vary and control the temperature within the sensor.

Page numbering as found in the original thesis

Appendix 1

List of Publications

1.- GERI Annual Research Symposium (GARS) 2007

Liverpool John Moores University, June 27th, 2007

Smart Microwave On-Line Sensor for Multiphase Metering In the Oil and Gas Industry

S. Al-Hajeri, S. R. Wylie, R. A. Stuart, A. I. Al-Shamma'a.

Abstract

A significant problem in the oil and gas industry is how to measure oil, gas, and water mixtures. The industry requires accurate on line sensors to monitor the fluid flow in pipelines, in order to manage wells efficiently. The sensor described in this paper uses the different relative permittivity values for the three phases: oil, gas and water to help determine the fraction of each phase in the pipeline, by monitoring the resonant frequencies that

occur within an electromagnetic cavity. The sensor has been designed to be non-intrusive. This is advantageous as it will prevent the sensor being damaged by the flow through the pipeline and allow pigging; the techniques used for cleaning rust and wax from the inside of the pipeline using blades or brushes. A laboratory prototype version of the sensor has been constructed and the results are compared to those simulated, using HFSS.

2.- 41st Annual International Microwave Symposium Proceedings 2007

Vancouver - Canada, August 1st - 3th, 2007

RF-Microwave Monitoring Sensor for the Oil Industry

S. Al-Hajeri, S.R. Wylie, A. Shaw, A.I. Al-Shamma'a

Abstract

A reliable monitoring system is an important component of the offshore.

Existing designs of monitor sensor(s) are widely used and often provide useful results, but they can require regular calibration and many struggle to provide reliable quantitative measurements. At Liverpool John Moores University we have been investigating the propagation of RF and

microwaves through various mediums within the oil pipe including oil, gas, water and sand in order to quantify the dielectric properties of medium mixtures. The sensor is non-invasive and relies on the relatively high dielectric constant of the pipeline mixtures. The electromagnetic wave field profiles within the pipeline have been modelled and simulated using a higher frequency structure simulator (HFSS) package. This paper describes the microwave system set-up including the transmitting and receiving antennas. Theoretical modelling and experimental results of various mixtures will be presented.

3.- IoP Sensors & their Applications XIV

The Instrument Science and technology group

Liverpool John Moores University, September 11th – 13th, 2007

An Electromagnetic Cavity Sensor for Multiphase Measurement in the Oil and gas industry

S. Al-Hajeri, S.R. Wylie, R.A. Stuart and A.I. Al-Shamma'a

Abstract

The oil and gas industry require accurate sensors to monitor fluid flow in pipelines in order to manage wells efficiently. The sensor described in this paper uses the different relative permittivity values for the three phases: oil, gas and water to help determine the fraction of each phase in the pipeline, by monitoring the resonant frequencies that occur within an electromagnetic cavity. The sensor has been designed to be non-intrusive. This is advantageous as it will prevent the sensor being damaged by the flow through the pipeline and allow pigging, the technique used for cleaning rust and wax from the inside of the pipeline using blades or brushes.

4.- GERI Annual Research Symposium (GARS) 2008

Liverpool John Moores University, June 25th, 2008

Smart Microwave On-Line Sensor for Multiphase Metering In the Oil and Gas Industry

S. H. Al-Hajeri, S. R. Wylie, A. Shaw and A. I. Al-Shamma'a

Abstract

Measuring oil, gas, and water fraction percentages in a dynamic pipeline is a significant problem in the oil and gas industry. In order to manage wells efficiently, the industry requires accurate on line sensors to monitor the fluid flow in pipelines. The sensor described in this paper uses different relative permittivity values of three phases: oil, gas and water to help determine the fraction of each phase in the pipeline, by monitoring the resonant frequencies that occur within an electromagnetic cavity. The sensor has been designed to be non-intrusive. This is advantageous as it will prevent the sensor being damaged by the flow through the pipeline and allow pigging. Techniques used for cleaning rust and wax from the inside of the pipeline using blades or brushes. A laboratory prototype version of the sensor system has been constructed, and the experimental results are compared to the simulation results which have been obtained by the use of High Frequency Structure Simulation (HFSS) software package. Finally, the system was automated, using National Instrumentation (NI) devices and Lab view software package, and an online real time results are read and captured.

5.- IoP Sensors & their Applications XV

The Instrument Science and technology group

Edinburgh, UK, October 5th – 7th, 2009

Real Time EM Waves Monitoring System for oil Industry Three Phase Flow Measurement

S. Al-Hajeri, S. R. Wylie, A. Shaw and A. I. Al-Shamma'a

Abstract

Monitoring fluid flow in a dynamic pipeline is a significant problem in the oil industry. In order to manage oil field wells efficiently, the oil industry requires accurate on line sensors to monitor the oil, gas, and water flow in the production pipelines. This paper describes a sensor that is based on an EM Waves cavity resonator. It determines and monitors the percentage volumes of each phase of three phase (oil, gas, and water) in the pipeline, using the resonant frequencies shifts that occur within an electromagnetic cavity resonator. The sensor was designed to not be intrusive. This advantage will prevent the sensor being damaged by the flow through the pipeline and allow pigging (technique used for cleaning rust and wax from the inside of the pipeline using blades or brushes). A laboratory prototype

version of the sensor system was constructed, and the experimental results were compared to the simulation results which were obtained by the use of High Frequency Structure Simulation (HFSS) software package. Finally, a software application was designed (using National Instrumentation (NI) devices, and software package), the system prototype was automated and tested, and a real time results were displayed.

PAGE NUMBERING AS IN THE ORIGINAL THESIS

CHAPTER 6

Results Analysis

6.1 Introduction

Prior to designing a software application to automate the developed sensors to monitor the multiphase flow online, the performance of the EMW2 and EMW3 sensors, developed in chapters 4 and 5, had to be evaluated. This was achieved by analysing the HFSS simulation results and experimental results for each sensor. The strategy used for analyzing the results was the descriptive statistic analysis.

The descriptive statistic analysis is used to describe the basic features of the quantitative data in a study, as it provides simple summaries about the predicted results and the measured results, together with simple tables and graphics analysis. Generally descriptive statistic is presented along with more formal analyses to give an overall sense of the data being analysed [21, 22].

Comparisons of the HFSS simulation results to the experimental results for both sensors are now presented in details. This will be followed by an analysis the

experimental results of the frequency temperature dependent. Finally, two phase (oil and gas, and water and gas), and three phase (oil, gas and water) experiment results for the EMW3 sensor developed in chapter 5 will be presented and analysed.

6.2. Electromagnetic Wave (EMW2) Sensor Results

Accuracy of the sensor can be evaluated by comparing its HFSS simulation results to the experimental results in term of Deviation or Error%. The experimental results and HFSS simulation results obtained in chapter 4 are compared and analysed in this section.

6.2.1 Experimental Results vs Simulation Results

As described earlier, the two phase experiments were carried out using the system set up shown in Figure 4.8. The experimental resonant frequencies and the HFSS simulated resonant frequencies provided in chapter 4 (sections 4.4 and 4.6) are analysed for both TE111 and TM010. The resolution of both TE111 and TM010 can be compared in terms of Deviation% or Error Percentages. This is illustrated in Tables 6.1 and 6.2 for the TE111 and the TM010 respectively.

It can be seen clearly from columns 1 and 5 in Table 6.1 that, as the water volume percentage in the sensor pipeline increases, the Error percentage or Deviation% decreases.

Table 6.1: Comparing HFSS simulated to experimental results for the TE111 mode in terms of the Deviation percentages or Error %.

Percentage		TE111 Mode		
Water%	Gas%	Exp. Freq(MHz)	HFSS Freq(MHz)	Deviation%
0%	100%	307.813	304.140	1.191
10%	90%	306.563	302.995	1.164
20%	80%	306.250	302.255	1.304
30%	70%	305.313	301.645	1.201
40%	60%	303.750	300.910	0.935
50%	50%	302.813	300.240	0.854
60%	40%	301.563	299.485	0.689
70%	30%	300.938	298.905	0.675
80%	20%	299.375	297.965	0.471
90%	10%	297.813	297.135	0.227
100%	0%	295.313	295.640	0.111

On the other hand, the error percentage increases as the volume percentage decreases and the resonant frequency increases.

The maximum and minimum Error percentage values are found to be 1.19% at 0%w and 0.11% at 100%w. The average error percentage value is found to be 0.65%. Consequently, the values of the experimental resonant frequency are slightly corresponding to the simulated frequencies values.

The Error percentage values for the TM010 mode are shown in Table 6.2. It can be seen that, the Error percentage increases as the water volume percentage increases.

Table 6.2: Comparing HFSS simulation results and the experimental results for the TM010 mode in term of the Deviation Percentage.

Percentage		TM010 mode		
Water%	Gas%	Exp. Freq.(MHz)	HFSS. Freq.(MHz)	Deviation%
0%	100%	248.750	247.76	0.398
10%	90%	245.625	243.53	0.853
20%	80%	243.125	239.11	1.651
30%	70%	240.625	234.67	2.475
40%	60%	238.125	230.29	3.290

50%	50%	236.250	226.02	4.330
60%	40%	234.0625	221.92	5.188
70%	30%	232.500	218.08	6.202
80%	20%	230.625	214.37	7.048
90%	10%	229.063	210.88	7.938
100%	0%	226.875	207.49	8.544

Table 6.2: Comparing HFSS simulation results and the experimental results for the TM010 mode in term of the Deviation Percentage.

In other words, the Error percentage increases as the resonant frequency decreases and the water volume percentage increases. The minimum and maximum Error percentage values are found to be 0.398% at 0%w and 8.544% at 100%w respectively. The average Error percentage value is found to be 4.5%.

These Error % values are much larger than those values found for the TE111 mode. This is indicated as an up normal deference between the simulated and the experimental resonant frequencies in the TM010 mode. Therefore, analysing lengths of PVC pipeline shows that the PVC pipeline length was not sufficient to prevent energy loss or leaking at both ends of the sensor pipeline.

In order to prevent energy leaking through the ends of the PVC pipeline, the length of the inner cavity resonator or PVC pipeline was extended, so that any microwaves propagating out of the PVC pipeline will be attenuated to a negligible magnitude at the ends of the PVC Cavity.

The cut off wavelength of the inner resonance cavity or PVC pipeline is given by Equation 6.1.

$$\lambda_c = \frac{D}{X_{nm}} \tag{6.1}$$

Where D is the internal diameter (42mm) of the PVC pipeline and Xnm is to be replaced by P'_{11} for the TM010 and P_{11} TE111. This gives cut off wavelengths of 22.81mm and 17.47mm, which correspond to cut off frequencies of 465MHz and 607MHz for the TE111 and TM010 modes respectively. Therefore, even at the maximum frequency 400MHz used in this system, the cut off frequency of the PVC pipeline is much larger, resulting in no lost energy.

The HFSS simulation results for the sensor with this new HFSS designed PVC pipeline are shown in (columns 2 and 6) Table 6.3 are now compared to previous results shown in (columns 2 and 7) Table 6.3.

Table 6.3: HFSS Resonant Frequencies for TM010 with new pipeline length 333mm

Water	Gas	TM010-L1	TM010-L2	TM010	Deviarion-L2	Deviarion-L1
%	%	HFSS. MHz	HFSS. MHz	Exp. MHz	%	%
0	100	247.76	247.80	248.750	0.382	0.398
10	90	243.53	244.71	245.625	0.373	0.853
20	80	239.11	242.98	243.125	0.060	1.651
30	70	234.67	239.49	240.625	0.472	2.475
40	60	230.29	237.16	238.125	0.405	3.290
50	50	226.02	234.86	236.250	0.588	4.330
60	40	221.92	232.60	234.063	0.625	5.188
70	30	218.08	230.45	232.500	0.882	6.202
80	20	214.37	228.26	230.625	1.025	7.048
90	10	210.88	226.13	229.063	1.280	7.938
100	0	207.49	223.50	226.875	1.488	8.544

Comparing the values shows that the maximum and minimum Error percentages values in TM010 are reduced from 8.544% and 0.398% to 1.5% and 0.06% respectively. As with the maximum and minimum Error percentages, the

average Error percentage value, which was 4.5%, has dropped down to 0.689% as well.

A graphical representation, which related the experimental and HFSS resonant frequencies to the volume percentages for both the new and old pipeline lengths, is shown in Figure 6.1.

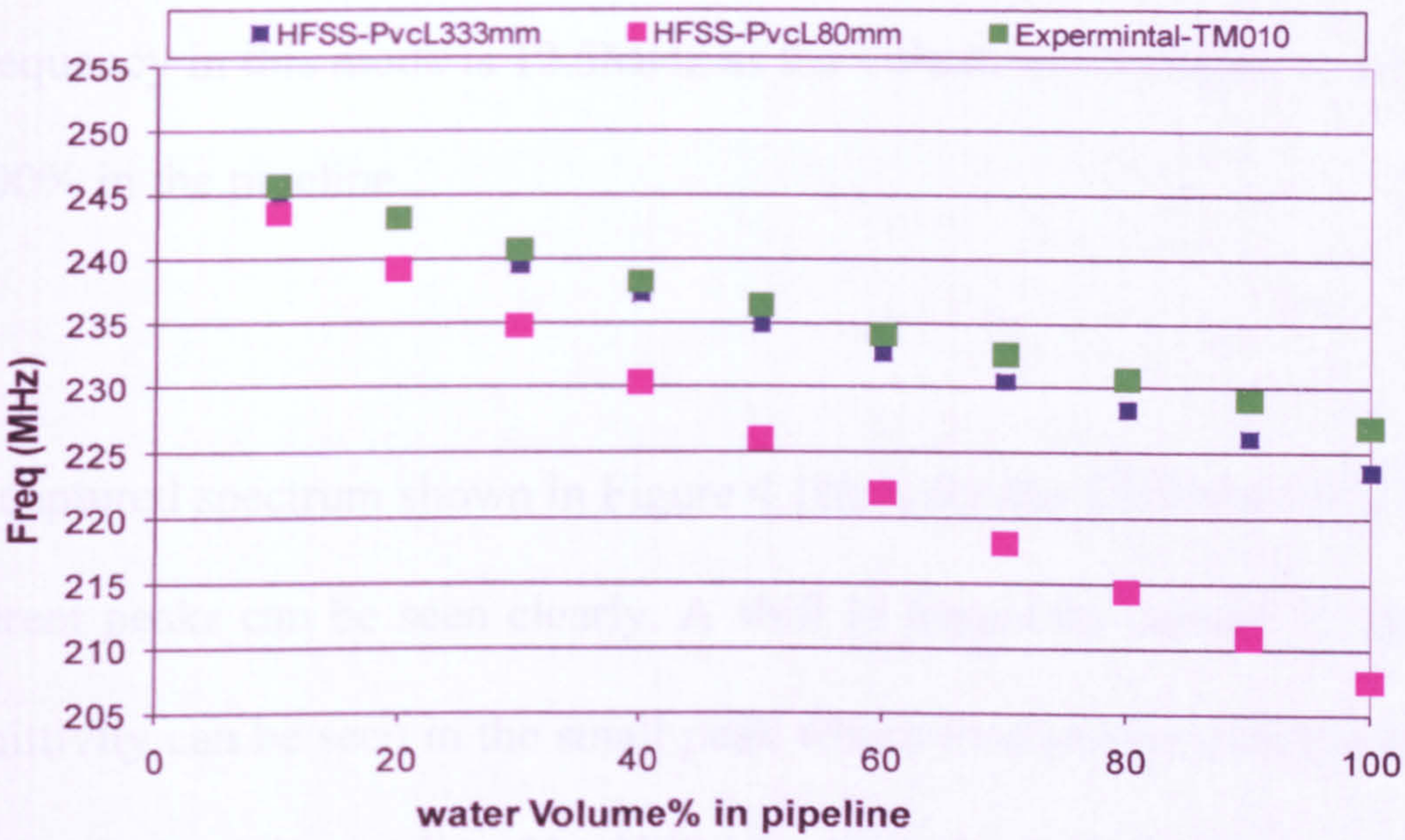

Figure 6.1: TM 010 HFSS resonant frequencies for two different lengths (80mm and 333mm) PVC pipeline.

The HFSS resonant frequencies with the new PVC pipeline length of 333mm (blue) closely correspond to the experimental frequencies (green) as shown in Figure 6.1.Values for the old PVC pipeline length (80mm) are included for comparison.

The spectrums captured during experiments are shown in Figure 4.12 for both the TE111 mode and TM010 mode respectively.

The peak of the TE111 mode as the mixture (water and gas) varies from 0 to 100% is shown in Figure 4.10a. The shifts in frequency caused by changes in the permittivity can be clearly seen in these peaks. The resonant frequencies correspond closely to the HFSS predicted resonant frequencies. The total shift in frequency in this mode is 12.5MHz as the volume percentages w vary from 0 to 100% in the pipeline

The captured spectrum shown in Figure 4.10b is for the TM010 mode where two different peaks can be seen clearly. A shift in frequency caused by changes in permittivity can be seen in the small peak where frequencies closely correspond with the frequencies predicted by HFSS for TM010 mode, as shown in Table 6.3 and Figure 6.1 respectively. The larger peak is assumed to be the TE111 mode peak, as it has discriminated against the TM010 mode. This discrimination occurred as a result of using the PVC material in the sensor pipeline.

6.3 Electromagnetic Wave (EMW3) Sensor Results

The two phase experiments and three phase experiments were carried out using the set up shown in Figure 5.1. The experimental results and HFSS simulation results obtained in chapter 5 for this sensor are compared and analysed to evaluate the performance of this sensor.

6.3.1 Experimental Results vs HFSS Simulation Results

The experimental and HFSS simulated resonant frequencies are listed in Table 6.4. It can be clearly seen from this table that the values of the experimental resonant frequencies closely correspond to the HFSS predicted resonant frequency values.

These results can be compared in terms of the deviation Error Percentages. From these results shown in Tables 6.4, show that as the water volume percentage increases, and the resonant frequency and gas volume percentages decrease, the Error percentage decreases as well.

Table 6.4: Comparison of the HFSS simulation and experimental resonant frequencies for the TE111 in terms of the percentage Error

Water %	Gas %	TE111-HFSS	TE111-Exp.	Deviation %
0	100	316.225	317.110	0.279
10	90	314.105	314.500	0.125
20	80	312.168	312.500	0.106
30	70	309.850	310.250	0.128
40	60	306.855	307.750	0.290
50	50	304.185	304.625	0.144
60	40	301.258	301.585	0.108
70	30	297.550	297.875	0.109
80	20	294.438	294.750	0.106
90	10	290.450	290.750	0.103
100	0	282.590	282.875	0.101

The minimum and maximum Error percentage values are found to be 0.101% and 0.29% respectively. The average error percentage value is found to be 0.145%.

A spectrum captured during the experiments is shown in figure 6.2 where peak of the TE111 mode has shifted as the permittivity is changed. The values of the experiential resonant frequencies closely correspond to the HFSS simulated frequency values.

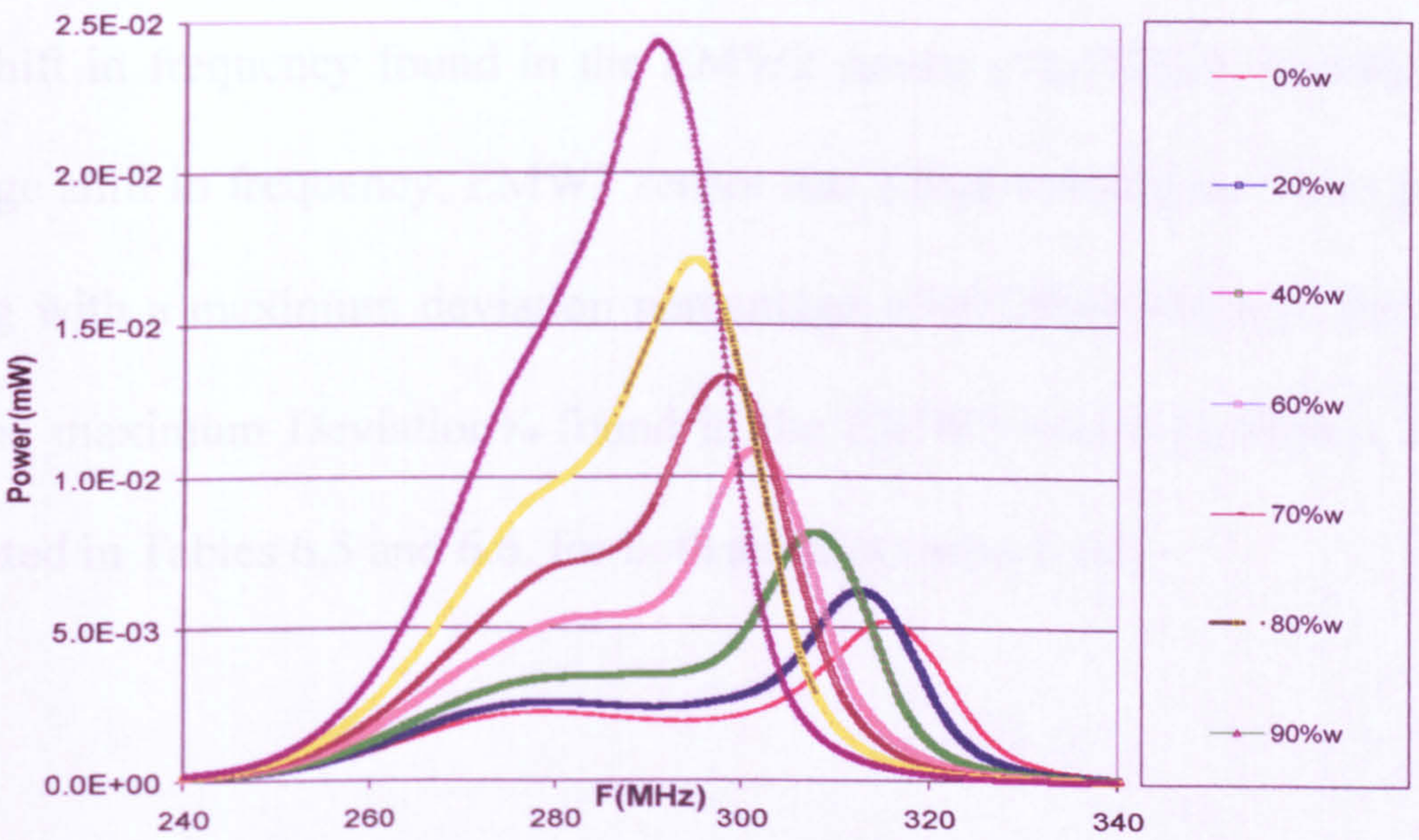

Figure 6.2.: Experimental results showing the changes in TE_{111} peak for two phases (gas and water), as the mixtures vary form 0-100% in the PVC pipeline.

6.4 EMW3 Sensor Experimental Results vs EMW2 Sensor Experiments Results

Analysing the HFSS simulation results and experimental results for the TE111 mode in both sensors show that both sensors can successfully measure two phase components.

Performance, on the other hand, is not identical in both sensors as the EMW3 sensor has a total shift in frequency of (34.235MHz) which is larger than the total shift in frequency found in the EMW2 sensor (12.5MHz). In addition to the large shift in frequency, EMW3 sensor has a high resolution. It can provide reading with a maximum deviation percentage of (0.29%) which is also lower than the maximum Deviation% found in the EMW2 sensor (1.304%). This is illustrated in Tables 6.5 and 6.6. for both sensors respectively.

Table 6.5: Comparison parameters for the EMW2 sensor for the TE111 mode

Water%	Gas%	Exp.(MHz)	HFSS.(MHz)	Deviation%	Shift (MHz)	Permittivty
0%	100%	307.813	304.14	1.191	1.25	56.333
10%	90%	306.563	302.995	1.164	1.5625	56.794
20%	80%	306.25	302.255	1.304	2.5	56.910
30%	70%	305.313	301.645	1.201	4.0625	57.259
40%	60%	303.75	300.91	0.935	5	57.850
50%	50%	302.813	300.24	0.854	6.25	58.209
60%	40%	301.563	299.485	0.689	6.875	58.692
70%	30%	300.938	298.905	0.675	8.4375	58.936
80%	20%	299.375	297.965	0.471	10	59.553
90%	10%	297.813	297.135	0.227	12.5	60.180
100%	0%	295.313	295.64	0.111	1.25	63.333

Table 6.6: Comparison of parameters for the EMW3 sensor (TE111)

Water%	Gas%	Exp.(MHz)	HFSS.(MHz)	Error%	Shift (MHz)	Permittivity
0%	100%	317.110	316.225	0.279	2.610	33.179
10%	90%	314.500	314.105	0.126	4.610	33.732
20%	80%	312.500	312.168	0.106	6.860	34.165
30%	70%	310.25	309.850	0.129	9.360	34.663
40%	60%	307.750	306.855	0.291	12.485	35.228
50%	50%	304.625	304.185	0.144	15.525	35.955
60%	40%	301.585	301.258	0.108	19.235	36.683
70%	30%	297.875	297.550	0.109	22.360	37.603
80%	20%	294.750	294.438	0.106	26.360	38.404
90%	10%	290.750	290.450	0.103	34.235	39.468
100%	0%	282.875	282.590	0.101	2.610	41.696

The changes in permittivity as a function of the resonator diameter are shown in (column 6) Tables 6.5 and 6.6. Another important factor to be taken into

account as a credit to the EMW3 sensor is the frequency shift per volume percentage as it can be used as a control data for designing a control program. Also, this can be seen clearly from (column 7) Tables (6.5 and 6.6) for both sensors EMW2 and EMW3 respectively. Control data will be discussed in chapter 7.

6.5 Frequency Temperature Dependence Experiments

The temperature as a factor affecting the resonant frequency was investigated experimentally. During the experimental works presented in chapters 4 and 5, the effect of the temperature on the frequency was noted, so that as the room temperature is changed, the measured peak frequency was changed as well. Therefore, temperature experiments were carried out using the system set up shown in Figures 5.1.

The PVC pipeline was filled with 100% water and the temperature was varied between 22 and 50^{0}C. Including the trend line Equation, the relation between the measured resonant frequency and the temperature is presented graphically as shown in Figure 6.3.

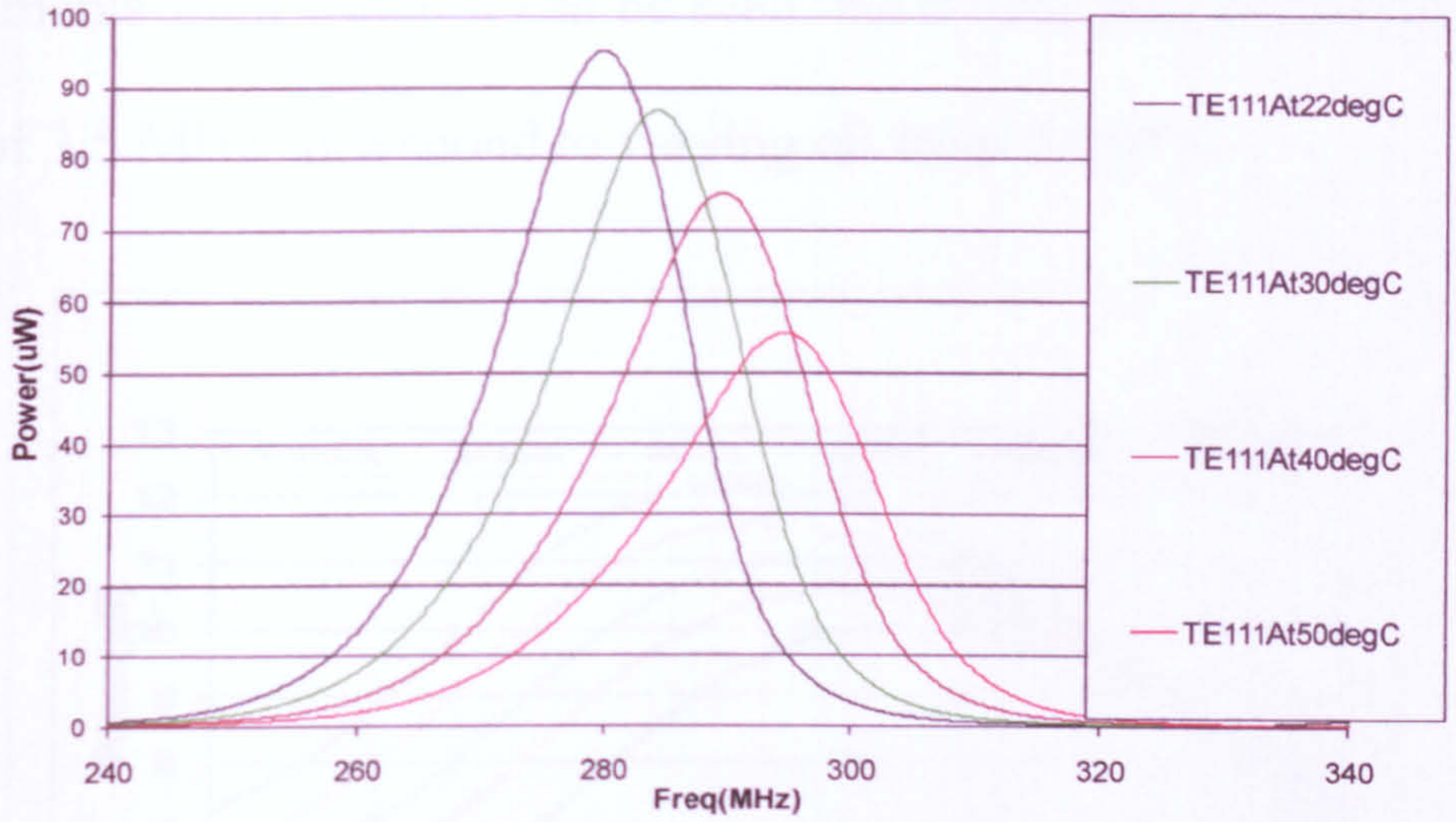

Figure 6.3: Experimental results for the temperature effect on the TE111 at 100%w in the PVC pipeline using EMW3 sensor.

The experimental results show that as the temperature rose by one C^0 degree, the frequency increased with average rate of 0.5MHz / C^0.

6.6 EMW3 Sensor (oil, gas, and water) Experimental Results

6.6.1 Two Phase Experimental Results (Oil and gas)

Two phase component experiments for (oil and gas mixture) were carried out using the system set up shown in Figure 5.1. As this mixture is varied from 0 to

100% in the PVC pipeline, the two phase components are measured in volume percentages as well. Figure 6.4 shows the spectrum captured during these experiments from which it can be seen that a total frequency shift in the TE111 peak of 3.5 MHz correspond to varying oil from 0-100%.

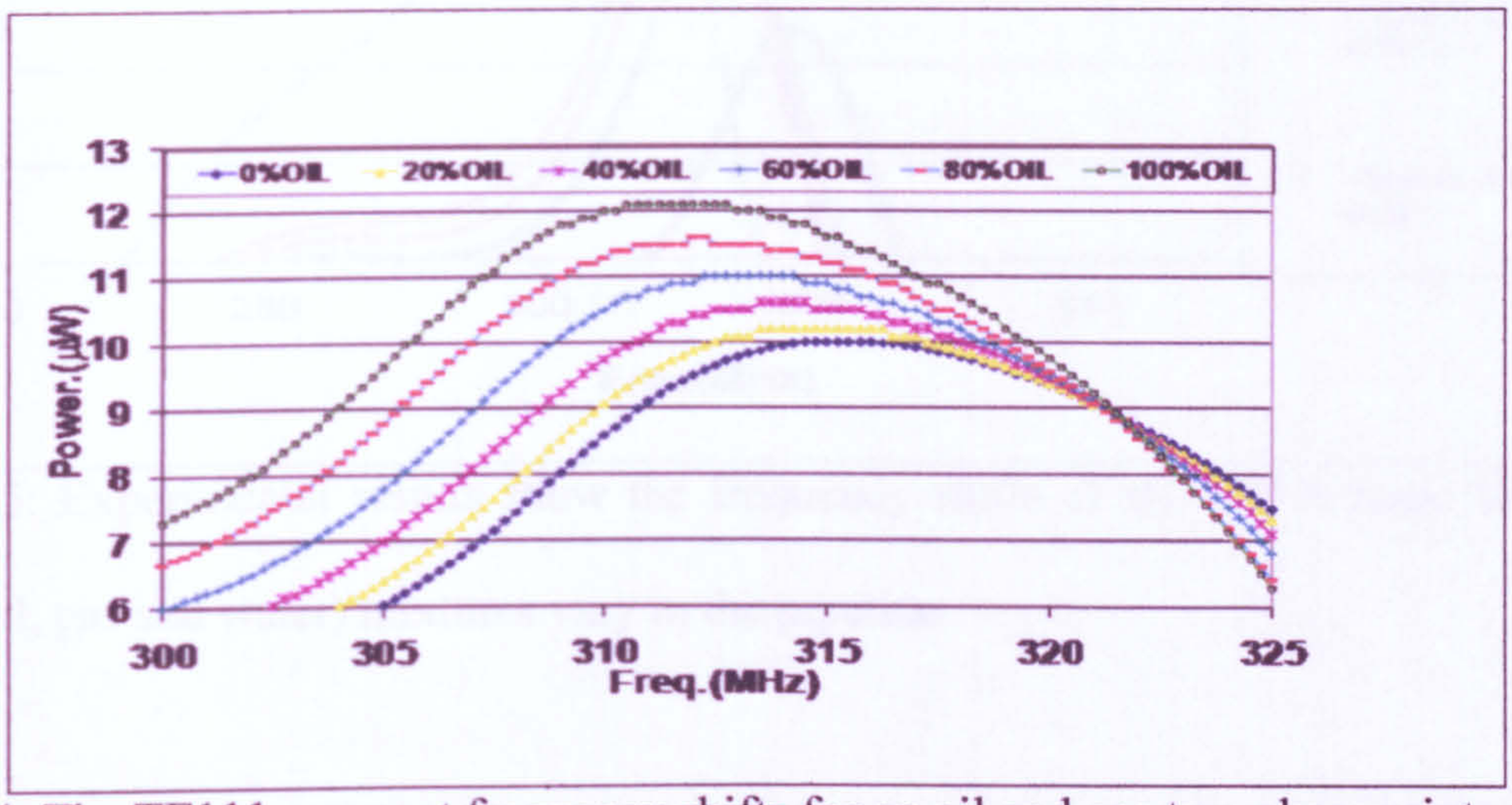

Figure 6.4: The TE111 resonant frequency shifts for an oil and gas two phase mixture as it varies from 0-100% in the sensor at room temperature.

6.6.2 Three Phase Experimental Results (Oil, gas, and water)

Three phase experiments were carried out using the set up shown in Figure 5.1. As multiphase flow (oil, gas, and water) mixture is varied from 0 to 100%, the resonant frequency is shifted as well.

The spectrums captured during the three phase experiments are shown in Figure 6.5.

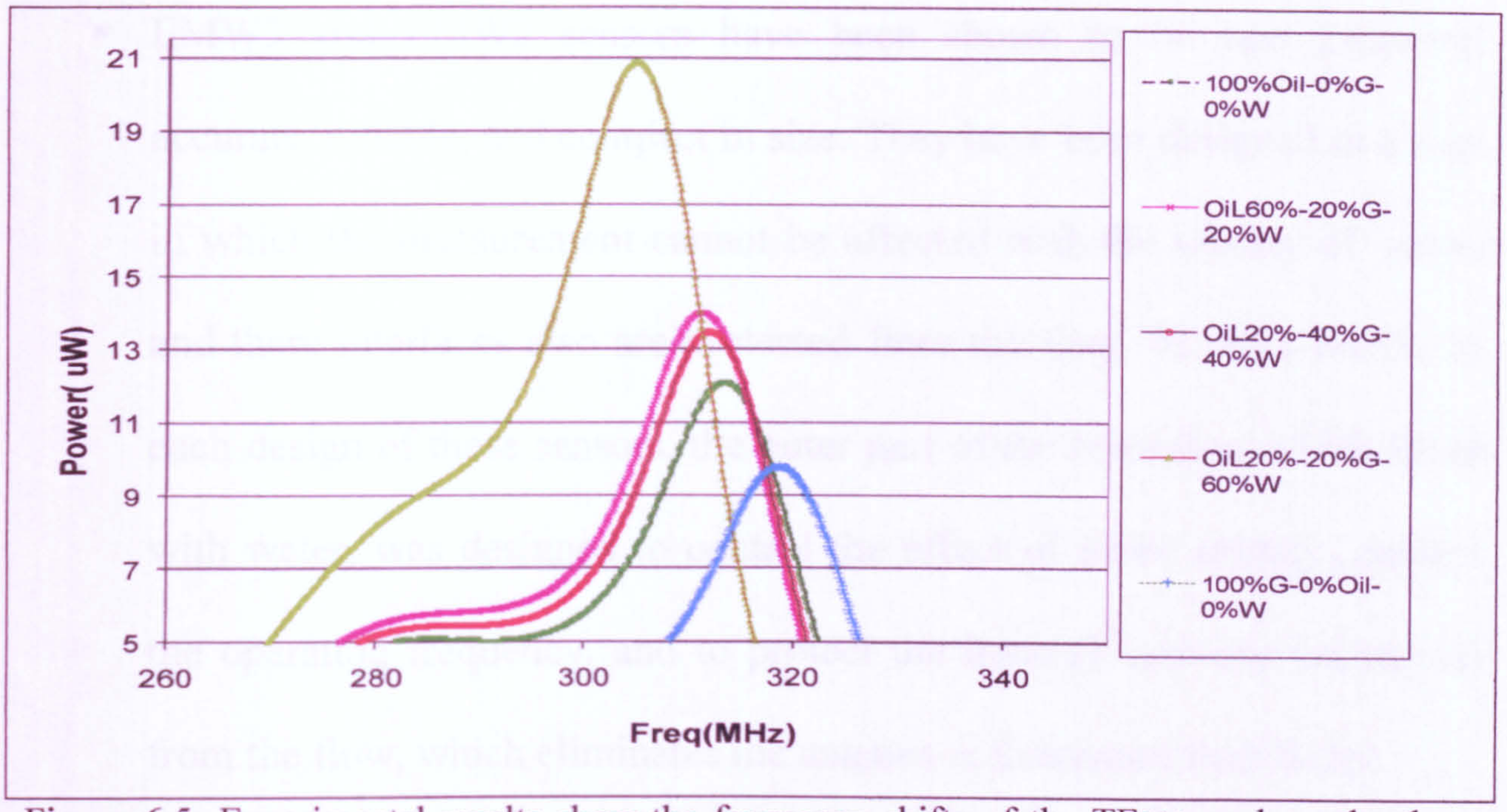

Figure 6.5: Experimental results show the frequency shifts of the TE111 peak as the three phases (oil, gas and water) mixtures vary in the pipeline.

From this Figure, it is can be seen clearly that as the mixture permittivity is changed, the resonant frequency is shifted as well. The value of this frequency shift depends on the component that has the highest permittivity value.

6.7 Conclusion

The HFSS simulation results and the experimental results for both sensors, the EMW2 and EMW3 were presented and analysed. Based on analysing these results, the conclusion drawn as follows:

- EMW3 and EMW2 sensors have been shown to be non intrusive, accurate, reliable, and compact in size. They have been designed in a way in which the measurement cannot be affected with the salinity of water, and there interfaces also are protected from the flow. In other words, in each design of these sensors, the outer part of the resonator, which filled with water, was designed to control the effect of water salinity, control the operating frequency, and to protect the internal interface (antennas) from the flow, which eliminates the antenna maintenance cost factor.
- The EMW2 sensor was found to be capable for detecting and measuring two phase (oil / gas or water/ gas) components in %volume in a pipeline with TE111 mode. However, the measurement with TM010 could not be achieved experimentally in this design.
- The EMW3 sensor was found to be more accurate than the EMW2 sensor, and capable for detecting and measuring two phase (oil and gas or water gas), and three phase (oil, gas, and water) quantities in % volume a pipeline with the TE111 mode. The total experimental frequency shift for EMW3 was found to be 34.235MHz, while the experimental frequency shift was found to be 12.5 MHz. The maximum deviation percentage was

found to be (0.29%), which is smaller than that one found for EMW2 (1.19%).

- The drawback of frequency temperature dependence was analysed experimentally using EMW3 sensor. The PVC pipeline was filled with 100% water and the temperature was varied between 22 and50^{0}C. The experimental results show that as the temperature rose by one C^{0}degree, the frequency increased with average rate of 0.5MHz /C^0. This impact has been prevented with additional control unit which was used to vary and control the temperature for both sensors. These data have been used to control the online system described in chapter 7.

CHAPTER 7

Online EM Wave Monitoring System

7.1 Introduction

The non intrusive electromagnetic wave EMW3 sensor described in chapter 5 was upgraded with new control hardware and automated with a new software application [75]. The software program controlled the sensor system parameters, and allowed the sensor to measure and monitor multiphase flow component fractions in a pipeline (in real time), and express them in volume percentage.

7.2 Online Sensor Design

As it was described earlier, the permittivity is temperature dependent. Therefore, a thermally controlled unit was used to vary and control the temperatures for both the brass cavity resonator and the PVC pipeline contents [76]. The temperatures were measured using a National Instruments NI-USP 9162 multichannel thermocouple module [77]. In addition to the thermal control

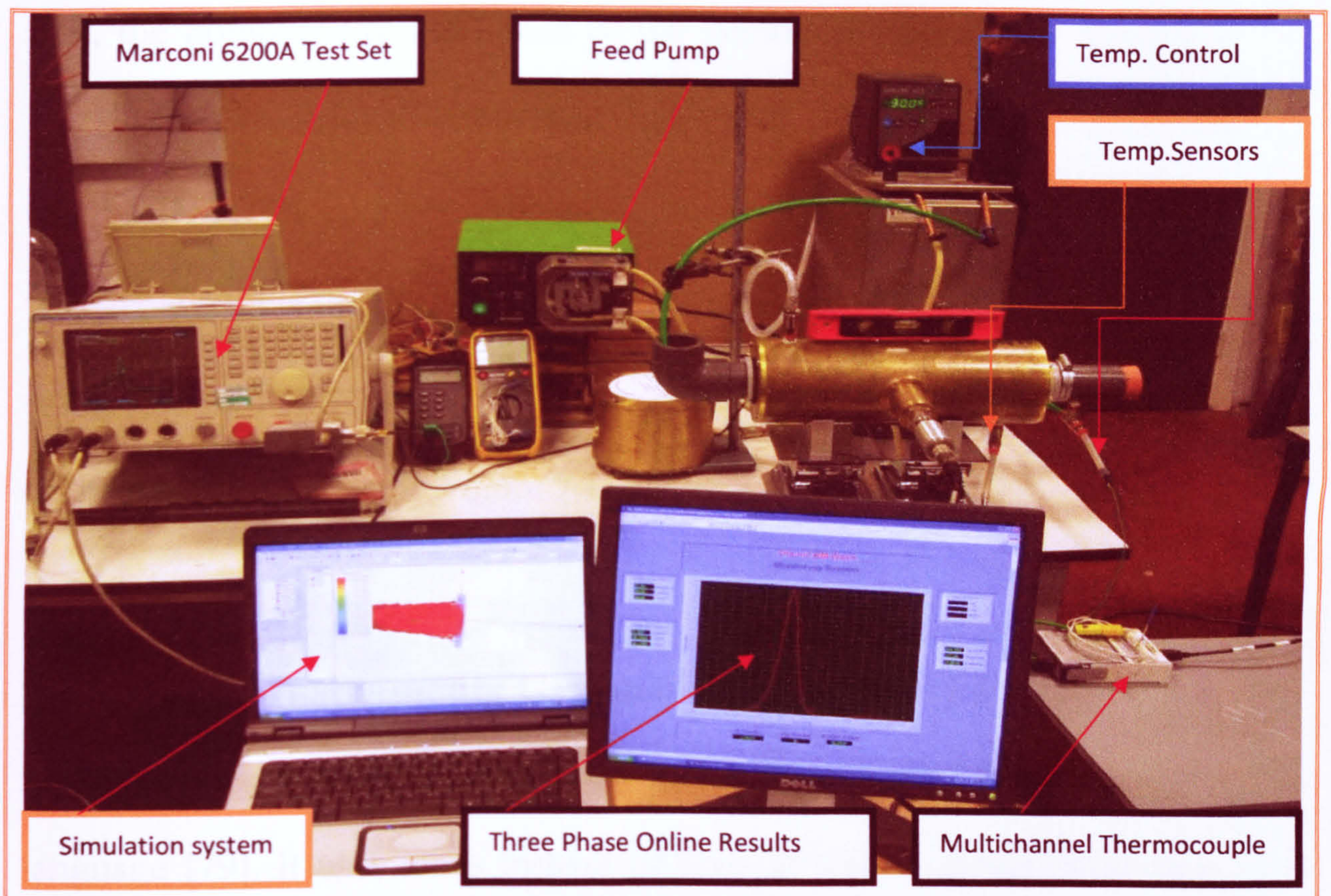

(a)

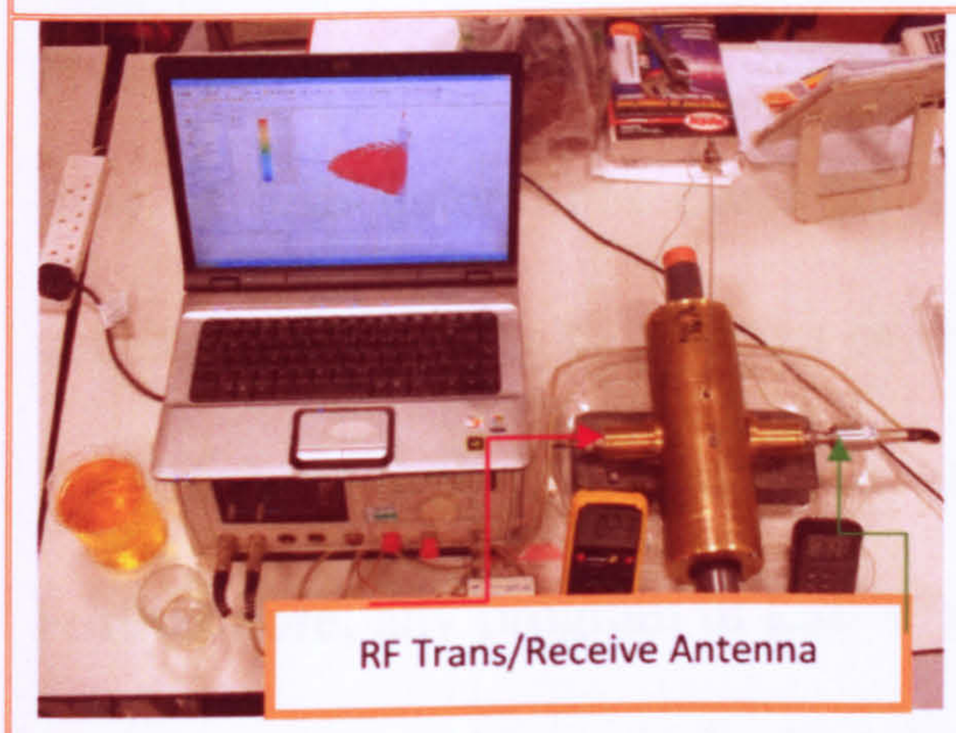

(b)

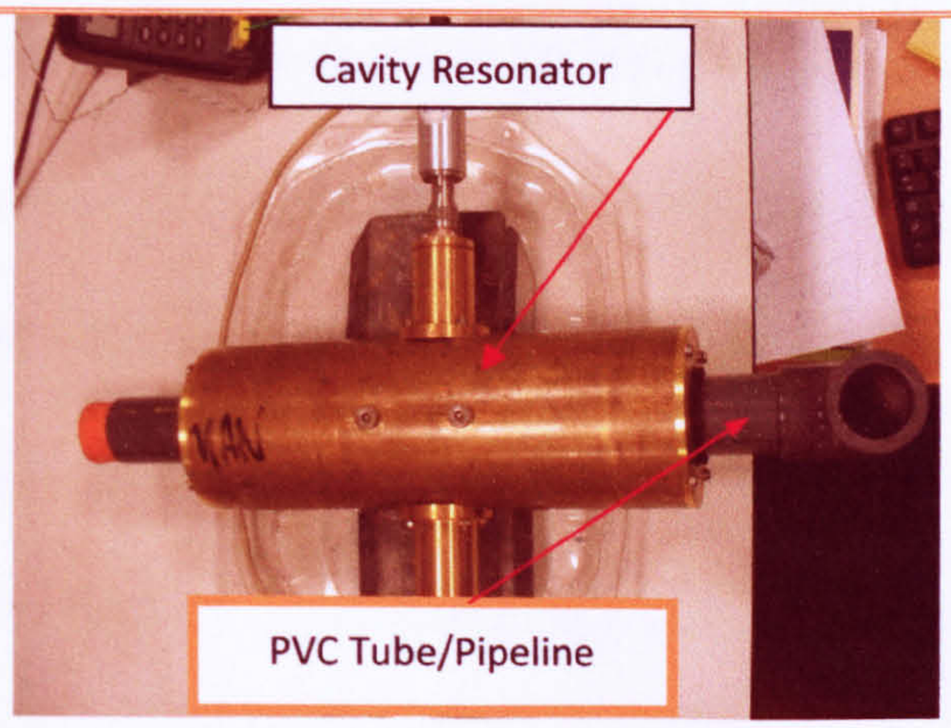

(c)

Figure 7.1: Online control and monitoring sensor system set up

unit, the homogeneity and speed of the homogeneous mixture flowing in the pipeline was controlled with a feed pump [78]. The system is coupled to a PC via the IN GPIB interface. Automatic identification of the system components was achieved via the PC with the IN test software. A new software program was designed and implemented, and a real time results were achieved. An overview of the system is shown in Figure 7.1.

7.3 National Instruments Graphical Language (Lab View)

Lab View is a programming software that utilizes as a graphical programming language [79]. It uses icons instead of lines of text to create applications. In contrast to text-based programming languages, where instructions determine program execution [80, 81], Lab View uses dataflow programming, where the flow of data determines execution. Further, if it is necessary to use external codes, Lab View can call source codes written in other programming languages. For example Lab View can call source codes written in C language [82]. Furthermore, any program in Lab View is written by connecting icons (controls and indicators) with special wires (see Figure 7.2). Controls and indicators, on the other hand, correspond to subprograms in text-based programming languages.

The interface of Lab View consists of a front panel which is known as the graphical user interface (GUI) and block diagram (code). This is illustrated in Figure 7.2.

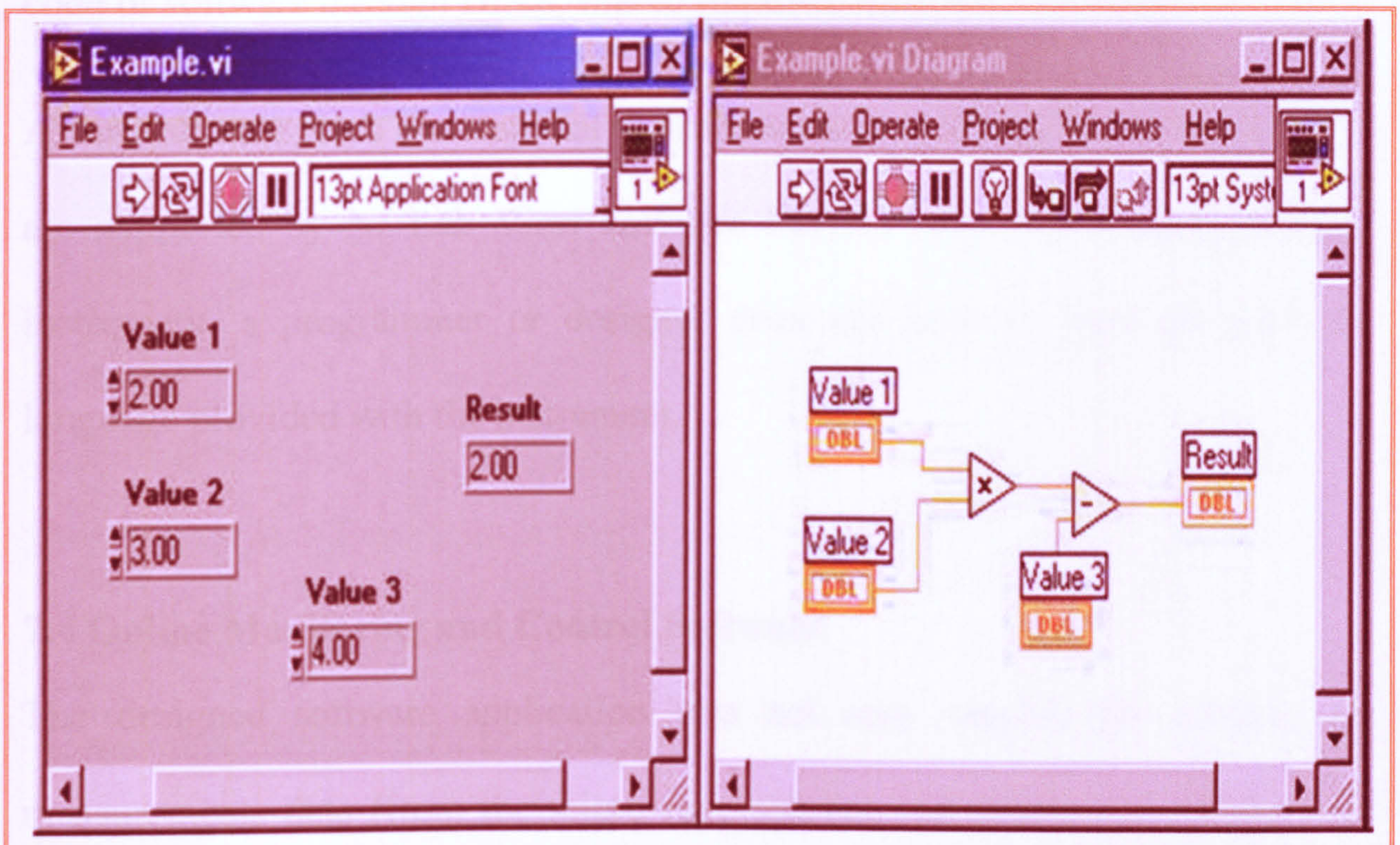

Figure 7.2: An example showing a Lab View program front panel (a) and block diagram (b).

Lab View has excellent capabilities for managing very complex data structures, signal acquisition and processing. Because it is fully integrated with data acquisition cards from National Instruments or NI, it is rapidly used for signal acquisition.

Lab View has built-in features for connecting application to the Internet using the Lab View web server and software standards such as TCP/IP networking and ActiveX. It also provides numerous mechanisms for connecting to external code or software through DLLs, shared libraries, ActiveX, and more.

All instruments from the National Instruments and most modern instrumements are supported by NI Lab View software Drivers [83]. When using such an instrument, a programmer or designer does not have to learn the protocol language provided with the instrument.

7.4 Online Monitoring and Control Software

The designed software application was not only capable for reading the measurements data (from the microwave source), but it also was designed to control the sensor system components, variables, initialize the input and output of the microwave source, and display the spectrum online and the volume percentages for each phase components (oil, gas, and water). The Marconi Microwave Test Set 6200A was not supported with an NI Lab View driver [83]. Therefore, we have designed this software application programme to provide two functions in one. It drives the Marconi Microwave Test Set 6200A as a Lab

View driver, and controls the sensor system as a control software application programme as well.

Control of the system was achieved from a remote PC with a control panel or user graphical interface (GUI). Figures (7.3, 7.4, and 7.5) show the control panel created in Lab View to control and initialize the system, and to carry out the measurement and display the results online respectively.

The initial program application was designed to initialize the system in a couple of messages. It initiates an instruction to identify the Marconi Test Set via the NI GPIB. If the identification fails, the communication is ended as well. If the Marconi is correctly identified, then another instruction is sent to flash the communication bus and reset the Marconi to the manufacture setting values [62]. Once the system is correctly initialized, the parameter including, the output power, the start and stop frequency values, and the measurements units are assigned. The default values assigned to these parameters by the program are shown in Figure 7.3

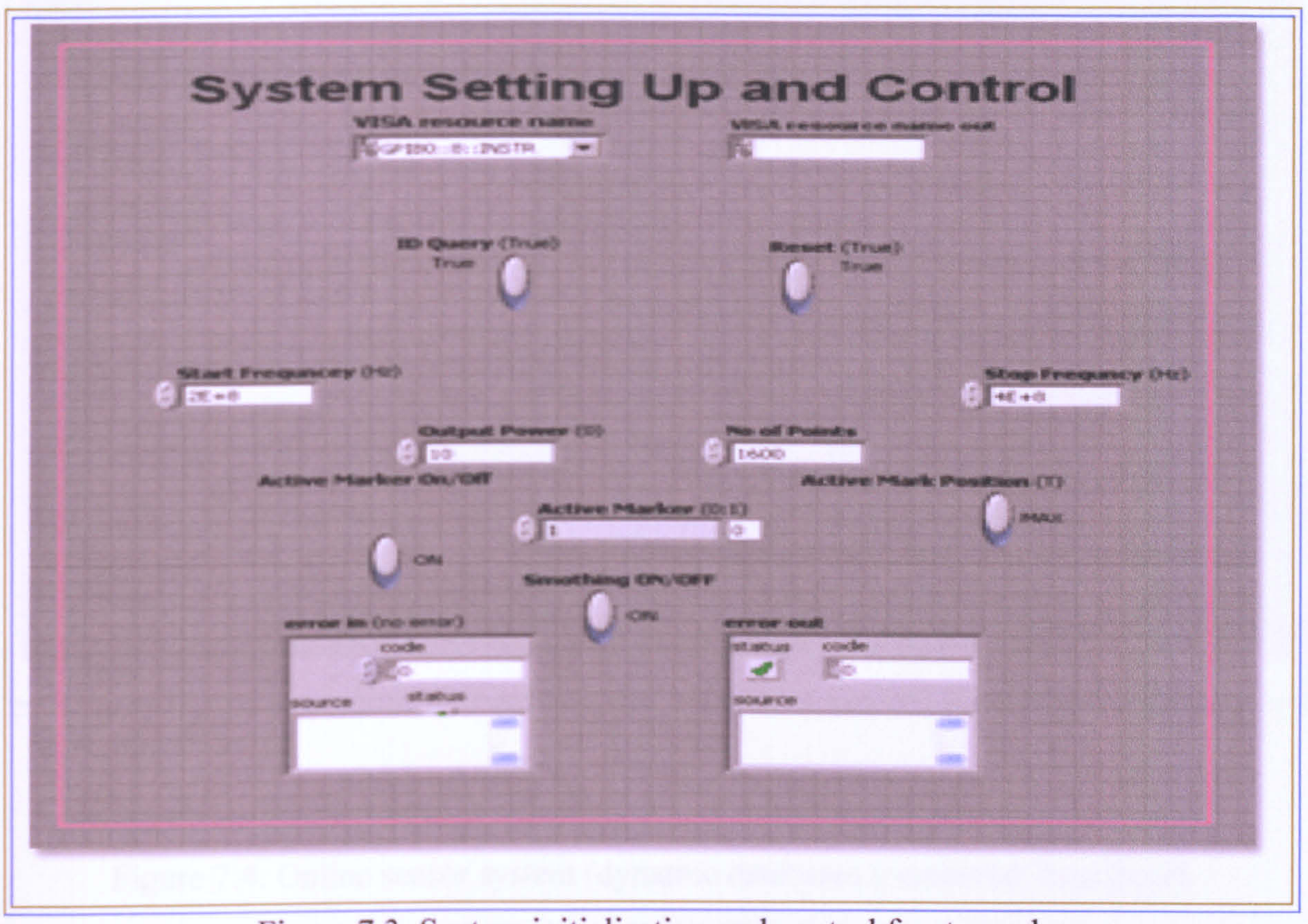

Figure 7.3: System initialisation and control front panel.

For controlling just one instrument, the identification operation can be ignored.

This application, however, was designed to control more than one instrument as required; therefore, the identification and resetting of the instrument are kept optional for the user.

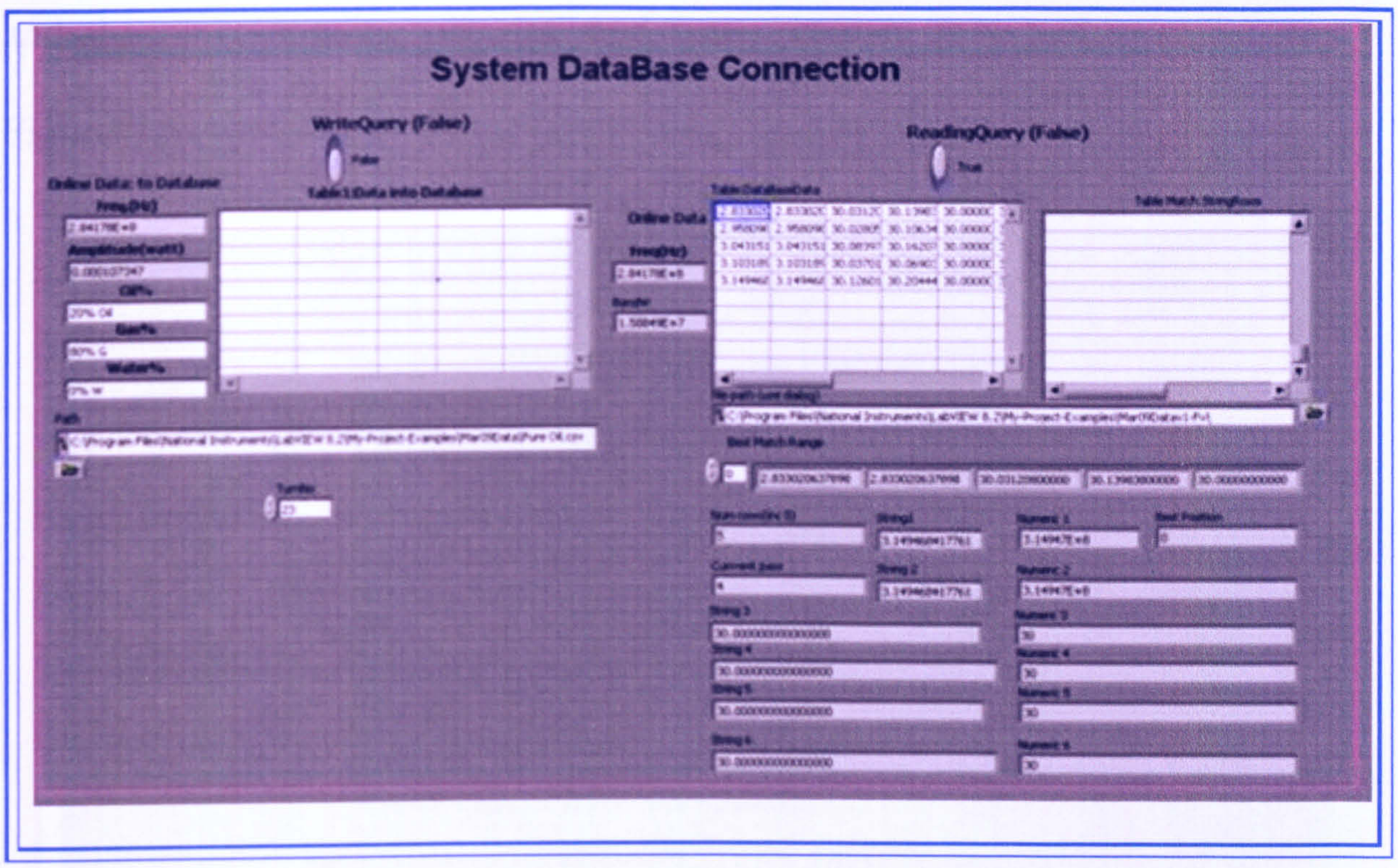

Figure 7.4: Online sensor system (dynamic database) connection front panel.

The main program was designed to display online results by executing two operations. The sensor dynamically reads the Marconi output waveform, the resonant frequency, and the temperatures for both the cavity resonator and the pipeline. It then compares these values (the resonant frequency and temperatures) to the control data stored in the system database using a dynamic database connection shown in Figure 7.4. Finally, depending on the comparison results, the application displays the waveform, the frequency, the temperatures,

and the corresponding oil, gas, and water volume percentages, as shown in Figure 7.5.

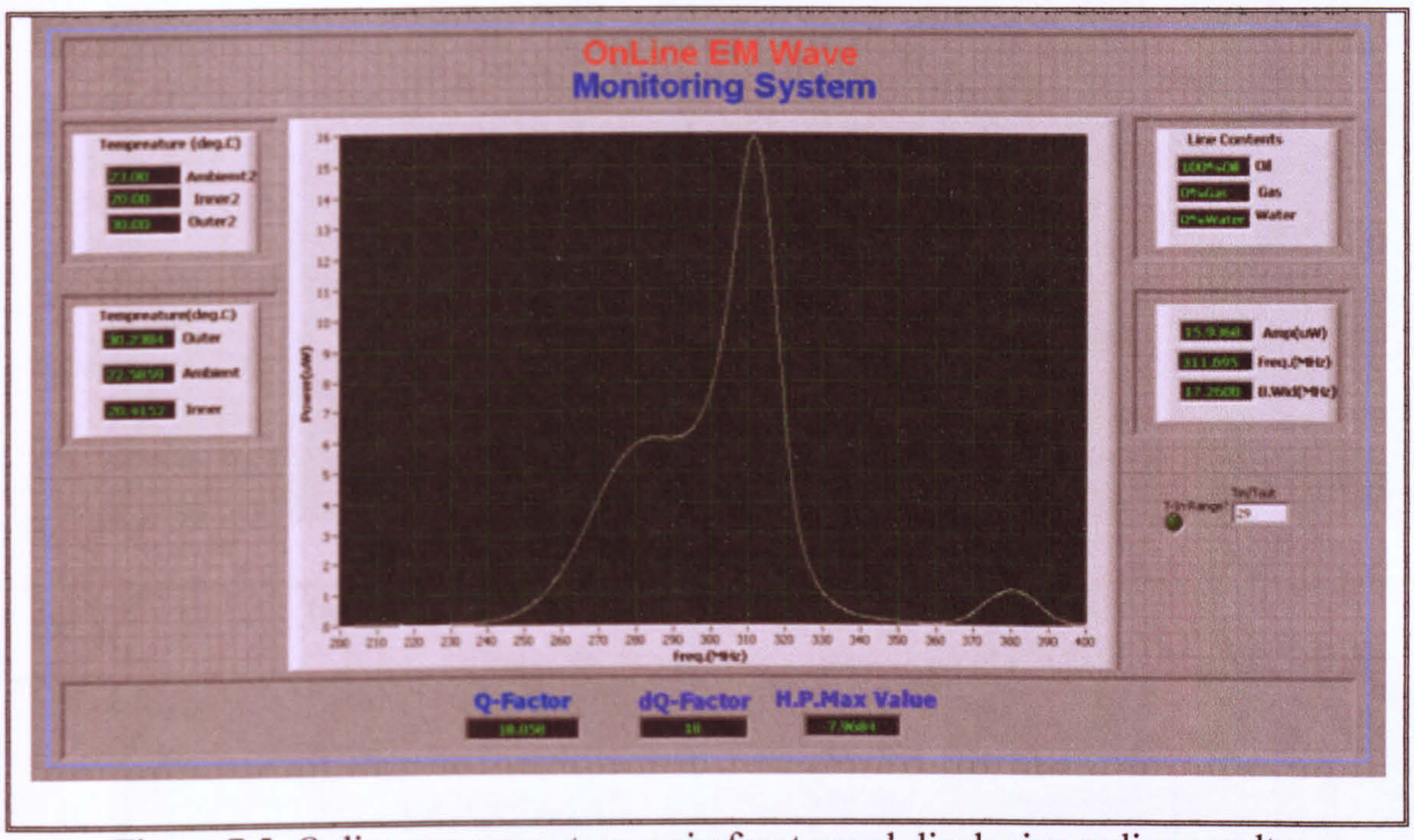

Figure 7.5: Online sensor system main front panel displaying online results.

7.5 Online Two Phase Results

As described above, the application software was implemented and experiments were carried out in a real time using the system set up shown in Figure 7.1. Consequently, online results were achieved. Figure 7.6a shows screen shot captured during online two phase (oil and gas mixtures) experiments.

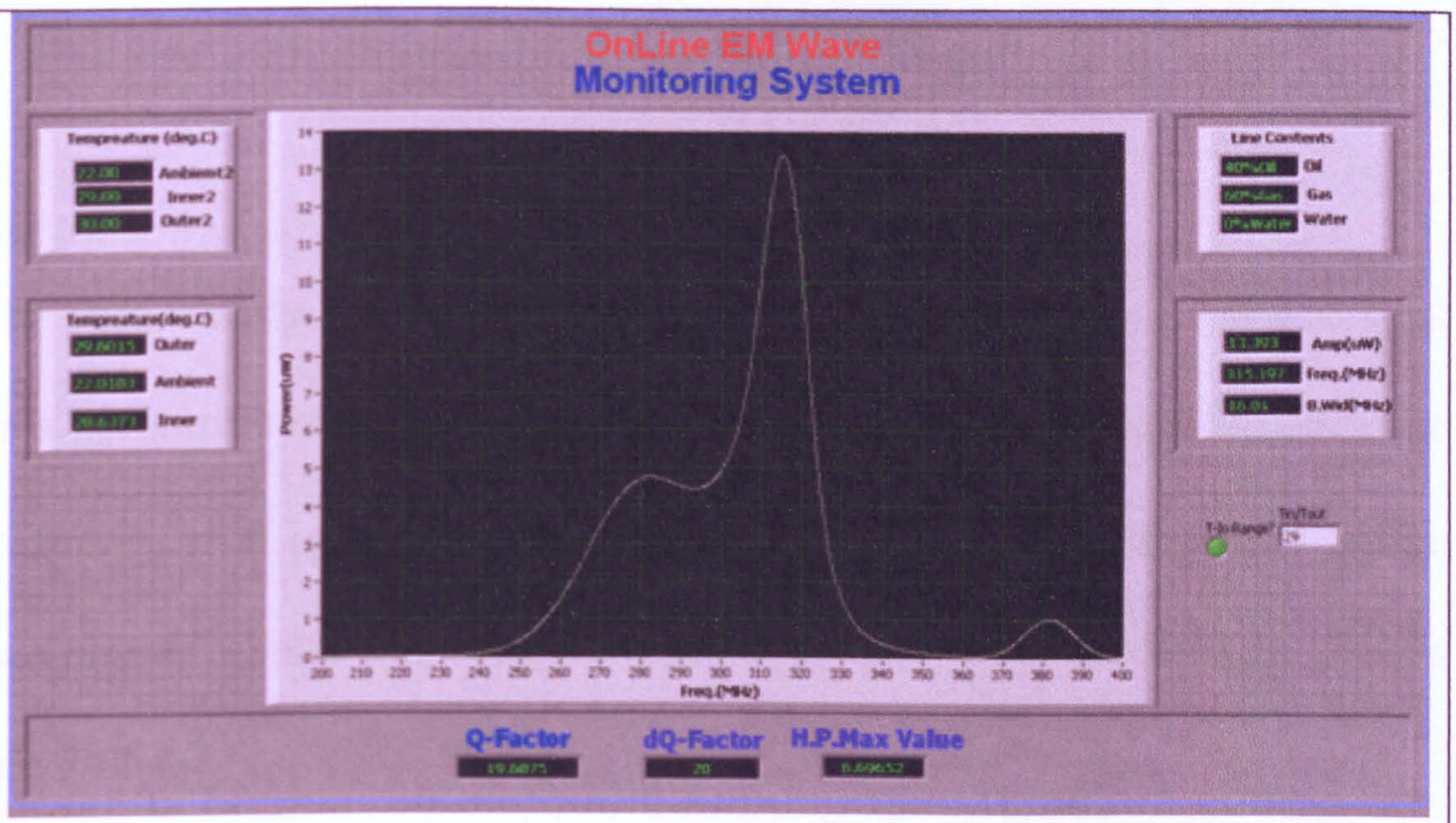

(a) : (40%Oil, 60%Gas, 0%Water), Freq 315.197MHz

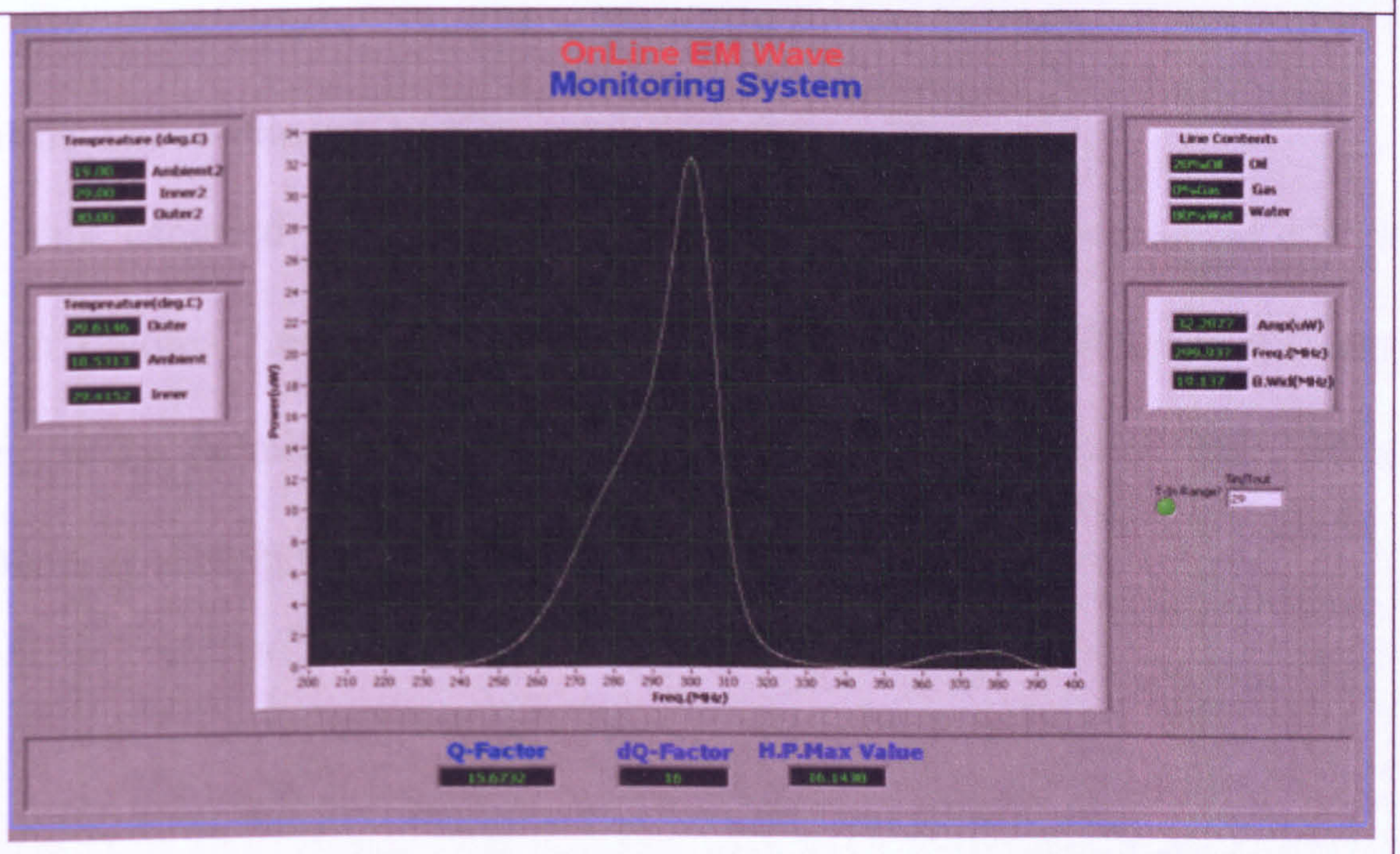

(b) : (20% Oil, 80%Water, and 0%Gas), Freq 299.937MHz

Figure 7.6: Screen shot showing online results of two phase (oil and water mixtures) in (a), and two phase (oil and gas mixtures) in (b).

It can be seen clearly from figure (7.6 a) that, as the two phase (oil and gas) mixture's permittivity is changed the resonant frequency is shifted as well. The total frequency shift is found to be 4.6MHz. The screen shots captured online for a two phase (oil and water) mixture flowing through the pipeline are shown in Figure 7.6b.

7.6 Online Three Phase (Oil, Gas, and Water) Results

Screen shot captured during online three phase test of the sensor system is shown in Figures 7.6c. It can be clearly seen from this figure that for any changes in the permittivity of the (oil, gas, and water) mixture, there is a corresponding shift in the frequency.

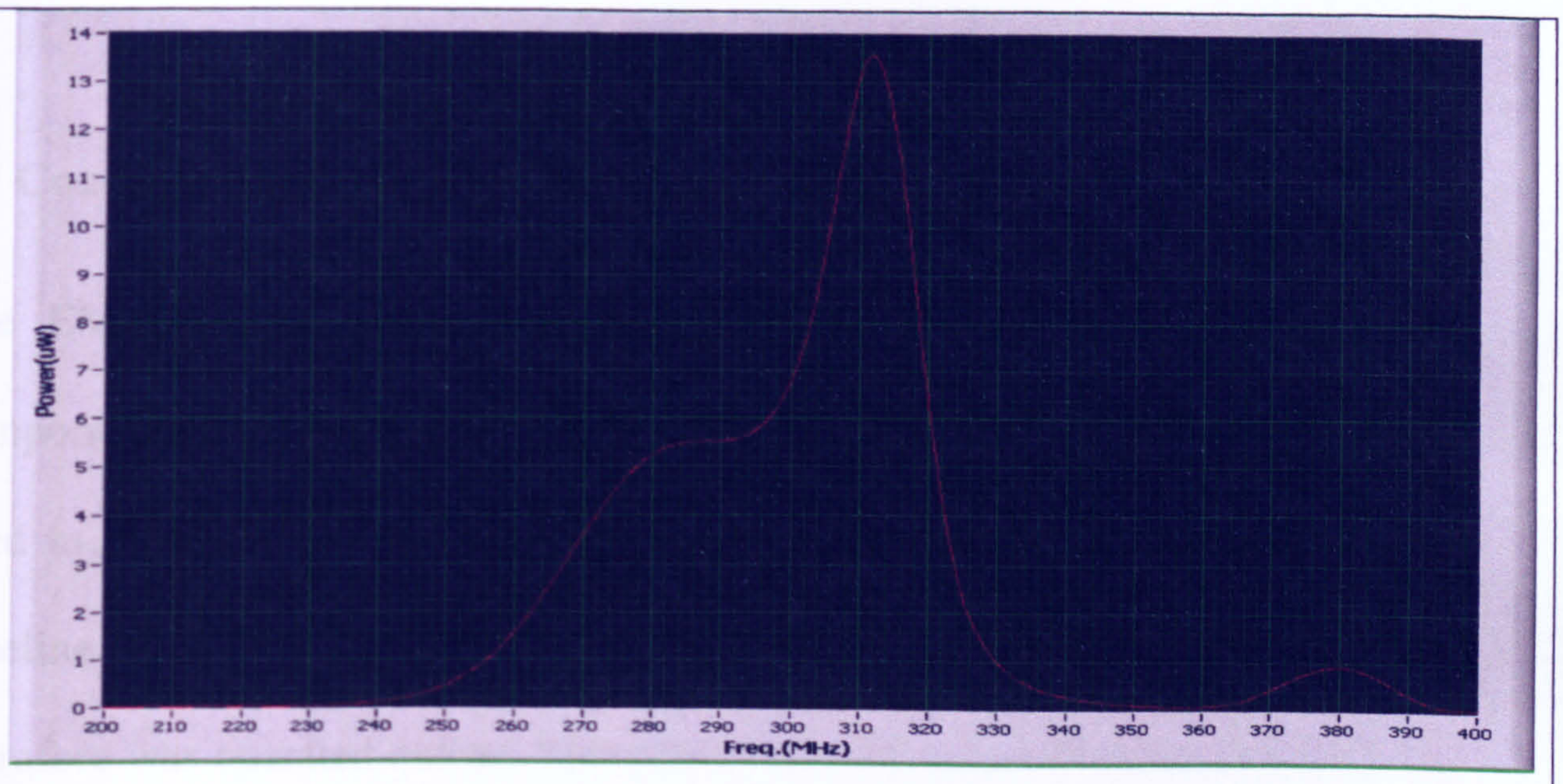

(a) : 20%Oil, 40%Water, 40%Gas, Freq 312.195MHz

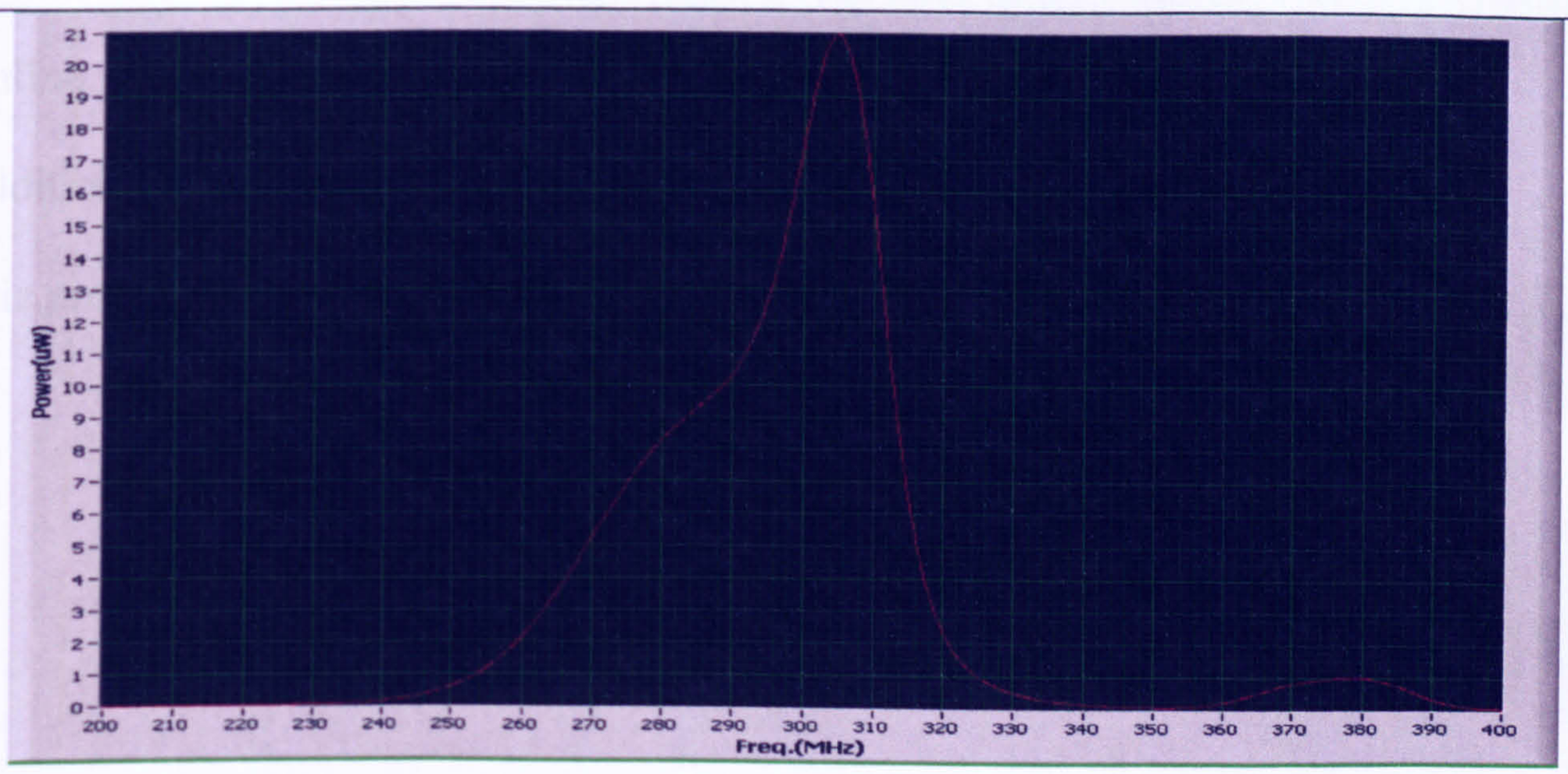

(b) : (20%Oil, 60%Water, 20%Gas), Freq 304.816MHz

Figure 7.7: Screen shot showing online results three phase (oil, gas, and water mixtures) in a pipeline.

7.7 Conclusion

The EMW3 sensor described in chapter 5 was upgraded with hardware components, and a software application was designed. These components were used to vary and control the temperature, and to homogenise the flow in the pipeline. The software application was implemented and the sensor system therefore was operated online. Two phase (oil and gas, and water and gas), and three phase (oil, gas, and water) online experiments were carried out, and the online results were presented. The main limitation with this design was the addition of the hardware units which has complicated the system size. However, this problem will be solved in the future works.

CHAPTER 8

Conclusion and Future Work

8.1 Conclusion

The problem of how to measure oil, water, and gas mixtures in a pipeline has been a challenging problem for the oil industry. Monitoring and measuring (oil, water, and gas mixture) fractions are very important for enhancing the quality aspects of production, and optimizing the process for both operation and transportation. Multiphase flow measurement provides valuable information for the management of oil field as it enables decisions to be made to maximize the hydrocarbons that are extracted from each well in the most efficient manner.

The major part of the work presented in this thesis was to design and implement non intrusive and accurate microwave sensors for monitoring and measuring (oil, gas, and water) mixture fractions in a pipeline (expressed in volume percentages) in real time, using a software program. As a result, electromagnetic

wave sensors operating at microwave frequencies were designed based on a cylindrical cavity resonator fitted in-line with a pipeline.

The EMW2 sensor was designed to detect and measure two phase components in a pipeline, expressed in volume percentages. The EMW3 sensor was designed for monitoring and measuring three phase (oil, gas, and water) in a pipeline, in real time. The EMW2 and the EMW3 sensors were described in chapters 4 and 5 respectively. The EMW3 sensor was upgraded with new hardware control units and automated with a new software application, using the NI Lab View graphical language.

Based on the HFSS simulation results and the experimental results analysis, the following conclusions can be drawn:

1. **EMW2 sensor:** This sensor was found to be accurate, compact in size, and capable for detecting and measuring the two phase components in a pipeline with the TE111 mode. The measurement of the two phase components using the TM010 mode in this sensor, on the other hand, was found to be impossible experimentally. It was found that even when the sensor was energized for TM mode, the TE111 still dominated. This

problem was referred to the presence of the (PVC) material of the pipeline. However, detecting and measuring two phase components with TE111 mode were achieved successfully. The HFSS simulation results and the experimental results were discussed, and compared and analyzed in chapters 4 and 6 respectively.

2. **EMW3 sensor:** This sensor was not only found to be compact in size and accurate for monitoring and measuring two phase and three phase (oil, gas, and water) fractions in a pipeline , in volume percentages, but also more accurate than the EMW sensor. The comparisons and analysis of the HFSS results and experimental results discussed in chapter 4 were compared and analyzed in chapter 6.

3. **Frequency temperature dependency**: This drawback was investigated experimentally in chapter 5, and has been overcome by adding a thermally controlled unit to vary and control the temperature in both the cavity resonator and the PVC pipeline as shown in Figure 7.1. The data collected has been used as a control data in this system database as described in chapter 7.

8.2 Future Work

The sensors, which are described in the thesis, all work satisfactorily and do not seem to have any major weaknesses. From a commercial point of view, there is no need for further studies of the sensors at the level treated in the thesis. However, for a higher level such as manufacturing a commercial three phase sensor or designing other sensors based on the same principles as the described ones, we suggest the following list of recommendations:

- In order to manufacture a commercial version of the online three phase sensor described in this thesis the system set up units must be integrated into a suitable package.
- The methods for designing the loop antenna should be studied further.
- The successful implementation of the monitoring and control system as an online three phase sensor was demonstrated in chapter 7 with online results. From a security point of view the system can be implemented at different locations along unsecured transportation pipeline. These locations of the system and the way of sending the system output to a security office need to be studied.
- The effect of temperature on the resonant frequency was examined experimentally up to 50^{0}C and taken into account for controlling the system

and providing online monitoring measurements. Depending upon the actual application in the oil industry, temperature effects above 50^{0}C should be studied further.

References

[1] Thorn R., G.A. Johansen, E.A. Hammer. Recent Developments in three phase flow measurement. Measurement Science Technology 8, 691–701, 1997.

[2] Kovel, N.I. Multiphase Flow Dynamics. Springer-Verlag Berlin Heidelberg, New York, Vol. 1, Fundamentals, 2nd edition, 2005.

[3] Ibrahim M.M. Babelli. In Search of an Ideal Multiphase Flowmeter for the Oil Industry. The Arabian Journal for Science and Engineering, Volume 27, Number 28, 2002.

[4] Parviz M., Jame Williamson, P.E. Principles of Multiphase Measurement. Alaska Oil and Gas Conservation Commission, 2004.

[5] Claudio Barrerios da Costa e Silva, Jose Alberto Pinheiro da Silva Filho Miguel Joao Borges Filho, Josaphat Dias da Mata . Multiphase Flow Metering Technology Update. 2002

[6] Sorensen, H. and Somme, B.F. Use of online PVT package on Sign Vest for converting meter flowrates to export conditions. Proc. 12thMultiphase Production Technology, pp.399-413, 2005.

[7] Thorn R., Johansen G. and Hammer, E. Three-Phase Flow Measurement in the Offshore Oil Industry Meas. 1st World Congress on Industrial Process Tomography, Buxton, Greater Manchester, April 14- 17, 1999.

[8] Van Santen, H., Kolar, Z.I. and Scheers, A.M. Photon Energy Selection for Dual Energy γ-and/or X-ray Absorption Composition Measurements in oil–water–gas Mixtures, Nucl. Geophysics. Vol. 9, pp: 193–202, 1995.

[9] Scheers, A.M. and Letton, W. An oil/water/gas composition meter based on multiple energy gamma ray absorption, (MEGRA) measurement Proc. 14th North Sea Flow Measurement Workshop (Peebles, Scotland), 1996.

[10] Dykesteen, E. Multiphase metering, Trans. IchemE, Vol. 70, part A, pp:32–37, 1992.

[11] Dykesteen, E., Hallanger, A., Hammer, E.A., Samnoy, E. and Thorn, R. Non-intrusive three-component ration measurement using an impedance sensor, J. Phys. E: Sci. Instrum. 18, pp:540–544, 1985.

[12] Ashton, S.L., Cutmore, N.G., Roach, G.L., Watt, J.S., Zastawny H.W. and McEwan, A. J. Development and trial of microwave techniques for measurement of multiphase flow of oil, water and gas, Proc. SPE Asia Pacific Oil and Gas Conf. (Melbourne, Australia)(Society of Petroleum Engineers), 1994.

[13] Handbook of Multiphase Flow Metering, 2005.

[14] Gainsford, S. and Hide, H.O. Field testing of the multi-fluid LP multiphase meter, Proc. 11th North Sea Flow Measurement Workshop (Bergen), Norway, 1993.

[15] Hogan, B., Al-Shamma'a, A.I. and Lucas, J. Real-Time Multiphase Metering Using Non- Intrusive Microwave Sensor, 2nd North American Conference on Multiphase Technology, ISBN 1- 86058252-4, pp:281-296, 2000.

[16] Bird, A. The role of multiphase flow in oil and gas production, Proc. Conf. Advances in Multiphase Operations, Offshore (London), 1995.

[17] Kruger, G.L., Birke A. and Weiss, R. Nuclear magnetic resonance (NMR) two-phase mass flow measurement, Flow Meas. Instrument. Vol. 7, pp: 25–37, 1996.

[18] Meyer, W., "Helical resonators for measuring dielectric properties of materials", IEEE Trans. Microwave Theory Tech., Vol. MTT-29, No. 3, pp. 240-247, 1981.

[19] Loether, H. J., and D. G. McTavish. Descriptive and Inferential Statistics: An Introduction, 3rd ed. Boston: Allyn and Bacon, 1988.

[20] McPherson, G. Statistics in Scientific Investigation: Its Basis, Application, and Interpretation. New York: Springer-Verlag, 1990.

[21] Creswell, John, Michael Fetters, and Nataliya Ivankova 2004 Designing a Mixed Methods Study In Primary Care. Annals of Family Medicine 2:7–12.

[22] Creswell, John W., and Vicki L. Plano Clark 2007 Designing and Conducting Mixed Methods Research.Thousand Oaks, CA: Sage Publications.

[23] David M. Pozar. Microwave Engineering. John Wiley & Sons Inc, 2005.

Cha2:

[24] Joseph J. Carr. Practical Antenna Handbook, page 8. McGraw-Hell, 2001.

[25] The American Heritage Dictionary, 1985.

[26] W.V.D. Glazier and E.R.L Lamont. Transmission Lines and Propagation, Volume 5. Her Majesty's Stationary Office, 1958.

[27] Scot AW. Understanding Microwaves. John wily & Sons, Inc., New Jersey, 1993.

[28] Kraus JD. Electromagnetics, Fourth Edition. MacGraw Hill, New York, 1992.

[29] Connor FR. Wave Transmission. Edward Arnold Ltd, London, 1975.

[30] Benson FA, Benson TM. Field Wave and Transmission Lines. Chapman &Hill, London, 1991.

[31] Oliver AD. Microwave and Optical Transmission. John wily & Sons, Ltd, New York, 1992.

[32] David M. Pozar. Microwave Engineering . John Wiley & Sons Inc, 2004.

[33] Collin RE. Foundattion for Microwave Engineering. John wily & Sons, Inc., New Jersey., 2001.

[34] Samuel Y. Liao, Microwave Devices and Circuits, 3rded . Prentic-Hall, Inc,2001.

[35] Om P. Gandhi. Microwave Engineering and Applications, pages 251-235. Pergamon Press ,1981.

[36] Simon Ramo , John R. Whinnery, and Theodore Van Duzer, Fields and Waves in Communications Electronics, John Wiley and Sons, 3rd ed., 1994.

[37] David. K. Cheng, Field and Wave Electromagnetics, Addison-Wesley Pub Co, 2nd ed., 1989.

[38] John D. Kraus and Ronald J. Marhefka, Antennas for all Applications, Tata McGraw-Hill, 2003.

[39] Nyfors E, Vainnikainen P. Industrial Microwave Sensor, Arech House, Norwood Ma, 1989a.

[40] Von Hippel, A.R., Dielectric Materials and Applications, Cambridge, MA: MIT Press, 438 p, 1954.

[41] Becher, P., Emulsions: Theory and Practice, New York: Reinhold, 2nd ed. 440 p, 1965.

[42] Klein, A., "Microwave determination of moisture in coal: Comparison of attenuation and phase measurement", J. Microwave Power, Vol. 16, No. 3-4, 1981, pp. 289-304.

[43] Brodwin, M., J. Benway, "Experimental evaluation of a microwave transmission moisture sensor", J. Microwave Power, Vol. 15, No. 4, 1980, pp. 261-265.

[44] Stuchly, M.A., and S.S. Stuchly, "Coaxial line reflection methods for measuring dielectric properties of biological substances at radio and microwave frequencies - A review", IEEE Trans. Instr. Meas., Vol. IM-29, No. 3,September 1980, pp. 176-183.

[45] Colpitts, B., Y. Pelletier, S. Cogswell, "Complex permittivity measurement of the colorado potato beetle using coaxial probe techniques", J. of Microwave Power and Electromagnetic Energy, Vol. 27, No. 3, 1992, pp. 175-182.

[46] Hasted, J.B., Aqueous Dielectrics, London: Chapman and Hall, 302 p, 1973.

[47] Scott, B.N., Cregger, B.B., and Shortes, S.R. "Technology for Full-Range Water-Cut Measurement," paper OTC 7233 presented at the Annual OTC in Houston, Texas, 3-6 May 1993.

[48] 13. Mehdizadeh, P.: "Multi-Phase Flow Metering Using Dissimilar Flow Sensors: Theory and Field Trial Results," paper SPE 29847 presented at the SPE Middle East Oil Show held in Bahrain, 11-14 March 1995.

[49] United States Patent: "Oil/Water Measurement", patent number 5,101,163.

[50] Basrawi, Y.F.: "Crude and Hydrocarbon Measurement Technologies," paper SPE 56808 presented at the SPE Annual Technical Conference and Exhibition held in Houston, Texas, 3-6 October 1999.

[51] United States Patent: "Emulsion Composition Monitor", patent number 6,182,504, 2001.

HFSS-3

[52] HFSS. http://www.ansoft.co.uk, 2006.

[53] Ali Mahmoudi. Negative refraction of a three-dimensional metallic photonic crystal. Eur. Phys. J. Appl. Phys. 39, 27-32 (2007)

[54] H. Seong-Tae, K. Jung-I, and P. Gun-Sik. Design of folded waveguide travelling-wave tube. Microwave. Opt. Techn.Let. , 38 (6):161-165, 2003.

[55] Y. Han and I. S. Kim. Practical design consideration of a modified structure for a planar multiport power divider at 2 GHz. Microwave J., 45(11):102-114, 2002.

[56] A. F. Abdelaziz and K. A. Zaki. Full wave analysis of rounded ends iris and its application in coupling. J. Electroman. Wave, 15(9):1215-1227, 2001.

[57] T. Kamei, H. Morishita, C. T. Cheung, and D.B. Rutledge. Design of a mode converter for quasi-optical ampliers by using 3D EM simulation software. IEICE T. Electron., E84C (7): 955-960, 2001.

[58] Vector Fields Concerto. http://www.vectorfields.com, 2007.

[59] E. da Silva. High Frequency and Microwave Engineering, pages 87-141. Butterworth – Heinemann, 2001.

[60] Al-Hajeri. S, Wylie. S. R, Stuart. R. A and Al-Shamma'a. A. I, "An Electromagnetic Cavity Sensor For Multiphase Measurement In The Oil And Gas Industry", Sensors And Their Applications XIV Conference (SENSORS07), Liverpool, UK, 11–13 September 2007, Journal of Physics: Conference Series, ISSN: 1742-6588, doi:10.1088/1742-6596/76/1/012007, Vol. 76, IOP Publishing, Article No. 012007, 2007.

[61] Wylie. S, Al-Hajeri. S, Shaw. A, Al-Shamma'a. A. I, "RF-Microwave Monitoring Sensor for the Oil Industry", 41st Annual International Microwave Symposium Proceedings, Vancouver, Canada, August 2007, ISBN 1070-0129, pp: 79-83, 2007.

[62] Aeroflex: http://www.reroflx.com. Marconi Microwave Test Set 6200A.

[63] Nyfors E., and P. Vainikainen, Industrial Microwave Sensors, Norwood, MA.: Artech House, 1989.

[64] Okamura, S., S. Miyagaki, Z. Ma, "Accurate resonance frequency detection in a microwave moisture measurement", J. of Microwave Power and Electromagnetic Energy, Vol. 33, No. 3, pp. 143-150, 1998.

[65] Saad, T.S., Ed., Microwave Engineers' Handbook, Vol. I, Norwood, MA: Artech House, 1971.

[66] National Instruments GPIB: http://www.ni.com/gpib/, 2007.

[67] Liquid Capture Software: http://www.ni.com./gpib/, 2007.

[68] Al-Hajeri. S, Wylie. S. R, Stuart. R. A and Al-Shamma'a. A. I, "Smart Microwave On-Line Sensor For Multiphase Metering In The Oil And Gas Industry", 3rd GERI Annual Research Symposium GARS-2007, Liverpool, UK, 27 June 2007.

[69] Al-Hajeri. S, Wylie. S. R, and Al-Shamma'a. A. I, "Smart Microwave On-Line Sensor For Multiphase Metering In The Oil And Gas Industry", 4the GERI Annual Research Symposium GARS-2008, Liverpool, UK, 25 June 2008.

[70] Hewlett-Packard Application Note 1217-1, Basics of measuring the dielectric properties of materials.

[71] Von Hippel, A.R., Dielectric Materials and Applications, Cambridge, MA: MIT Press, 1954.

[72] Handbook of Multiphase Metering, Norwegian Society for Oil and Gas Measurement, NFOGM Report No. 1, 64 p, 1995.

[73] Bramanti, M., E. Salerno, "Electromagnetic techniques for nondestructive testing of dielectric materials: Diffraction Tomography", J. Microwave Power and Electromagnetic Energy, Vol. 27, No. 4, pp. 233-240, 1992.

[74] Al-Hajeri. S, Wylie. S. R, Stuart. R. A and Al-Shamma'a. A. I. An Electromagnetic Cavity Sensor For Multiphase Measurement In The Oil And Gas Industry, Sensors And Their Applications XIV Conference (SENSORS07), Liverpool, UK, 11–13 September 2007, Journal of Physics: Conference Series, ISSN: 1742-6588, doi:10.1088/1742-6596/76/1/012007, Vol. 76, IOP Publishing, Article No. 012007, 2007.

[75] Thermal Control Unit: http://www.huberonline.com/html/produkte/plug_play_e.html, 2008.

[76] National Instruments: http://www.ni.com/labview/thermocouple, 2008.

[77] Watson Marlow Pump: http://www.watson-marlow.com/wmb-gb/p-rangegb3.html, 2008.

[78] National Instruments: http://www.ni.com/labview,2008.

[79] John Sharp. Microsoft Visual C++. Microsoft Press. Washington US. 2005.

[80] H.M Deitel &P.J Deitel. (Java) How to Program, Second Edition. Prentice-Hall, Inc. New Jersey, US.1998.

[81] H.M Deitel & P.J Deitel. (C Language) How to Program, Second Edition. Prentice-Hall, Inc. New Jersey, US.1998.

[82] National Instruments: http://www.ni.com/instrumentsdrivers, 2008.

[83] A.C Mettaxas & R.J Meredith. Indestrial Microwave Heating. John Wiley & Sons Inc, 2005.

Appendix 1

List of Publications

1.- GERI Annual Research Symposium (GARS) 2007

Liverpool John Moores University, June 27th, 2007

Smart Microwave On-Line Sensor for Multiphase Metering In the Oil and Gas Industry

S. Al-Hajeri, S. R. Wylie, R. A. Stuart, A. I. Al-Shamma'a.

Abstract

A significant problem in the oil and gas industry is how to measure oil, gas, and water mixtures. The industry requires accurate on line sensors to monitor the fluid flow in pipelines, in order to manage wells efficiently. The sensor described in this paper uses the different relative permittivity values for the three phases: oil, gas and water to help determine the fraction of each phase in the pipeline, by monitoring the resonant frequencies that

occur within an electromagnetic cavity. The sensor has been designed to be non-intrusive. This is advantageous as it will prevent the sensor being damaged by the flow through the pipeline and allow pigging; the techniques used for cleaning rust and wax from the inside of the pipeline using blades or brushes. A laboratory prototype version of the sensor has been constructed and the results are compared to those simulated, using HFSS.

2.- 41st Annual International Microwave Symposium Proceedings 2007

Vancouver - Canada, August 1st - 3th, 2007

RF-Microwave Monitoring Sensor for the Oil Industry

S. Al-Hajeri, S.R. Wylie, A. Shaw, A.I. Al-Shamma'a

Abstract

A reliable monitoring system is an important component of the offshore. Existing designs of monitor sensor(s) are widely used and often provide useful results, but they can require regular calibration and many struggle to provide reliable quantitative measurements. At Liverpool John Moores University we have been investigating the propagation of RF and

microwaves through various mediums within the oil pipe including oil, gas, water and sand in order to quantify the dielectric properties of medium mixtures. The sensor is non-invasive and relies on the relatively high dielectric constant of the pipeline mixtures. The electromagnetic wave field profiles within the pipeline have been modelled and simulated using a higher frequency structure simulator (HFSS) package. This paper describes the microwave system set-up including the transmitting and receiving antennas. Theoretical modelling and experimental results of various mixtures will be presented.

3.- IoP Sensors & their Applications XIV

The Instrument Science and technology group

Liverpool John Moores University, September 11th – 13th, 2007

An Electromagnetic Cavity Sensor for Multiphase Measurement in the Oil and gas industry

S. Al-Hajeri, S.R. Wylie, R.A. Stuart and A.I. Al-Shamma'a

Abstract

The oil and gas industry require accurate sensors to monitor fluid flow in pipelines in order to manage wells efficiently. The sensor described in this paper uses the different relative permittivity values for the three phases: oil, gas and water to help determine the fraction of each phase in the pipeline, by monitoring the resonant frequencies that occur within an electromagnetic cavity. The sensor has been designed to be non-intrusive. This is advantageous as it will prevent the sensor being damaged by the flow through the pipeline and allow pigging, the technique used for cleaning rust and wax from the inside of the pipeline using blades or brushes.

4.- GERI Annual Research Symposium (GARS) 2008

Liverpool John Moores University, June 25th, 2008

Smart Microwave On-Line Sensor for Multiphase Metering In the Oil and Gas Industry

S. H. Al-Hajeri, S. R. Wylie, A. Shaw and A. I. Al-Shamma'a

Abstract

Measuring oil, gas, and water fraction percentages in a dynamic pipeline is a significant problem in the oil and gas industry. In order to manage wells efficiently, the industry requires accurate on line sensors to monitor the fluid flow in pipelines. The sensor described in this paper uses different relative permittivity values of three phases: oil, gas and water to help determine the fraction of each phase in the pipeline, by monitoring the resonant frequencies that occur within an electromagnetic cavity. The sensor has been designed to be non-intrusive. This is advantageous as it will prevent the sensor being damaged by the flow through the pipeline and allow pigging. Techniques used for cleaning rust and wax from the inside of the pipeline using blades or brushes. A laboratory prototype version of the sensor system has been constructed, and the experimental results are compared to the simulation results which have been obtained by the use of High Frequency Structure Simulation (HFSS) software package. Finally, the system was automated, using National Instrumentation (NI) devices and Lab view software package, and an online real time results are read and captured.

5.- IoP Sensors & their Applications XV

The Instrument Science and technology group

Edinburgh, UK, October 5th – 7th, 2009

Real Time EM Waves Monitoring System for oil Industry Three Phase Flow Measurement

S. Al-Hajeri, S. R. Wylie, A. Shaw and A. I. Al-Shamma'a

Abstract

Monitoring fluid flow in a dynamic pipeline is a significant problem in the oil industry. In order to manage oil field wells efficiently, the oil industry requires accurate on line sensors to monitor the oil, gas, and water flow in the production pipelines. This paper describes a sensor that is based on an EM Waves cavity resonator. It determines and monitors the percentage volumes of each phase of three phase (oil, gas, and water) in the pipeline, using the resonant frequencies shifts that occur within an electromagnetic cavity resonator. The sensor was designed to not be intrusive. This advantage will prevent the sensor being damaged by the flow through the pipeline and allow pigging (technique used for cleaning rust and wax from the inside of the pipeline using blades or brushes). A laboratory prototype

version of the sensor system was constructed, and the experimental results were compared to the simulation results which were obtained by the use of High Frequency Structure Simulation (HFSS) software package. Finally, a software application was designed (using National Instrumentation (NI) devices, and software package), the system prototype was automated and tested, and a real time results were displayed.